Pre-construction Biogeochemical Analysis of Mercury in Wetlands Bordering the Hamilton Army Airfield (HAAF) Wetlands Restoration Site

Interim Report 2004

For

USACE District, San Francisco

Prepared by

USACE Engineer Research and Development Center
Waterways Experiment Station
Environmental Laboratory
Vicksburg, MS

DRAFT November 2004

Authors

The following scientists were responsible for the conduct of the research and the preparation of the report:

Elly P.H.Best[1], Herbert L.Fredrickson[1], Victor A. McFarland[1], Holger Hintelmann[2], Robert P. Jones[1], Charles H. Lutz[1], Gregory A. Kiker[1], Anthony J. Bednar[1], Rod N. Millward[3], Richard A. Price[1], Guy R. Lotufo[1], Gary L. Ray[1]

[1] U.S. Army U.S. Army Engineer Research and Development Center, Environmental Laboratory, Vicksburg, Mississippi, USA:

[2] Trent University, Department of Chemistry, Peterborough, Ontario, Canada:

[3] Applied Research Associates, Inc., Vicksburg, Mississippi, USA:

The report should be cited as:

Best, E.P.H., Fredrickson, H.L., MacFarland, V.A., Hintelmann, H., Jones, R.P., Lutz, C.H., Kiker, G.A., Bednar, A.J., Millward, R.N., Price, R.A., Lotufo, G.R., Ray, G.L., 2004. Pre-construction Biogeochemical Analysis of Mercury in Wetlands bordering the Hamilton Army Airfield (HAAF) Wetlands Restoration Site. Interim Report 2004 to USACE District, San Francisco, by USACE Engineer Research and Development Center, Waterways Experiment Station, Vicksburg, MS, November, 2004.

Contents

List of Figures

List of Tables

Chapter 1.

TOC = total organic carbon.

Chapter 5.

Interim Report Summary

Problem

Long-term goals for San Francisco Bay development include extensive wetland restoration. The current wetlands bordering San Pablo Bay are to be increased from 16,200 ha to 42,525 ha by the year 2055 (Project Goals, 1999). Dikes currently protect most of the areas targeted for restoration. Drying and oxidation of the soils on the landward side of the dikes has resulted in subsidence such that current soil elevations are often meters below the mean tide level. Breaching the dikes would result in lakes, not wetlands. Considerable amounts of fill material are required to raise the elevation of subsided areas to a level that would support aquatic macrophytes that would in turn trap sediments required to sustain the elevation of the wetland. For example, the Hamilton Army Airfield site will require approximately 10.6 million cubic yards of material. Sediments derived from operations and maintenance of navigation channels in the Bay could be used for this purpose. On one hand this beneficial use of local dredged materials would save the Government the cost of obtaining other fill material, and on the other hand save the Government the cost of transporting the material to more distal disposal sites.

The high current levels of mercury in the San Francisco Bay fishery complicate this potential win-win situation. The San Francisco Bay watershed is impacted by the legacy of mercury mines in the Coastal Range and placer gold mining in much of the Sierra Nevada watershed. Wetlands, and particularly intertidal wetlands, are notorious for converting mercury to methylmercury. Methylmercury is a potent neurotoxin that efficiently biomagnifies in many aquatic food webs. In this context, the immediate concern of the U.S. Army Corps of Engineers focuses on the use of mercury containing dredged material for the restoration of wetlands. However, the level of mercury in these dredged materials will be generally typical of that found in the majority of the Bay sediments. The larger environmental issue affecting the use of dredged material for wetland restoration becomes the contribution of Bay salt marshes to mercury in the Bay fishery, no matter the source of the mercury.

Most of the work in this interim report was designed to address consensus technical questions formulated at the CALFED Stakeholders' Workshop on Mercury in San Francisco Bay, held 8-9 October 2002 at Moss Point Landing. These included:

1. What are the present levels of MeHg in SF Bay wetlands with respect to biota, sub-habitats, and location within the Bay?
2. What are the rates of MeHg production?
3. What factors control MeHg production? Can these be managed?
4. Are some wetlands larger mercury exporters than others?
5. Can we model/predict the effects of wetland restoration on MeHg production and export?

Chapter 1: HAAF Sediment Mercury Pool Sizes and Dynamics in Relation to Primary Producers

- An exploratory field study was conducted to: (1) measure total Hg and MeHg levels concurrently in sediments from low marsh (mud), middle marsh (*Spartina foliosa*), high marsh (*Salicornia virginica*), and epipelon-vegetated mud from different locations in and adjacent to HAAF; (2) determine rates of Hg^{2+} methylation and MeHg demethylation potential in sediments from low marsh (mud), middle marsh (*Spartina foliosa*), high marsh (*Salicornia virginica*), and epipelon-vegetated mud; and (3) explore the following factors potentially influencing

methylation and demethylation rates: illumination, plant species, redox potential and pH, and composition of the microbial community.

We collected and incubated samples during the period of 9-11 June 2003, i.e. in the dry season, in two tidal marshes, a marsh bordering the HAAF and a reference marsh. The test site was situated at the HAAF Bay Edge and the reference site in the China Camp State Park wetland. Where possible, locations within each site were chosen to represent the low marsh (mud), middle marsh (*Spartina foliosa*), and high marsh (*Salicornia virginica*).

We incubated mud- and vegetated-mud-cores with stable Hg isotopes on site, and recorded redox potential and pH in the incubated cores. After incubation, the cores were flash-frozen and shipped to the laboratory for further analyses.

Mean MeHg concentrations in sediments were in the same order of magnitude at HAAF and China Camp, and ranged from 0.79 to 1.80 ng g^{-1} DW. Mean MeHg concentrations in the macrophytes varied between 1.08 ng g^{-1} DW in *S. foliosa* stems to 5.59 ng g^{-1} DW in *S. foliosa* roots. Plant levels usually exceeded those in the sediments in which they rooted, particularly when incubated under ambient irradiance.

Net MeHg production is the result of methylation and demethylation rates in the sediment. Methylation rates were 1.44 ng MeHg g^{-1} DW per day in non-vegetated sediments of HAAF. Rates were usually higher in vegetated than in non-vegetated sediments. Rates were also usually higher in the light than in darkness. Methylation rates varied with location within the Bay, and were lower at HAAF than at China Camp. Demethylation rates were 0.59 ng MeHg g^{-1} DW per day in non-vegetated sediments. Rates were equal or lower in vegetated sediments. Among all sediments studied, the epipelon-vegetated sediment exhibited the highest potential for net MeHg production, since it had a methylation:demethylation ratio of 12. Bare and *S. foliosa* - vegetated sediment had the lowest ratio, i.e. of 2, while *S. virginica*-vegetated sediment had a ratio of 7.

Methylation and demethylation rates appear to be higher in the sediment surface layers than in deeper layers. In the surface layers, the microbial biomass is also highest, and the composition of the microbial communities is strongly influenced by the presence/absence of vegetation, and by the vegetating species (epipelon, *S. foliosa*, *S. virginica*). The largest variations in redox potential occur in the surface layer due to tidal inundation and plant-sediment interactions.

Our mass balance and export estimations are speculative, but begin to frame the problem and help identify critical information gaps. They are not meant for TMDL use but for the purpose of identifying current knowledge gaps that prevent the calculation of meaningful TMDLs. Based on the assumptions detailed in this report our initial estimated annual net MeHg production of the 2005 HAAF system is 12.8 kg. The annual export of MeHg with tidal waters to the Bay is projected to be in the order of 0.1 kg (0.8 percent of the MeHg in the top 5 cm of sediment). These values will serve as the basis for research hypotheses for future work. Although the levels of MeHg in salt marsh standing biomass are higher than those in the sediment, the mass of this biomass is much lower that of the 0-5 cm sediment. The MeHg trophic transfer mechanisms and efficiencies from salt marsh biomasses into Bay fisheries are important but unknown. Also important but unknown are the roles that the atmosphere serves as a source of bioavailable mercury and as a sink for mercury volatilized from aquatic systems.

The limited availability of data on Hg and MeHg cycling in salt marshes and the large variability in the existing data cause large uncertainties in projections using these data. To decrease this uncertainty we will select key, sensitive parameters on which future efforts should

focus. These include collecting more data on methylation and demethylation rates of bare and vegetated sediments using the best techniques, measuring the atmospheric flux of mercury to/from the salt marsh, measuring the exchange of Hg and MeHg between sediment and tidal waters, and determining the mechanisms and efficiencies of MeHg transfer in relevant aquatic food webs originating from the dominant primary producers

Chapter 2: Spatial Distribution and Concentrations of Mercury Species in the Vegetated Marsh Zones of Salt Marshes Bordering the HAAF Wetland Restoration Site

- The purpose of this study was to determine a tentative relationship between marsh zones and THg and MeHg levels in the sediments, and assess the THg and MeHg concentrations in live and dead plant materials collected from these zones.

For this, a tentative relationship between marsh zonation and THg or MeHg concentrations in the sediment was explored by regrouping previously collected data on mercury species concentrations in surficial sediment cores according to vegetation zone, and calculating mean values for each zone. Furthermore, tissues from live plant shoots and of plant detritus were collected from as many zones as possible, and analyzed for mercury species. The following zones were distinguished: non-vegetated mudflats, *S. foliosa*-vegetated tidal marsh, *S. virginica*-vegetated upper marsh, and upland-seasonally flooded wetland.

The THg and MeHg levels in the surficial sediments of the marsh zones varied by zone. The mean THg concentrations in the surface sediments decreased in the order Low marsh>High marsh>Diked high marsh>Mudflat. No distinct effect of dry and wet season on THg concentration was noted. Mean THg concentrations, in ng g^{-1} DW, in the dry season were: Low marsh 346, High marsh 292, Diked high marsh 261, Mudflat 236.

Mean MeHg concentrations increased in the sediments of all zones during the wet season except in the mudflats. Mean MeHg concentrations, in ng g^{-1} DW, decreased in the order High marsh 7.29 >Low marsh 5.17 > Diked high marsh 1.82 > Mudflat 0.73.

In plant shoots, the mean concentrations of THg ranged from 14 to 25 ng g^{-1} DW, and of MeHg from 0.17 to 0.96 ng g^{-1} DW in *S. foliosa* and *S. virginica*. THg and MeHg levels in the plant shoots did not appear to be related to species or zone, but the number of locations sampled was low. The THg and MeHg levels in plant detritus were far higher than in live shoots, i.e., a factor of 5 to 8.

Chapter 3: Geochemical Characterization of HAAF Sediment Profiles and Mercury Species Levels in Macrofauna.

- This chapter details the results obtained from a field study conducted in June, 2003. The purpose of this effort was to measure total mercury (THg) and methylmercury (MeHg) levels in the sediment in relation to depth at intertidal sites at Hamilton Army Airfield (HAAF) and China Camp State Park (as a reference), as well as inland sites at HAAF and Bel Marin Creek. Other parameters important for the cycling of Hg and MeHg in sediments were also determined with the goal of establishing site-specific relationships between these parameters and THg and MeHg. Finally, Hg and MeHg were measured in macrofauna collected at the above-mentioned intertidal sites for the purpose of calculating site-specific biota-sediment bioaccumulation factors (BAFs).

For sediments, the highest MeHg concentrations were found in the upper 2.5 – 5.1 cm of the cores, and levels decreased with depth suggesting that conditions for the methylation of mercury are most favorable near the surface. THg levels increased with depth, correlating inversely with MeHg. The significance of this is unclear, but may suggest a net loss of mercury

from the surface through volatilization or surface runoff/tidal transport of MeHg from the sediment surface. MeHg correlated directly with redox potential (E_h), total organic carbon (TOC), and phosphorus (P) suggesting that these parameters were associated with MeHg levels in HAAF marsh sediment. The predicted influence of E_h and pH on the bioavailability of mercury is consistent with the observed MeHg profile with more positive E_h values representing oxic conditions near the surface favoring mercury in the bioavailable Hg^0 state, and more negative E_h values (anoxic) at increasing depths favoring formation of non-bioavailable HgS.

For macrofauna, significant levels of THg and MeHg were detected in tissues of animals collected at intertidal sites at HAAF and China Camp, suggesting that both THg and MeHg are available for uptake. MeHg comprised on average 40 % of THg (range 20% to 70%), indicating that a significant portion of the invertebrate THg body burden is in the form of MeHg. Calculated BAFs (greater than 1) suggest that MeHg has a strong tendency toward bioaccumulation, and BAFs for MeHg ranged from about 3 to 50. Snails were the highest Hg bioaccumulators. Because the diet of these animals is composed largely by plant material, it is likely that MeHg in plants represents an important MeHg source for terrestrial trophic transfer.

Chapter 4: Bioavailability of Mercury to Benthic Invertebrates: Characterization and Remediation Effects in HAAF Wetland Sediments

- Many studies have identified the potential adverse effects, bioaccumulation and biomagnification of Hg. As such, it is imperative that the bioavailability of Hg, and in particular the MeHg species, be ascertained as part of any assessment of environmental and human risk. The study incorporated two research goals, (1) to establish baseline bioaccumulation of Hg and MeHg in a representative and locally abundant benthic organism, the bent nosed clam *Macoma nasuta*, and (2) whether Hg uptake might be reduced by the addition of Hg-sorbing materials into the sediment. In the bioaccumulation experiment we measured the uptake and elimination of THg and MeHg in *M. nasuta* exposed to HAAF Bay Edge (SM-1 and SM-10) and the reference site China Camp State Park (R44) cores. A similar pattern of THg temporal bioaccumulation and similar final THg body burden at termination of the uptake phase of the experiment suggest that the bioavailability of THg was similar at all sites. The uptake phase was characterized by a rapid increase in body burden followed by a slower increase whereas during the elimination phase a rapid decrease in body burden was followed by a slower decrease. Overall, the bioaccumulation study indicated that the elimination of Hg is very slow in benthic clams, as the apparent steady state body burden was not reached following a 56-d exposure. The body burdens of the experimentally exposed clams were only approximately half of those recorded in clams inhabiting Bay Edge sediments, further suggesting that longer exposure periods longer than 56-d are needed for THg to approach apparent steady-state in clam tissues. The tissue MeHg concentrations varied considerably between replicates throughout the exposure hampering the observation of temporal changes in body burden during the uptake and elimination phases of the bioaccumulation experiment.

In the remediation study, sediment from the SM-10 site was used to test the effects of granular activated carbon (GAC) and sulfonated Kraft lignin on speciation and bioaccumulation of THg and MeHg in 56-d exposures using *M. nasuta*. Results were mixed but promising. GAC significantly decreased the bioaccumulation of spiked MeHg, and MeHg methylated from spiked Hg^{2+}, despite the higher concentration of those substances in the amended sediment, while it did not affect the bioaccumulation of legacy $Me^{202}Hg$. We suggest that GAC was more effective in reducing the uptake of spiked Hg species, since these were more labile and hence were freer to

associate with GAC particles. In contrast, ambient Hg is more likely to be in closer association with sediment ligands, and hence would be more refractile and less available for contact with GAC. We suggest that further experiments should contact sediment with GAC for periods longer than 16 days, to address efficacy of GAC on ambient Hg availability. Sulfonated Kraft lignin was extremely soluble in seawater, suggesting a short theoretical contact time with Hg in the sediments and raising issues of transportation of any lignin-sorbed Hg out of the system. Therefore, lignin was eliminated as a viable sorption candidate.

Chapter 5: Integrating Physical, Chemical and Biological Processes that Drive Mercury and Methylmercury Cycling in San Pablo Bay Salt Marshes into a Screening-Level Model

- The *Questions and Decisions* ™ (QnD): screening model system was created to provide an effective tool to incorporate ecosystem and management issues into a user-friendly framework. The QnD model links the spatial components within GIS files to the prevalent abiotic, climatic, and biotic interactions in an ecosystem. QnD has a simple design and can be upgraded easily. This modeling approach has been applied to the Hamilton Army Airfield wetland restoration project (QnD:HAAF). The purpose of the current QnD:HAAF version 1.0 is to integrate the field and laboratory data detailed in the preceding chapters of this report. QnD:HAAF is being applied in an iterative, interactive, manner to identify critical abiotic and biotic drivers of salt marsh mercury and methylmercury cycling and guide subsequent work on HAAF and San Francisco Bay salt marshes. It is planned to also incorporate and link scientific, economic and social issues in a manner that enables the evaluation of their relative impacts through scenario projections. As further learning occurs, those drivers that are shown to be important can be explored and subsequently expanded, those judged unimportant be discarded. Whereas these changes would require substantial code rewriting of other models, they are rapidly made in QnD.

The QnD:HAAF v1.0 is composed by four spatial areas (High *Salicornia*-vegetated Marsh, Mid *Spartina*-vegetated Marsh, Mud Flat, and Sub Tidal), three drivers (day-time light, dry and wet season, and tide-dependent redox potential), and two processes (methylation and demethylation). Biota are represented by typical plant and animal species.

Although QnD:HAAF v1.0 development is based for only 10 percent on concepts and literature data, and for 90 percent on data measured in one year only, i.e. 2003, the model results have generated several interesting points for discussion and further exploration.Two fourteen-day scenario's were simulated, i.e., one scenario representing the wet season (Feb 1 –14, 2004) and one scenario representing the dry season (June 1 – 14, 2003). Simulated MeHg levels in biota indicated a significant bioaccumulation potential from lower to higher trophic levels, regardless of season. Elevation was an important factor influencing net MeHg production. Simulated MeHg concentrations in the sediment greatly exceeded the measured levels while simulated methylation and demethylation rates were in the same order of magnitude as measured values.. The difference between the simulated and measured mercury levels in the sediment and biota can provide a first estimate of the magnitude of the HAAF mercury export term. Validation of the value of the HAAF mercury export term and the processes by which this export is realized is the focus of current work plans.

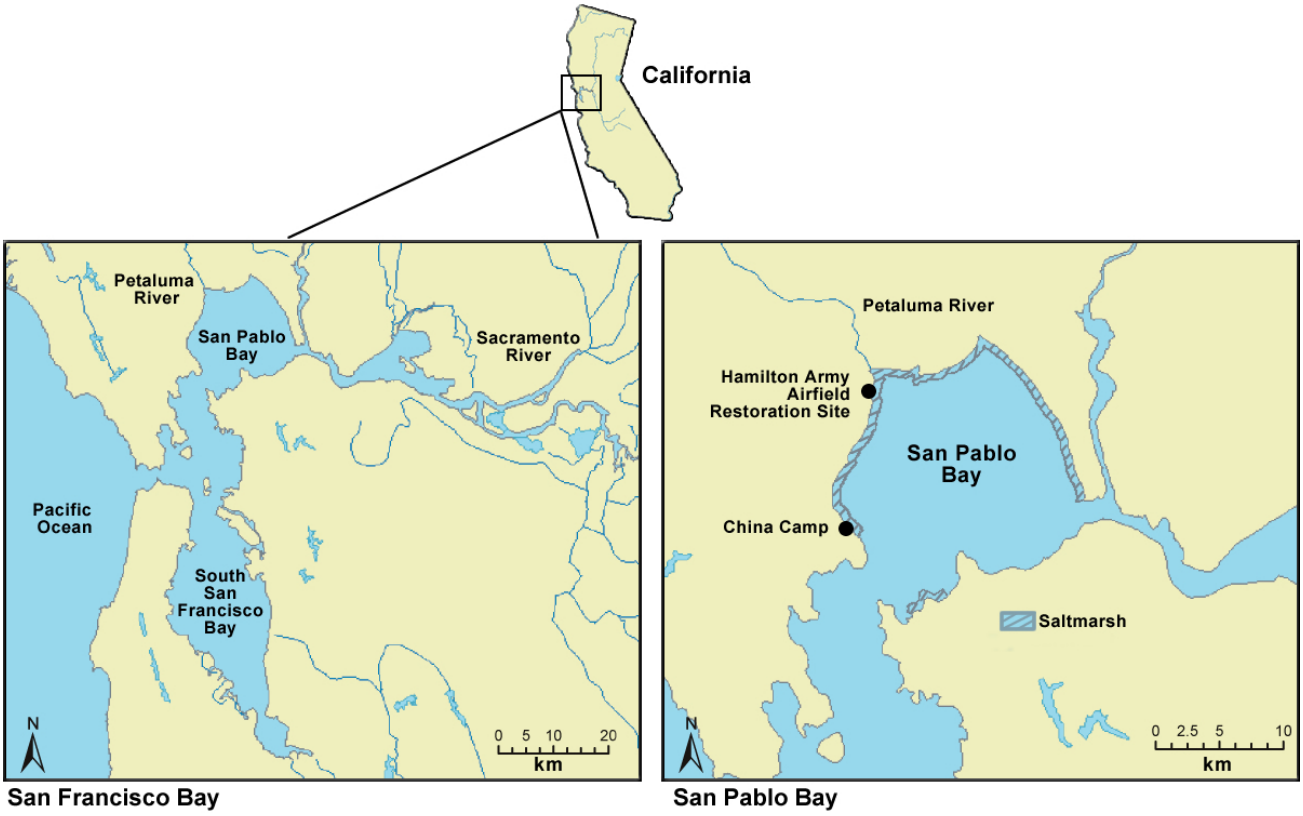

Site map showing the location of San Pablo Bay within San Francisco Bay (left) and the location of the Hamilton Army Airfield Restoration Site and the China Camp reference site (right).

Background

In March, 2003, the US Army Engineer District, San Francisco (CESPN) requested an expansion of pre-construction monitoring of mercury concentrations (total and methylmercury) in sediments and soils of existing wetlands bordering the Hamilton Army Airfield (HAAF) Wetlands Restoration Site on San Pablo Bay, California. The purpose of the expanded activities was to gain site-specific knowledge of the geochemical/geophysical, microbial, predominant plant- and animal related interactions that affect the stabilization and mobilization of mercury and methylmercury in the sediments/soils of the area. Based on these results a first-generation site-specific screening-level model was created for estimating mercury and methylmercury mobility during wetlands reconstruction.

The potential for methylation of mercury in sediments and soils of tidal marsh and seasonal wetlands bordering the Hamilton Army Airfield (HAAF) Wetlands Restoration Site was assessed by same-sample analysis for total mercury (THg) and monomethylmercury (CH_3Hg^+, MMHg, or MeHg) during the dry season (McFarland et al., 2001, and appendices therein) and during the wet season in 2002-2003 (McFarland et al. 2001, -----, 2003a). The surficial 1-2 cm of sediments at sixty sites (replicated five times) divided among seven locations were sampled. Results served as the basis for selection of sites for intensive study as described in the HAAF Mercury Characterization Project Management Plan (MacFarland et al., 2003b). The results of the subsequent feasibility studies, conducted during 2003 and largely interpreted during 2004, are described in the current Interim Report 2004.

McFarland, V.A., Clarke, J.U., Lutz, C.H., and MacMillan, D.K. (2002). "Mercury Concentrations Bordering The Hamilton Army Air Field Remediation Site: September, 2001," Report to USACE District, San Francisco, by USACE Engineer Research and Development Center, Waterways Experiment Station, Vicksburg, MS, October 4, 2002.

McFarland, V.A., Clarke, J.U., Lutz, C.H., and MacMillan, D.K. (2003a). "Mercury Concentrations Bordering The Hamilton Army Air Field Remediation Site: February, 2003. Wet Season - Dry Season Contrast," Draft Report to USACE District, San Francisco, by USACE Engineer Research and Development Center, Waterways Experiment Station, Vicksburg, MS, September 30, 2003.

McFarland, V.A., Lutz, C.H., Bednar, A.H., Jones, R.P., Fredrickson, H., Ray, G.L., Lotufo, G.R., Kiker, G.A., Price, R.A., Sturgis, T., Best, E. (2003b). "Project Management Plan for Detailed Characterization of Existing Mercury and Methylmercury Contamination Bordering the Hamilton Army Airfield Wetlands Restoration Site, April – September 2003," Prepared for USACE District, San Francisco, by USACE Engineer Research and Development Center, Waterways Experiment Station, Vicksburg, MS, June 02, 2003.

PROJECT MANAGER:
Herbert L. Fredrickson
U.S. Army U.S. Army Engineer Research and Development Center, Environmental Laboratory, Vicksburg, Mississippi, USA
Ph: 601-634-3716; Email: herbert.l.fredrickson@erdc.usace.army.mil

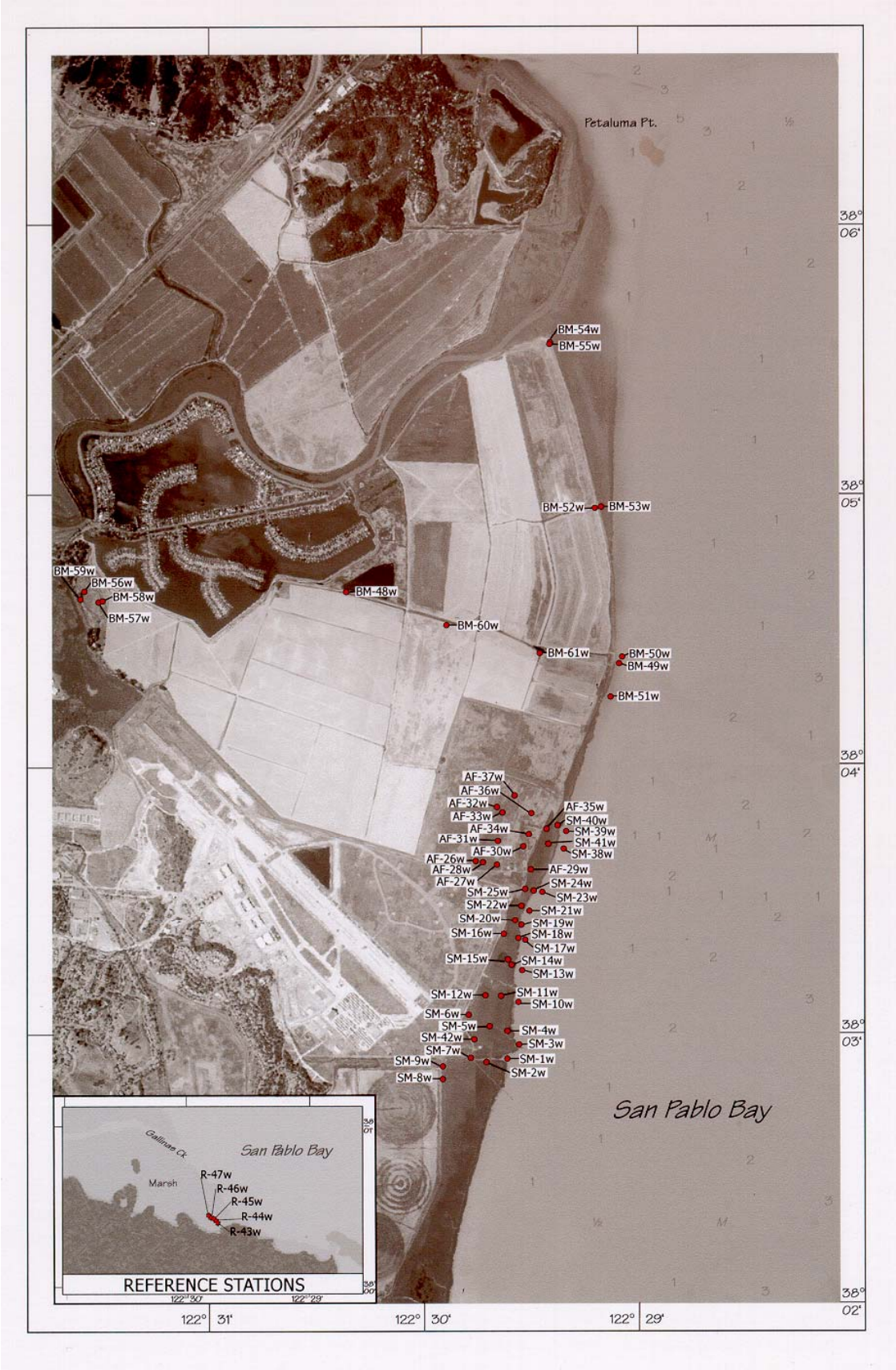

Map of sampling locations HAAF and China Camp (inset).

1- HAAF Sediment Mercury Pool Sizes and Dynamics in Relation to Primary Producers

SUMMARY

An exploratory field study was conducted to: (1) measure total Hg and MeHg levels concurrently in sediments from low marsh (mud), middle marsh (*Spartina foliosa*), high marsh (*Salicornia virginica*), and epipelon-vegetated mud from different locations in and adjacent to HAAF; (2) determine rates of Hg^{2+} methylation and MeHg demethylation potential in sediments from low marsh (mud), middle marsh (*Spartina foliosa*), high marsh (*Salicornia virginica*), and epipelon-vegetated mud; and (3) explore the following factors potentially influencing methylation and demethylation rates: illumination, plant species, redox potential and pH, and composition of the microbial community.

We collected and incubated samples during the period of 9-11 June 2003, i.e. in the dry season, in two tidal marshes, a marsh bordering the HAAF and a reference marsh. The test site was situated at the HAAF Bay Edge and the reference site in the China Camp State Park wetland. Where possible, locations within each site were chosen to represent the low marsh (mud), middle marsh (*Spartina foliosa*), and high marsh (*Salicornia virginica*).

We incubated mud- and vegetated-mud-cores with stable Hg isotopes on site, and recorded redox potential and pH in the incubated cores. After incubation, the cores were flash-frozen and shipped to the laboratory for further analyses.

Mean MeHg concentrations in sediments were in the same order of magnitude at HAAF and China Camp, and ranged from 0.79 to 1.80 ng g^{-1} DW. Mean MeHg concentrations in the macrophytes varied between 1.08 ng g^{-1} DW in *S. foliosa* stems to 5.59 ng g^{-1} DW in *S. foliosa* roots. Plant levels usually exceeded those in the sediments in which they rooted, particularly when incubated under ambient irradiance.

Net MeHg production is the result of methylation and demethylation rates in the sediment. Methylation rates were 1.44 ng MeHg g^{-1} DW per day in non-vegetated sediments of HAAF. Rates were usually higher in vegetated than in non-vegetated sediments. Rates were also usually higher in the light than in darkness. Methylation rates varied with location within the Bay, and were lower at HAAF than at China Camp. Demethylation rates were 0.59 ng MeHg g^{-1} DW per day in non-vegetated sediments. Rates were equal or lower in vegetated sediments. Among all sediments studied, the epipelon-vegetated sediment exhibited the highest potential for net MeHg production, since it had a methylation:demethylation ratio of 12. Bare and *S. foliosa* -vegetated sediment had the lowest ratio, i.e. of 2, while *S. virginica*-vegetated sediment had a ratio of 7.

Methylation and demethylation rates appear to be higher in the sediment surface layers than in deeper layers. In the surface layers, the microbial biomass is also highest, and the composition of the microbial communities is strongly influenced by the presence/absence of vegetation, and by the vegetating species (epipelon, *S. foliosa*, *S. virginica*). The largest variations in redox potential occur in the surface layer due to tidal inundation and plant-sediment interactions.

Our mass balance and export estimations are speculative, but begin to frame the problem and help identify critical information gaps. They are not meant for TMDL use but for the purpose of identifying current knowledge gaps that prevent the calculation of meaningful TMDLs. Based on the assumptions detailed in this report our initial estimated annual net MeHg production of the 2005 HAAF system is 12.8 kg. The annual export of MeHg with tidal waters to the Bay is projected to be in the order of 0.1 kg (0.8 percent of the MeHg in the top 5 cm of sediment). These values will serve as the basis for research hypotheses for future work. Although the levels of MeHg in salt marsh standing biomass are higher than those in the sediment, the mass of this biomass is much lower that of the 0-5 cm sediment. The MeHg trophic transfer mechanisms and efficiencies from salt marsh biomasses into Bay fisheries are important but unknown. Also important but unknown are the roles that the atmosphere serves as a source of bioavailable mercury and as a sink for mercury volatilized from aquatic systems.

The limited availability of data on Hg and MeHg cycling in salt marshes and the large variability in the existing data cause large uncertainties in projections using these data. To decrease this uncertainty we will select key, sensitive parameters on which future efforts should focus. These include collecting more data on methylation and demethylation rates of bare and vegetated sediments using the best techniques, measuring the atmospheric flux of mercury to/from the salt marsh, measuring the exchange of Hg and MeHg between sediment and tidal waters, and determining the mechanisms and efficiencies of MeHg transfer in relevant aquatic food webs originating from the dominant primary producers

INTRODUCTION

The total Hg (THg) levels in San Francisco Bay sediments range from 0.04 -1.08 $\mu g\ g^{-1}$ dry weight. Due to a history of placer gold and mercury mining the Bay's watershed contains high levels of THg. Furthermore, one of the world's largest Hg mines operated in the South Bay for many years. This has resulted in total sedimentary THg levels at or higher than those in sediments relative to other aquatic ecosystems perceived to present a Hg environmental toxicity risk (e.g., the Everglades). These high levels of total mercury (THg) in the Bay and adjacent watershed will not be easily changed. Although environmental regulations are based on THg levels, methylmercury (MeHg) is the most toxic Hg species and cause of the greatest concern. Levels of MeHg might be effectively managed if we can develop a mechanistic understanding of its' formation, bioaccumulation into biota, and biomagnification up aquatic food webs.

Although MeHg generally comprises less than 1% of the THg in most soils and sediments, MeHg generally comprises approximately 99% of the total Hg in biomass. MeHg biomagnifies up food chains and is neurotoxic. MeHg is the form of Hg that is of greatest concern with respect to human health and risk assessment. Knowledge of the environmental factors that control the standing pool size of MeHg, and its introduction into and magnification up food chains is needed for assessing the potential impacts of MeHg in the San Francisco Bay system. This is particularly true for the environmental risk posed by the construction of intertidal wetlands, systems that are known to produce MeHg.

Microorganisms are the agents responsible for both the methylation of Hg^{2+} to MeHg and the demethylation of MeHg to Hg^{2+}. It is unclear why bacteria catalyze these reactions. Detoxification has been suggested but it is unclear which species of Hg are more toxic to

bacteria. Electron transport for metabolic energy production is another potential, but unproven, motivation. Under reducing conditions anaerobic bacteria (especially some sulfate-reducing bacteria) oxidize sediment organic matter and transfer the resulting electrons through their cytochrome systems to available electron acceptors. When preferred terminal respiratory electron acceptors (e.g., sulfate) are limiting, some anaerobic bacteria will use whatever electron acceptor available to them (perhaps $Hg^{2+} + e^{-} \rightarrow$ MeHg). Mercury methylation requires the presence of appropriate bacteria (e.g., some sulfate-reducing bacteria), a bioavailable and reactive form of mercury, and a carbon and energy source for respiration. Temporally/spatially fluctuating level of the preferred terminal electron acceptor (e.g., sulfate) appear to stimulate MeHg production. On the other side of the ledger, many genera of aerobic microorganisms can demethylate MeHg back to Hg^{2+}. This can be a fortuitous process but some microorganisms may be able to benefit from the carbon and energy produced in this reaction. The standing pool size of MeHg is then the difference between the rates of the competing methylation and demethylation reactions. The standing MeHg pool is believed to be very dynamic, but the factors that drive the competing methylation and demethylation reactions are not currently known. Moreover, the potential for the standing pool of MeHg to be introduced into the food web is a function of the size of the MeHg pool and its availability to biota.

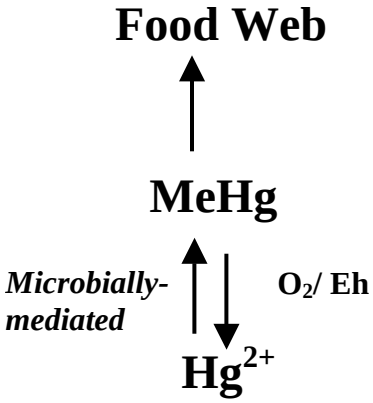

Spartina foliosa and *Salicornia virginica* are the most abundant plant genera at the HAAF site and will be the dominant genera in the reconstructed wetland. These wetland plants are typical for the low and high marsh parts, respectively. These aquatic macrophytes trap sediment particles that sustain the wetland, provide habitat for wetland fauna, and are the main sources of organic carbon, and energy to the wetland system. Marshes usually serve as net sources of MeHg in aquatic systems. With respect to mercury geochemistry these dominant plants will trap mercury-containing sediments in the marsh and affect the microbial metabolism in their root zones. Accumulation of MeHg directly into plant biomass is probably a major route of MeHg accommodation into the aquatic food web. However this process is poorly understood, as is the fate of MeHg in plant detritus.

Marsh plants may accumulate Hg and MeHg in their tissues, and as such serve as sources for biomagnification of these compounds for higher trophic levels. Additionally, they directly affect the species composition, and types and levels of metabolic activities of microbial communities in their root zones. Plants release a variety of organic nutrients that selectively enhance a beneficial microbial community around their roots. During the photoperiod some

plants actively pump oxygen from their roots into the sediment. These plant activities create a metabolically active, diurnally dynamic habitat in surface sediments. In addition, water inundations driven by tidal cycles profoundly affect physicochemical parameters such as oxygen diffusion into sediment and advective transport (e.g., sulfate, Hg^{2+}, MeHg, Fe^{2+}, etc.).

PURPOSE

A large part of the research addressed in this feasibility study (Tasks II and VII in the Scope of Work for FY2003) was designed to address consensus technical questions formulated at the CALFED Stakeholders' Workshop on Mercury in San Francisco Bay, held 8-9 October 2002 at Moss Point Landing.

These included:

1. What are the present levels of MeHg in SF Bay wetlands with respect to biota, sub-habitats, and location within the Bay ?
2. What are the rates of MeHg production ?
3. What factors control MeHg production ? Can these be managed?
4. Are some wetlands larger mercury exporters than others ?
5. Can we model/predict the effects of wetland restoration on MeHg production and export?

This exploratory field study was initiated in 2003 to specifically:

(1) Measure total Hg and MeHg levels in sediments from low marsh (mud), middle marsh (*Spartina foliosa*), high marsh (*Salicornia virginica*), and epipelon-vegetated mud from different locations in and adjacent to HAAF.

(2) Concurrently measure rates of Hg^{2+} methylation and MeHg demethylation potential in sediments from low marsh (mud), middle marsh (*Spartina foliosa*), high marsh (*Salicornia virginica*), and epipelon-vegetated mud from different locations in and adjacent to HAAF.

(3) Explore the following factors potentially influencing methylation and demethylation rates:
   i) illumination
   ii) plant species
   iii) redox potential and pH
   iv) composition of the microbial community.

STUDY SITE

The Hamilton Army Airfield on San Pablo Bay is part of the San Francisco Baylands. It is located in the North Bay Subregion. The Baylands consist of the shallow water habitats around the San Francisco Bay between the maximum and minimum elevations of the tides. The Baylands ecosystem includes the areas of maximium and minimum tidal fluctuations, adjacent habitats, and their associated plants and animals. The boundaries of the ecosystem vary with the bayward and landward movements of fish and wildlife that depend upon the Baylands for

survival. Many habitats of the Baylands are wetlands. Habitat goals selected for the restored HAAF include tidal marshes, with natural transitions into upland areas with seasonal wetlands. The restored HAAF area is expected to increase the habitat of the regionally rare clapper rail, because it will contain a large tidal wetland and is remote from predator outposts and corridors (Goals Project, 1999).

We collected and incubated samples in two tidal marshes, a marsh bordering the HAAF and a reference marsh. The test site was situated at the HAAF Bay Edge (**SM-10**; 38°03.116 N, 122° 29.550W; Fig. 1) and the reference site in the China Camp State Park wetland (**R-44**; 38° 04.379 N, 122° 28.758 W). Where possible, locations within each site were chosen to represent the low marsh (mud), middle marsh (*Spartina foliosa*), and high marsh (*Salicornia virginica*).

APPROACH

Sediment Sampling

A special sediment corer was constructed by the Engineer Research and Development Center's (ERDC) shops (Fig. 2). Undisturbed 9.5 cm diameter sediment cores were collected and used for the on-site incubations to derive methylation and demethylation rate measurements. This corer was placed over an intact plant, twisted into the sediment to a depth of approximately 20 cm, and used to extract the entire plant, roots, and adjacent sediment. A solution of $^{199}Hg^{2+}$ and $CH_3{}^{200}Hg^{+}$ was injected through pre-drilled ports in the acrylic tube core liner at three different depths (2.5, 5 and 9-10 cm) of each core. Epipelon, the micro-algal mat complex growing in patches on the sediment surface, was collected by scraping off the top 1-cm layer of mat, transferring the material into plastic centrifuge tubes, adding water from the same site, and amendment with isotopes. After injection of isotopes, all cores and tubes were set back into their original location and incubated in place for 5 h. Control tubes with epipelon were placed within the undisturbed vegetation, in which the tubes were exposed to the typical light climate within a *S. foliosa* vegetation. This procedure is described below.

Smaller diameter PVC cores (5 cm) were collected immediately adjacent to the large diameter cores. Sediment samples from 2, 5 and 10 cm depths of these small were analyzed for polar membrane lipid fatty acid (PLFA) analyses. PLFA analyses provide a measure of sedimentary microbial community biomass and taxonomic composition. This procedure is described below.

Light - Dark Core Manipulations

Two approaches were planned to determine the effects of the dominant marsh plants on microorganisms that mediate Hg^{2+} methylation and MeHg demethylation. Relevant parameters were measured in the plant root zones and compared to those parameters measured in non-vegetated areas. However, in practice it was very difficult to find sediment where plant roots were not present. The second approach was to cover for 5 hours selected vegetated and non-vegetated sediment cores with black plastic bags, and compare relevant root zone measures in illuminated and darkened sediment cores (Fig. s 3 and 4).

Redox Potential and pH Measurements

The redox potential (E_h) is a relative measure of oxidizing/reducing conditions in a soil. E_h depends on both the presence of electron acceptors (oxygen and other oxidizing agents) and

pH. In a well-drained soil the E_h is in the 400-700 mV range. In flooded conditions E_h values as low as –300 mV can be found. Microbial transformation rates in soils are strongly influenced by E_h. E_h's in root zones of plants, are influenced through oxidation due to oxygen loss from the plants' photosynthesis in the light, and through reduction due to the plants' respiration in darkness. Sediment redox and pH measurements were taken at the end of the incubation period using an Orion pH/mV meter (Model 250A) adapted with a self-manufactured platinum-tip redox electrode (Boehn 1971; Faulkner et al. 1989), or a pH electrode (Orion model 91-05). Electrodes were calibrated with quinhydrone solution or pH buffers (Orion, Beverly MA), respectively, prior to use. Electrodes were inserted into the sediment with the tips contacting sediment at 2.5, 5, and 10 cm depth at the beginning of the incubation period. E_h was measured at all sites (2 test and one reference) at three sediment depths, 0.5, 5, and 10 cm, as close as possible to 3 of the incubated cores. At only one site, i.e. the China Camp reference site, E_h was measured also inside the darkened and non-darkened cores. E_h values were calculated from measured mV readings of Pt-electrodes and corrected for the potential of the reference AgCl electrode (222.34 mV). pH was measured also at all sites, but only in the surface sediment.

Polar Lipid Fatty Acid Analyses

Polar lipid fatty acid analysis has been detailed elsewhere (Fredrickson et al. 1986). Briefly, a 2 g (wet weight) sediment samples were collected from the frozen cores at depths of 2, 5, and 10 cm. These samples were extracted for 3 hours at room temperature in 6 ml of a mixture of dichloromethane:methanol:water (1:2:0.8, v:v:v). Amino-propyl solid phase extraction columns (Supelco, Bellefonte, PA) were used to separate the total lipid into neutral, glyco- and polar lipid fractions. Phospholipid fatty acid methyl esters (from the polar lipid fraction) were prepared for gas chromatography/mass spectrometry (GC/MS) by mild alkaline methanolic transesterification. The resulting phospholipid fatty acid methyl esters were dissolved in hexane containing methyl nonadecanoate (50 pmol μL^{-1}) as an internal standard and analyzed using a gas chromatograph equipped with a 50m x 0.25mm (ID) DB-1 capillary column (0.1 µm film thickness, J&W Scientific, Folsom, CA) and a flame ionization detector. Peak identities were confirmed using a gas chromatograph-mass selective detector (Hewlett Packard GC6890-5973 MSD) with electron impact ionization at 70eV. Areas under the peaks were converted to concentrations, summed and then normalized to the gram weight extracted for biomass determinations. For community comparisons, the percent contribution of each peak was calculated and then normalized using an arcsine square root transformation.

Stable Hg Isotopic Tracer Studies

$^{199}HgCl_2$ was used for the methylation assay. ^{199}HgO (Oak Ridge National Laboratories) was converted into $^{199}HgCl_2$ by dissolving 0.690 mg of ^{199}Hg enriched (91.95 % purity) HgO in 1 mL of hydrochloric acid (10 mM), resulting in a solution with a concentration of 0.588 mg/mL ^{199}Hg. $CH_3{}^{200}HgCl$ was prepared for the demethylation assay. ^{200}Hg enriched (96.41 % purity) HgO (Oak Ridge National Laboratories) was synthesized using the methylcobalamin method as described in Hintelmann et al. (2000). The final isotopic solution had a concentration of 345 ng/mL ^{200}Hg (as $Me^{200}Hg$). 250µL of the ^{199}Hg solution were mixed with 266 µL of $Me^{200}Hg$ solution and diluted to 10 mL.

The solution (100 µL) of $^{199}Hg^{2+}$ and $CH_3{}^{200}Hg^+$ was injected through predrilled ports in the acrylic tube into three different layers (2, 5 and 9-10 cm) of each core. A total of 1470 ng of $^{199}Hg(II)$ and 0.918 ng of $Me^{200}Hg$ were injected into each layer. One set of samples was placed

into a black plastic bag to assess the effects of plant photosynthesis. After injection of isotopes, all cores were set back into their original location and incubated in place for 5 h. Incubation was terminated by quick-freezing of cores, including plants, with dry ice in the field. Samples remained frozen until analysis in the lab.

Frozen Core Sample Handling

The above ground plant material was cut off from the sediment core and weighed. The frozen cores were extruded from the plastic tube and cut into 1/2" slices using a diamond tipped cutting blade. The area injected with mercury isotopes was further isolated by cutting out a 1/2" strip from the center area around the injection point resulting in a 1/2" x 1/2" x 4" sediment core containing the injected solution of isotopes. This sub-core was further homogenized and sub-samples were taken for the various measurements. Root material was obtained by washing a sub-sample of the isolated core over a fine meshed sieved to remove clay and silt particles from the roots. The relative amounts of sediments and root material (wet weight) were determined at this stage. Wet sediment was dried at 50 °C overnight or until weight consistency was obtained to determine the dry/wet weight ratio (% solids). The loss on ignition (LOI) was determined by ashing the dried sample at 500 °C for 4 hours or until weight consistency was obtained.

Total Hg Determination

About 0.2 g of sample was weighed into 30 mL acid washed glass vials. 12.2 ng of $^{201}HgCl_2$ was added as an internal standard. After addition of 5 mL of concentrated H_2SO_4/HNO_3, the mixture was left to react for one hour at room temperature. Digestion was finished by heating vials in an Al block at 120 ^{0}C on a hot plate for 3 hours or until formation of brown nitrous gases had ceased. The digest was diluted with Milli-Q water to the mark.

The concentration of Hg isotopes in the digest was quantified using continuous-flow cold-vapor generation with ICP/MS detection (Finnigan MAT, Model Element 2). The acidified sample was continuously mixed with a solution of stannous chloride by means of a peristaltic pump. The formed mercury vapor was separated from the liquid in a gas-liquid separator (Model L1-2) and the elemental mercury swept into the plasma of the ICP/MS. The following isotopes of Hg were measured: ^{199}Hg (added isotope for the methylation assay), ^{200}Hg (added isotope for the demethylation assay), ^{201}Hg (internal standard) and ^{202}Hg (to calculate ambient total Hg). Concentrations of individual isotopes were calculated using an excel spreadsheet, employing matrix algebra, as described in Hintelmann and Ogrinc (2003).

Methylmercury Determination

A method modified from Hintelmann and Evans (1997) was used. Approximately 0.2 g of sample was weighed into 30 mL Teflon vials. $CH_3{}^{201}HgCl$ (55 pg) was added as an internal standard. 200µL of H_2SO_4 (9 M) and 500µL of KCl (20%) were added, the vessel placed into a heating block at 140 °C. Methylmercury distilled from the sample under a supporting nitrogen stream (80 mL min^{-1}). Distillation time was approximately 60-90 min per sample.

A reaction vessel was filled with 100 ml Milli-Q water, and the distillate was added for measurement of methylmercury. 0.2 ml of acetate buffer (2 M) was added to adjust the pH to 4.9. Sodium tetraethylborate (100 uL, 1 % w/v) was added and the solution left sitting at room temperature for 20 min for the tetraethylborate to react. Tenax adsorber traps were connected to the reaction vessel and the generated methylethylmercury was purged from the solution using nitrogen (200 mL min^{-1}) and collected on the Tenax trap. Finally, mercury species were

thermally desorbed from the trap (250^{o}C), separated by gas chromatography and quantified by ICP/MS (Micromass Platform). The following isotopes of Hg were measured: ^{199}Hg (methylated Hg), ^{200}Hg (methylmercury demethylation assay), ^{201}Hg (internal standard) and ^{202}Hg (to calculate ambient methylmercury). Peak areas were used for quantification and concentrations of individual isotopes were calculated using an excel spreadsheet, employing matrix algebra, as described in Hintelmann and Ogrinc (2003).

Hg Analysis QA/QC

For each batch of samples the following set of QA/QC samples was measured: 3 reagent blanks (HgT) or bubbler blanks (MeHg) and a certified reference material (IAEA 356 marine sediment and MESS-3 marine estuary sediment for sediment analysis and NIST 1515 apple leaves for plant analysis). Individual distillation yields were determined using the added internal ^{201}Hg isotope standard.

RESULTS AND DISCUSSION

Background Information on Tidal Marsh Structure and Function

A central question arising from the biogeochemical study of mercury is, "How do concentrations of parts per trillion of mercury in water yield concentrations of parts per million in fish?" (Gilmour and Henry, 1991; Morel et al.,1998). To address this question it is important to understand the behavior of mercury in coastal systems in the context of the structure and function of that system. To this end we provide the following synopsis of selected relevant features of tidal marshes in San Francisco Bay.

Importance of Hydrology and Elevation

Coastal wetlands depend upon tides and rainfall for their moisture. Rainfall is usually restricted to the cool season, and freshwater runoff is limited largely to the wet periods. Hence, during most of the warm growing season, the salt marsh vegetation receives water only from the sea. Any alteration of tidal circulation, therefore, has a major effect on the entire wetland ecosystem, both by changing the frequency of wetting and by altering salinities.

Intertidal wetlands exist as a continuum of habitats within coastal and estuarine systems (Callaway, 2001). At HAAF, our experimental site, and China Camp, our reference site, this range of habitats includes subtidal areas, intertidal flats, tidal creeks and channels, salt marsh, and wetland-upland ecotones. In most natural marshes, sedimentation rates are in equilibrium with relative sea-level rise, resulting in a stable elevation of the marsh plain. The marsh plain usually stabilizes at elevations between Mean High Water (MHW) and Mean Higher High Water (MHHW; Allen, 1990; Pethick, 1992; Allen, 1994). The relative elevation of the marsh surface is affected by many factors. In addition to the feedback between elevation and sediment inputs (both tidal and storm inputs), other factors are also linked to elevation via a feedback mechanism. These include biomass production (above- and belowground) and decomposition of the vegetation. Eustatic sea-level rise, subsidence, and tectonic activity affect the relative elevation of the marsh, but without any feedback mechanism.

Tidal Marsh Vegetation Zones

Three general zones of vegetation typically characterize the tidal salt marsh, each of which is related to tidal elevation and distance from shore. Low tidal salt marsh occurs between the lowest margin of the marsh and MHW. Middle tidal marsh occurs between MHW and MHHW. High tidal marsh occurs between MHHW and the highest margin of the marsh. Tidal marshes have a variety of important components including tidal channels. Large tidal channels and their smaller tributaries form drainage networks that distribute tidal waters throughout the marsh. Channel density (i.e., the amount of channel habitat per area of marsh plain) is directly related to tidal prism, the volume of water that flows into and out of the marsh. Channel density may also be related to salinity; salt marshes generally have denser networks of tidal channels than do brackish marshes (Grossinger, 1995).

Spartina foliosa (Pacific cordgrass) and *Salicornia virginica* (common pickleweed) are the dominant higher plant species in the San Francisco Bay tidal salt marshes. Pacific cordgrass is usually the primary colonizer on broad tidal mudflats that fringe tidal marsh plains, and it occurs in virtually pure stands in the low marsh between Mean Tidal Level (MTL) and MHW. Midway within this tidal range it intermixes with *Salicornia virginica* (common pickelweed), especially in the depressions in the marsh plain. In the middle tidal marsh, at elevations near and above MHW, Pacific cordgrass yields to common pickleweed. The latter species is a perennial succulent that dominates around the Bay. In the high tidal marsh, between MHW and the maximum extent of the tides, common pickleweed occurs in association with peripheral halophytes such as *Distichlis spicata* (saltgrass) and *Atriplex triangularis* (fathen). All three zones described occur at both HAAF and China Camp.

Primary production, decomposition, and importance for the food web - Because MeHg is efficiently biomagnified up many aquatic food webs, it is important to study mercury biogeochemistry against the backdrop of wetland trophic structure. Marshes generally have a net primary production rate that is higher than that of any other ecosystem type. In an overview of primary production and biomass estimates for the world, salt marshes are listed as harboring on average a mean biomass of 6.8 kg carbon m^{-2}, and having a net primary production rate of 1125 g carbon m^{-2} yr^{-1} (Schlesinger, 1991). Primary production values published for California salt marsh vegetation vary greatly, between 70 and 2858 g C m^{-2} yr^{-1} (Table 1) depending on the elevation within the marsh, influence of freshwater inputs, climate (latitude) and species composition. Based on the latter production rates, a maximum aboveground biomass production of 715 g DW per year was expected (2858 g C m^{-2} yr^{-1} x 0.25) in natural marshes, and of 996 g DW m^{-2} in multi-species, planted, marshes (Callaway et al., 2003). Inferences as to rates of primary production based on casual observations of standing biomass can be misleading, because of the differences in growth and senescence strategies among vascular macrophyte species, and between algae and vascular macrophytes. For instance, in Mugu Lagoon, CA, primary production of vascular macrophytes in the low marsh was lower than that of epipelic algal mats, while primary production of vascular macrophytes in the high marsh was lower than that of submerged macrophytes, but higher than that of phytoplankton (Onuf, 1987).

Part of the primary production is utilized by macroconsumers directly via herbivory of live plant tissues or indirectly via the detritus pool. The importance of the various primary producers of the marsh for the consumers is strongly influenced by the tissue quality of live and dead plant material, situation within the marsh landscape relative to the sea, creeks and upland area, and the physical-temporal separation between the primary producers and consumers (Table

2; Onuf, 1987; Winfield, 1980). Strong food web linkages were found between macrophytes of the low and high marsh, microalgae of marsh pools, macroalgae from the mid-marsh, and invertebrates, fish, and clapper rails in San Dieguito Lagoon and Tiyuana Bay in southern California, using a multiple stable isotope ratio approach (Table 3; Kwak and Zedler, 1997). At this time a limited number of food web studies has been conducted, but none of these takes biomagnification of MeHg into consideration.

Effects of Macrophytes on Their Rhizospheres

Besides influencing marsh elevation by trapping sediment (see above), marsh plants can change the chemistry in their rhizosphere through physiological processes. These plant-mediated changes can greatly affect the competing mercury methylation and demethylation competing reactions in wetland surface sediments. Proton extrusion by roots may reduce rhizosphere pH (by more than 2 units from that in the bulk sediment). By their reducing and oxidizing activities, roots affect the redox potential in the sediment. Reduction in the rhizosphere is particularly important for the acquisition of iron or other metals when present in their less-mobile oxidized states in the sediment. On the other hand, roots in sediments can oxidize compounds in the rhizosphere, largely by the release of oxygen. This can reduce the solubility of potentially toxic ions like mercury, aluminum and sulfide. Roots often excrete exudates (e.g. organic acids) that mobilize sparingly soluble micronutrients, or stimulate the activity of rhizosphere microorganisms (after Lambers et al.,1998).

Our field observations in salt marshes bordering San Pablo Bay indicated that the redox potential (E_h) was below zero in all sediments (Table 4). In undisturbed compartments (i.e., outside the *in situ* incubated cores), E_h fluctuated between –91 and -202 mV in non-vegetated sediments, between –114 and –222 in epipelon-associated sediments, between –110 and –248 mV in *S. foliosa*-vegetated sediments, and between –127 and –213 mV in *S. virginica*-vegetated sediments. In vegetated sediments fluctuations tended to be larger and showed lower negative extremes than in non-vegetated sediments. Vegetation clearly affected E_h in the sediments of the incubated cores (Fig. 5). E_h tended to be less negative in illuminated vegetated cores than in darkened vegetated cores, particularly at 10 cm depth in the sediment. E_h in non-vegetated cores fluctuated between –99 and -203 mV and did not exhibit this trend. The main difference between the E_h profiles of vegetated and non-vegetated cores appeared to be that E_h was more negative at 2.5 and 5 cm depth (in both light and dark conditions) in the presence than in the absence of vegetation. This suggests a relationship between anoxic decomposition of plant materials at these depths possibly establishing E_h conditions conducive for MeHg production (see section 'Factors controlling MeHg production'). pH values in the surficial sediments of HAAF and China Camp (outside the incubated cores) ranged from 7.0 to 7.5 (Table 4). pH values decreased in incubated cores to 6.6-6.7. Conditions in the sediment with pH 6.6 and E_h ranging from –180 to 0 mV or more positive would favor Hg speciation into Hg^0, while those of pH 6.6 and E_h ranging from –180 to –450 mV would favor Hg speciation into Hg^{2+} (Fig. 6).

Current Levels of THg and MeHg in San Francisco Bay Wetlands

Several studies indicate that wetlands may contain considerable stores of MeHg in both organic matter and pore water (Heyes, 1996), and may serve as source for the water body immediately adjacent to it (St. Louis et al., 1994; 1996). However, although the potential

importance of wetlands as sources of MeHg has been realized, only recently have studies of the internal cycling of Hg or production of MeHg been initiated.

THg and MeHg in Sediment and Plant Portions

A summary of the THg and MeHg concentrations expressed on a dry weight (DW) basis is shown in Table 5. THg concentrations in sediments were variable, but in the same order of magnitude at HAAF and China Camp sites. Mean sediment concentrations ranged from 304 to 407 ng g^{-1} DW. THg concentrations were generally lower in plant material than in sediments, and mean concentrations varied in macrophytes between 18 ng g^{-1} DW (*S. foliosa* stems) and 330 ng g^{-1} DW (*S. virginica* roots), and in epipelon between 288 and 296 ng g^{-1} DW. THg concentrations varied greatly with plant organ, and were higher in roots than in aboveground plant organs.

MeHg concentrations in sediments were also variable, and in the same order of magnitude at HAAF and China Camp. Mean sediment concentrations ranged from 0.79 to 1.80 ng g^{-1} DW, and varied between 0.11 and 2.58 percent THg. MeHg concentrations in the macrophytes usually exceeded those in the sediments in which they rooted, particularly when incubated under ambient irradiance. Mean MeHg concentrations in plant materials varied between 1.08 ng g^{-1} DW in *S. foliosa* stems to 5.59 ng g^{-1} DW in *S. foliosa* roots. Also in this case, concentrations varied greatly with plant organ, and were higher in roots than in aboveground plant organs.

The THg concentrations in plant portions found in this study are high relative to those measured in other studies, but the MeHg concentrations are in the same range as published for other wetlands. Our values are 13-205 ng g^{-1} for THg in aboveground, and 217-297 ng g^{-1} in belowground biomass. MeHg was 0.55-1.64 ng g^{-1} in aboveground and 0.98-5.26 ng g^{-1} in belowground biomass (Table 6). The high THg and MeHg values measured in the stems of *S. foliosa* are probably artifacts due to adhering sediment particles. For comparison we provide mercury levels measured in other wetland plants. Mercury levels in plants from a freshwater wetland in Ontario, Canada, are 22 to 80 THg ng g^{-1} DW and 0.18 to 1.04 ng g^{-1} MeHg DW (Heyes et al., 1998). Plants in Chapman's Marsh salt marsh in New Hampshire are 8 to 34 ng g^{-1} THg DW, and 0.1 to 4 ng g^{-1} MeHg DW (Heller and Weber, 1998).

Light-Dark Comparison

In our study concentrations of THg were higher in aboveground plant organs incubated in light than those incubated in darkness, particularly in the stems. In contrast, the concentrations were similar in roots incubated in the light and in darkness (Table 6). This may indicate transport of THg from roots to shoots is driven by light, possibly by increased evapotranspiration. These results support the recently suggested hypothesis that Hg^0 emissions above cattail and sawgrass vegetation increase with increased evapotranspiration and photosynthesis while emissions were negligible at night (Lindberg et al., 2002; Dong et al. in press).

In the current study, the MeHg concentrations were higher in the aboveground plant organs of *S. foliosa* incubated in light compared to those incubated in darkness. There were no differences in mercury levels in the roots between light and dark incubations in the roots of *S. foliosa*. No difference was seen for *Salicornia virginica*. This may indicate a higher availability of MeHg in the sediment for uptake by *S. foliosa*, or a higher availability of energy in the plant species itself to fuel uptake and root-shoot transport.

Rates of MeHg Production

Rates of Methylation and Demethylation in Sediments of Marsh Zones

The standing pool sizes of MeHg are the difference between the rates of methylation of Hg^{2+} and demethylation of MeHg. We injected a mixture of $^{199}Hg^{2+}$ and $Me^{200}Hg$ into three different sediment horizons and incubated the sediments *in situ*. We assume that $^{199}Hg^{2+}$ and $Me^{200}Hg$ were equally available to the microorganisms in the effected areas of the sediment. This method produces the best data on ratio of rates of methylation to demethylation currently available. However, because the $^{199}Hg^{2+}$ labeled tracer is diluted by the sedimentary pool size of mercury available for methylation, calculations of methylation rates require measures of mercury available for methylation. Since no one knows how to measure the size of the bioavailable mercury pool we assume that the mercury in the sediment, THg, is available for methylation. However, the amount of mercury available for methylation is probably only a fraction of THg, and, therefore, our methylation rates may be considered as 'potential' rates.

Data generated in this study and by others (Hintelmann et al., 2000) have shown that the MeHg standing pool size is very variable with respect to space and time. The first indication of this variability is seen in the relatively large standard deviations around mean MeHg measurements within a given habitat (e.g., Table 6). Since the standard error of this measurement on homogenized HAAF sediment was shown to be less than 5%, the observed standard deviations must represent the actual spatial heterogeneity. These standard deviations may have been reduced by slurrying the root zone sediments, but this would have probably resulted in artificially raising the rates measured. However, our standard deviations were not wider than others recently reported.

The trends in mean rates of ^{199}Hg methylation consistently showed that photosynthetic activity increased the rates of Hg methylation in the root zones of *S. foliosa* and *S. virginica* in HAAF sediment (Table 7, 8). The same trend was seen for the sediment covered by an epipelic mat and sediments containing benthic algae without a visible algal mat cover. This trend was not obvious in China Camp sediments. No clear trend was noticeable in the mean rates of $Me^{200}Hg$ demethylation (Table 8). By recalculation of the methylation and demethylation rates on a dry sediment basis using the appropriate LOI values (Table 5, foot note), it was found that the methylation:demethylation ratio was >1 in all sediments (Table 9). The epipelon-vegetated sediments exhibited the highest ratio and the non-vegetated sediments the lowest ratio. The methylation:demethylation ratios found in this study for non-vegetated sediments are higher than found by Marvin DiPasquale et al. (2003), i.e. 2.45 versus 1.24. This study's methylation: demethylation ratio for vegetated sediments ranges from 2.45 to 7.13, while Marvin DiPasquale et al. (2003) reported a ratio of 3.38.

Sedimentary Microbial Community Biomass

Microorganisms are the agents that are primarily responsible for both the methylation of Hg^{2+} and the demethylation of MeHg. In non-vegetated sediments microbial biomass rapidly decreases with depth. This trend was generally observed at HAAF (Table 10). Epipelic mats at the sediment-water interface resulted in very high biomass. Both epipelon and the macrophytes increased the levels of microbial biomass in the surface sediments when compared to that of the non- vegetated sediment. Penetration of the lower sediments by macrophyte roots supports a dense microbial community to depths of 10 cm. The PLFAME analysis has been shown to give an accurate estimate of the microbial cells present in sediments because it does not require the

cultivation of fastidious environmental microorganisms. Assuming 1 pmole of PLFAME is equivalent to 2.5 x 10^7 microbial cells (Pinkart et al. 2002), these sediments support relatively high microbial population (> 10^9 cells g^{-1} DW).

Sedimentary Microbial Community Composition

Macrophytes not only affected levels and depth distributions of microbial community biomass but also affected the taxonomic composition of the uppermost sediments. The microbial community compositions of all surface sediment samples differed (Fig. 7). The PLFAME profiles of epipelic mats were similar no matter where in HAAF they were collected. They were very different from those from surface sediments vegetated by *S. foliosa* that were in turn very different from those vegetated by *S. virginica*. The PLFAME community profiles of all the deeper sediments (5-10 cm) were similar to each other and most closely resembled those of the non-vegetated sediment. Sulfate-reducing bacteria of the genus *Desulfobacter* contain a unique PLFAME, 10-methyl 16:0 while those of the genus *Desulfovibrio* contain *iso* methyl branched 17:1. The relative abundances of these biomarker PLFAME indicate that *Desulfobacter* biomass was 10 times that of *Desulfovibrio* biomass in almost all sediments examined. *Desulfobacter* methylates Hg^{2+} faster than *Desulfovibrio*. Similar correlations have recently been shown for acid mine drainage-impacted streams in the California Coastal Range (Batten and Scow, 2003).

Factors Controlling MeHg Production

The transfer of a methyl anion (CH_3^-) group to a metal ion is not an easy reaction because CH_3^- is a strong, unstable base in aqueous solution. This reaction may be photochemically driven but this is not seen as a significant environmental reaction mechanism in sediments. Microbial methylation of Hg is probably the main environmental source of MeHg. Microbial methylation of Hg requires the presence of microorganisms capable of catalyzing the reaction, the physiological conditions conducive for active microbial metabolisms, and a biologically available source of Hg.

A large and growing amount of circumstantial evidence has been amassed implicating sulfate-reducing bacteria as the primary agents of the environmental production of methyl mercury. Sulfate-reducing bacteria (SRB) are anaerobes that oxidize a limited range of organic substrates. They use sulfate as a terminal electron acceptor for their respiration and produce sulfide. Molybdate, a specific inhibitor of sulfate respiration, has been repeatedly shown to simultaneously inhibit mercury methylation. *Desulfovibrio desulfuricans* LS is believed to transfer a methyl group originating from serine or the acetyl-CoA synthesis pathway through methyl-tetrahydrofolate and cobalamin to Hg. However, not all SRB methylate Hg. Those that do, do so at very different rates. Marine sediments amended with acetate produced more methyl mercury than those amended with lactate. The SRB that can completely oxidize acetate (e.g., *Desulfobacter*) appear to be more proficient at methylating mercury than the lactate-oxidizing SRB that are unable to use acetate (*Desulfovibrio*). However, there appear to be many exceptions to this generalization. If Hg methylation proved to the SRB an energetic metabolic advantage, then the number of mercury-methylating SRB would be expected to increase to completely exploit the niche.

The availability of reactive Hg species that are available to the methylating SRB may be the rate-limiting factor in the environment. No active transport system for Hg has been demonstrated for the Hg methylating sulfate-reducing bacteria. Membrane diffusion of neutral, lipophilic Hg species is believed to be the way Hg enters SRB. However, a very large number of

Hg species can exist in natural waters and their behavior is complex. $HgCl_2$ (K_{ow} = 3.3) is believed to be an important species for membrane transport in oxic waters (Morel et al. 1998). $HgCl_2$ relative abundance is affected by the levels of chloride ion (salinity). Environmental sulfide levels are probably also a major determinant of the bioavailability of mercury to SRB. Water soluble mercury complexes include HgS^0, $Hg(SH)_2{}^0$, $Hg(SH)^+$, $HgS_2{}^{2+}$ and $HgHS_2^-$ (Benoit et al. 2003). Increasing the sulfide level drives the water chemistry so as to favor the charged mercury - sulfide complexes at the expense of the neutral complexes. This decreases the availability of mercury to SRB and would reduce rates of methylation. This leads to a situation that has been reported in the Everglades. The highest levels of Hg methylation and highest levels of methyl mercury in fish are found associated with sediments showing intermediate levels of sulfate and rates of sulfate reduction. Rates of Hg methylation and levels of methyl mercury in fish are lower in areas where intense sulfate respiration produces levels of sulfide that in turn decrease the availability of Hg to SRB (Benoit et al., 2003).

From this short discussion it can be realized that we have still much to learn about the mechanisms that drive environmental mercury methylation. However, we are in a position to test some hypotheses related to means to engineering means to mitigate methyl mercury production in wetlands.

Initial Answers to Questions Raised at the CALFED Stakeholders' Workshop on Mercury in San Francisco Bay, held 8-9 October 2002 at Moss Point Landing

While the environmental risk posed by the potential transport of mercury from dredged material into the HAAF food web is the immediate concern of this study, the potential cumulative impact of Hg from dredged materials and other sources in the context of the numerous ongoing and proposed wetland restorations on San Francisco Bay is an overarching concern. For both of these ends a mass balance of mercury for the HAAF wetlands would be useful. This section is meant to stimulate thought and identify critical gaps in knowledge of wetland mercury biogeochemistry with respect to physical/biological processes and trophic transfer of mercury from reconstructed wetlands into San Francisco Bay. The numerical values in these processes may change as the assumptions are replaced by measured or calculated values.

What Are the Present Levels of MeHg in SF Bay Wetlands with Respect to Biota, Sub-habitats, and Location Within the Bay?

Mean MeHg concentrations in sediments were in the same order of magnitude at HAAF and China Camp, and ranged from 0.79 to 1.80 ng g^{-1} DW. Mean MeHg concentrations in the macrophytes varied between 1.08 ng g^{-1} DW in *S. foliosa* stems to 5.59 ng g^{-1} DW in *S. foliosa* roots. They usually exceeded those in the sediments in which they rooted, particularly when incubated under ambient irradiance.

Based on the levels of mercury measured in this study we calculated a projection of the levels and distribution of mercury species in the HAAF marsh once it is reconstructed (Table 11). To create this projection we assumed that the 10.6 million cubic yards of dredged material needed to elevate the HAAF site (Phillip Williams and Associates 1998) will contain the same levels of total mercury (THg) and methyl mercury (MeHg) as currently in the HAAF surface sediments, and assumed this will be the primary source of Hg. We realize that this assumption is simplistic. If the source of the dredged material is the geological formation to be excavated for

the expansion of the Oakland Harbor, the level of Hg in this material will be far lower. Sediment trapped by the HAAF wetland as it develops will originate up the North Bay rivers and contain levels of Hg comparable to those currently in North Bay surficial sediments. The amounts and bioavailability for methylation of atmospherically deposited mercury is currently unclear and was considered for this projection.

In 2005, when the dredged material has been deposited into the target area and the initial wetland construction activities have been completed, the total aerial surface of the HAAF wetland will be approximately 203 hectare. The top (0-10 cm) of sediment will weigh 81.2 x 10^6 kg (dry weight), and (based on the above assumption) contain 30.7 kg of THg and 0.145 kg of MeHg (Table 11).

Standing crop values of 1 kg DW m^{-2} for aboveground and 1 kg DW m^{-2} for belowground macrophyte mass have been used for the marsh mass balance estimates (Table 1). S. *foliosa* will initially colonize HAAF and by 2015 occupy 117 hectare and produce a biomass of 2.34 x 10^6 kg dry weight (DW). At this point in time *S. virginica* will have colonized 86 hectare and constitute a biomass of 1.72 x 10^6 kg. The current average levels of mercury in these plants are as follows. *S. foliosa* standing stock will contain 90 ng THg and 2.52 ng MeHg per gram DW. *S. virginica* will contain 135 ng THg and 1.64 ng MeHg per gram DW. Based on present plant tissue levels the year 2015 *S. foliosa* biomass will contain 211 gram of THg and 6 gram of MeHg. Likewise the *S. virginica* biomass will contain approximately 232 gram of THg and 3 gram of MeHg (Table 11). In 2015, only 1.4 percent of the THg and 5.6 percent of the MeHg standing stocks of the system will be in the plant mass, while the remainder resides in the top 0-10 cm sediment layer.

The mass balance of mercury in HAAF during 2055 shown in Table 11 assume little change from the current distributions and levels in sediment and vegetation due to the increase in wetland aerial surface area. This table puts into perspective the mass of THg and MeHg in the surface sediments that is potentially available to the HAAF food web. It shows macrophytic marsh vegetation as a dominant biological presence in the marsh. THg and MeHg contents in macrophytes amount to 2 and 4 percent, respectively, of contents in surficial sediments. Perhaps most significantly, given the role of macrophyte biomass in wetland trophodynamics, it shows that the sediment - plant exposure route is potentially an important route for Hg to enter the wetland food web.

What are the Rates of MeHg Production?

Net MeHg production is the result of methylation and demethylation rates in the sediment. Methylation rates were 1.44 ng MeHg g^{-1} DW per day in non-vegetated sediments of HAAF. Rates were usually higher in vegetated than in non-vegetated sediments. Rates were also usually higher in the light than in darkness. Methylation rates varied with location within the Bay, and were lower at HAAF than at China Camp. Demethylation rates were 0.59 ng MeHg g^{-1} DW per day in non-vegetated sediments. Rates were equal or lower in vegetated sediments. Among all sediments studied, the epipelon-vegetated sediment exhibited the highest potential for net MeHg production, since it had a methylation: demethylation ratio of 12. Bare and *S. foliosa* - vegetated sediment had the lowest ratio, i.e. of 2, while *S. virginica*-vegetated sediment had a ratio of 7.

What Factors Control MeHg Production?

Although a number of plausible mechanisms have been proposed (see discussion above), no data currently exist to support any proposed mechanism. Trends in our data suggest methylation and demethylation rates are higher in the sediment surface layers than in deeper layers. In the surface layers, the microbial biomass is also highest, and the composition of the microbial communities is strongly influenced by the presence/absence of vegetation, and by the vegetating species (epipelon, *S. foliosa*, *S. virginica*). In the surface layer also the largest variations in redox potential due to tidal inundation and plant-sediment interactions occur. We and others will continue to work to find answers to this important question.

Can we Predict the Effects of Wetland Restoration on MeHg Production and Export? Are Some Wetlands Larger Mercury Exporters than Others?

HAAF- After placing the dredged material into the HAAF and breaching the dike, suspended sediments from the bay will enter HAAF. HAAF must be structured to trap sediments if the saltmarsh is to become sustainable. During the initial 10 years (2005-2015), the marsh plain will be composed largely by non-vegetated sediment (Phillip Williams and Associates, 1996). This sediment will be exposed to regular tides at elevations below MHW. Sediments at higher elevations will be wetted only by higher tides and storms. During this period these elevations will be primarily vegetated by epipelon that can greatly affect the cycling of Hg and MeHg in and export from the wetland. We have found that the ratio methylation:demethyation in epipelon-vegetated sediments are far higher than of bare and macrophyte-vegetated sediments (Table 9). A high net MeHg production would be expected and these high food quality algal mats would probably be associated with efficient MeHg trophic transfer. However, at present we lack data on the biomass of epipelon per m^2 basis and efficiency of trophic transfer. We are not able to estimate how large the epipelon-vegetated part will be, and, therefore, we did not use these values in our projections.

To identify gaps in our knowledge required to produce useful estimates of MeHg export from saltmarshes we have made initial estimates of MeHg export from HAAF noting the assumptions required to make this estimate. If we assume that the entire HAAF will be intertidal and non-vegetated, and that the tides will export 0.8 percent of the net MeHg (Brannon et al. 1980) produced in the upper 5 cm of the sediment to the Bay per year, a potential net export of 101 g MeHg per year is calculated (Table 12). Storms are expected to increase the amounts of THg and MeHg exported into the Bay, since sediments will be contacted to greater depths than 5 cm by waves. The 0.8 percent value is obviously a critical value that must be validated with HAAF sediment. Additionally, we have not yet measured mercury volatilization from HAAF sediment and vegetation but it is expected to be a quantitatively significant process. Volatilization was recently measured above the vegetation in the freshwater wetlands in the Everglades and amounted to 1-2 ng THg m^{-2} h^{-1} during daylight hours (Lindberg et al. 2002). Based on these values, volatilization in a system of the HAAF size would be 89 g THg per year. This amount would be in the same order of magnitude as MeHg predicted to be flushed from HAAF in tidal waters.

Succession of macrophytic communities in HAAF is predicted to result in a *S. virginica* dominated system in 2055. The vegetation contributes via three different routes to the export of MeHg from the wetland. First of all, the standing biomass will contribute daily relatively small amounts of THg and MeHg to the export by leaching processes. These amounts are expected to be at least 10 percent of the internal THg and MeHg concentrations in the aboveground plant

material per day, values commonly published for nutrients. Far higher values for Hg-leaching have been found for another plant species commonly found in saltmarshes, *S. alterniflora* (Windham et al., 2001). Based on the 10 percent leaching values, leaching amounts of 0.029 g THg/d and 0.00015 MeHg/d are expected. However, since it is not clear if these amounts are available for export or directly re-absorbed by the vegetation upon reaching the sediment, these amounts have not been included in our current export estimates. Secondly, large part of the plant biomass will scenesce, and almost all aboveground plant litter of *S. foliosa* will be exported into the Bay during storms in winter and spring. Scenescence and decomposition of *S. virginica* will be a more gradual, but continuous process throughout the year. The contribution of the vegetation to the MeHg export from the marsh via decomposition processes would amount to 4.36 g MeHg per year in 2015 and 2055 (Table 12). Thirdly, volatilization of THg from the vegetation is expected. Volatilization was not measured in *S. foliosa* and *S. virginica*, and, therefore, better estimates than indicated above cannot be made at this time.

Our current goal is to identify the key processes and values required to make useful estimates of MeHg export and provide initial estimates only for this purpose. These initial estimates are not intended to be used as quantitative values. From our estimates on MeHg standing stocks and potential export from a restored HAAF wetland, it is obvious that values of net MeHg production in surficial sediments are crucial. Aside from the values provided herein, little other data are available. However, one recent study reports values on methylation, demethylation rates, and ratio's measured in surficial bay sediments and in one marsh site, obtained using the less sensitive ^{14}C-method (Marvin DiPasquale et al. 2003). If we use the latter values, the estimates of annual potential MeHg export would change significantly, from 3 g MeHg for a non-vegetated HAAF to 405 g MeHg for a vegetated HAAF (Table 13). The latter export would be 2.8 times higher than projected when the values generated by our study would be used. Reasons for the differences in methylation, demethylation rates and methylation:demethylation ratio's in our study and in the Marvin DiPasquale et al. study may be the following. We used a more sensitive stable isotope approach than the radioactive isotope approach used by Marvin DiPasquale et al., and our methylation rates are above our method-detection level, while the methylation rates measured by Marvin DiPasquale et al. in Bay sediments are below their, higher, detection level. The non-vegetated Bay sediments assayed by us originate from the marsh currently bordering the HAAF that are richer in organic matter and have a higher LOI than the Bay sediments assayed by Marvin DiPasquale et al., possibly causing higher methylation rates. This comparison demonstrates the sensitivity of this value to MeHg export projections.

Potential Export of MeHg from Restoration of Whole Target Salt Marsh Area in San Pablo Bay-

Large uncertainties in projections of MeHg export from HAAF will be multiplied when calculating total MeHg exports from all salt marshes bordering San Pablo Bay. In spite of these uncertainties it is still useful to perform these calculations for the purpose of identifying key variables and initial attempts to delimit the solution space. Recommendations for salt marsh restoration in the San Pablo Bay (Goals Project 1999) include the restoration of salt marshes from a total area of 16,200 ha in 2005 to 42,525 ha in the future while keeping an open water area in the Bay of 102,870 ha intact. Our net MeHg production rates of non-vegetated HAAF sediments are not an order of magnitude different from those measured by DiPasquale et al in open water San Pablo Bay sediments. With all else being equal one would expect that a 42

percent increase in aerial surface area of wet estuarine sediment would result in a 42 percent increase in the aerial production of MeHg in San Pablo Bay. In this context it is critically important to determine what part of the net MeHg production in bordering salt marshes is exported into San Pablo Bay in a manner that impacts the food web. If one chooses to assume that only 0.8 percent of the net MeHg production in the top 0-5 cm of sediment is exported to the Bay with out-flowing tides and all of the MeHg produced in the open Bay sediments impacts the food web, then 42,525 ha. of restored wetland would contribute only 0.6 percent of San Pablo Bay MeHg. This estimate does not include a trophic transfer link and is simplistic.

In this context comprehensive information on the spatial sedimentary distribution of net MeHg rates in San Pablo Bay is needed. The impact on the trophic system of 1 mole of MeHg produced in open water sediment relative to 1 mole produced in a bordering salt marsh must be determined. This will require analysis of volatilization of mercury from wetlands because it has been shown to be a major route of export from other wetland systems (Lindberg et al., 2002).

POINT OF CONTACT CHAPTER 1:

Elly P.H. Best
U.S. Army U.S. Army Engineer Research and Development Center,
Environmental Laboratory, Vicksburg, Mississippi, USA
Ph: 601-634-4246; Email: elly.p.best@erdc.usace.army.mil

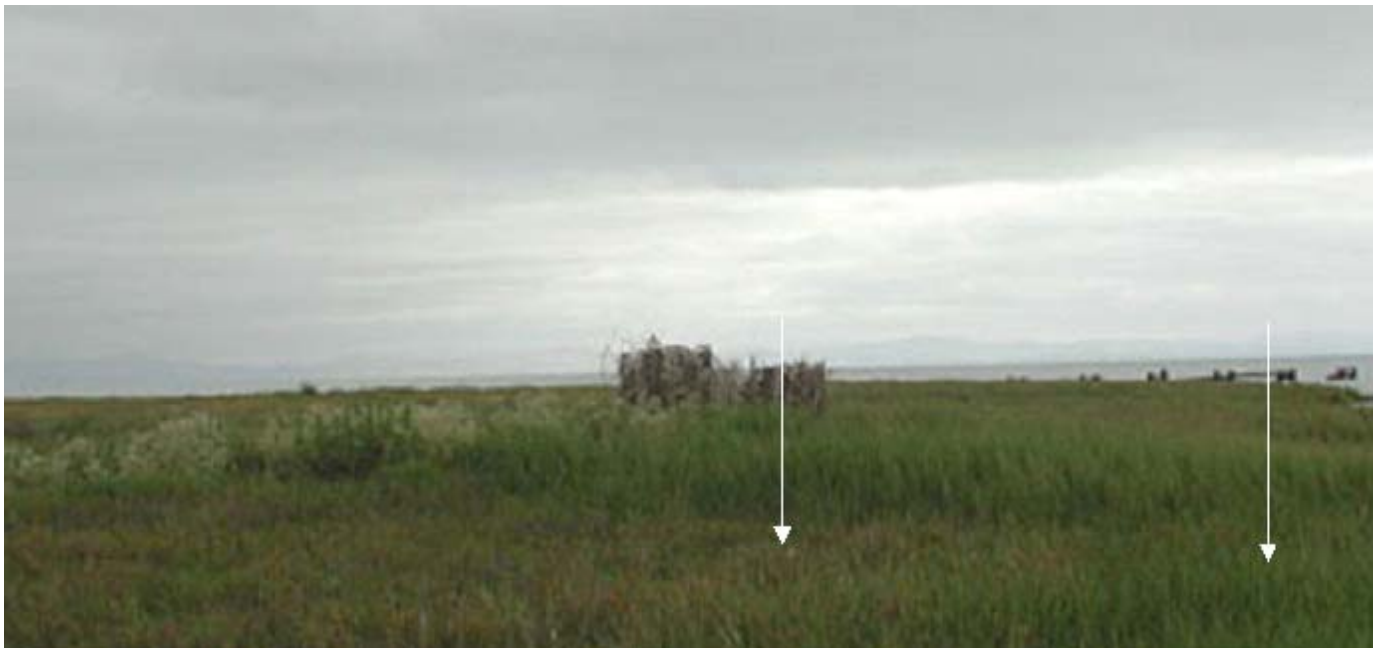

Figure 1. Study site at the Hamilton Air Field Wetlands restoration site. Location where the measurements were performed marked by arrows.

Figure 2. Sediment corer constructed to collect 9.5-cm-diameter vegetated sediment cores.

Figure 3. Administering isotopes to sediment cores and epipelon suspensions.

Figure 4. Incubation of vegetated cores in light and in darkness (upper); and on-site determinations of redox potential and pH (lower).

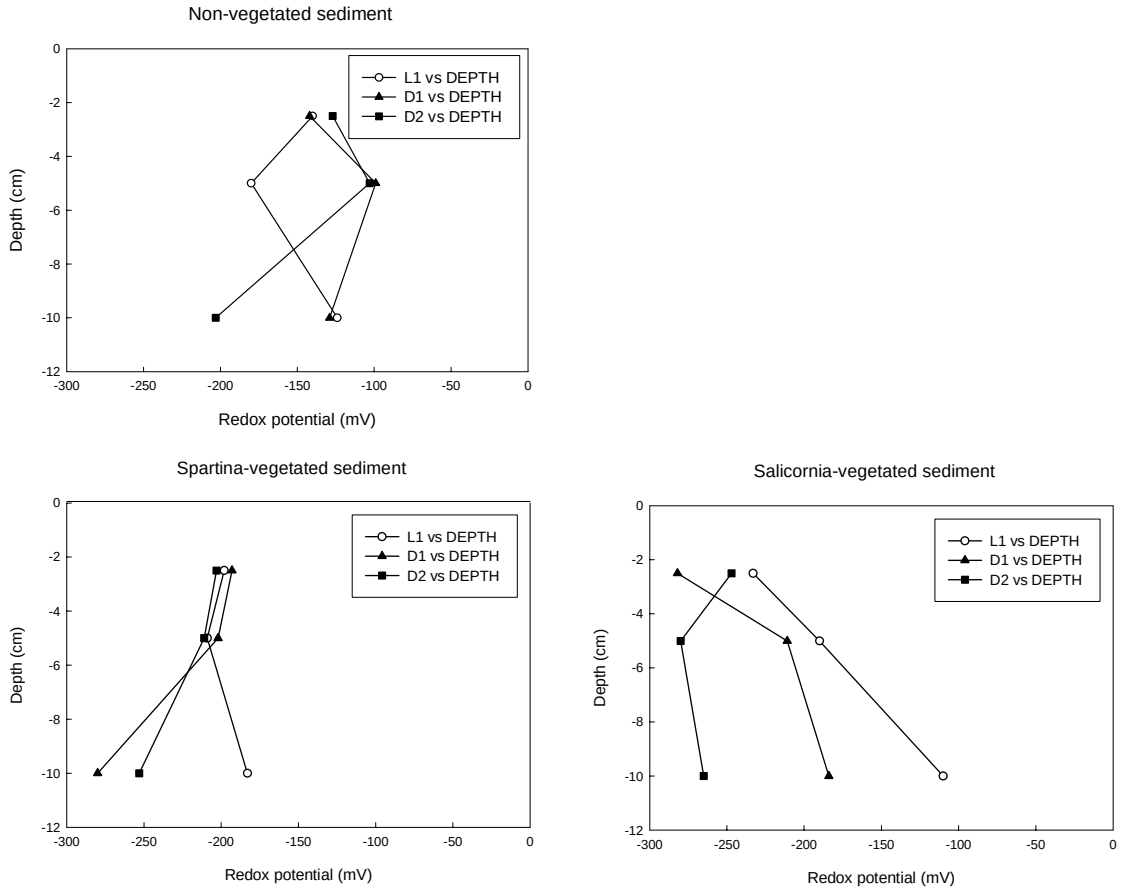

Figure 5. Depth profiles of redox potential in non-vegetated and vegetated sediment cores incubated in situ at HAAF in light (L) and in darkness (D).

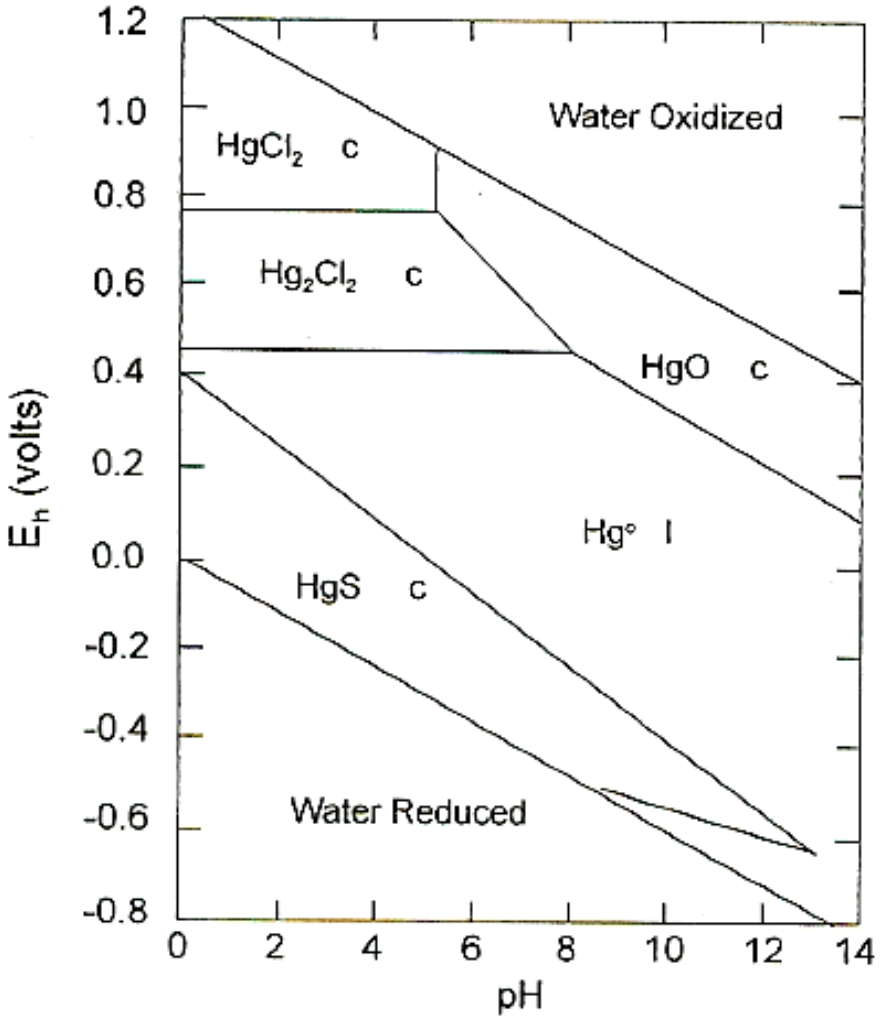

Figure 6. Abiotic conditions determining the various speciations of mercury.

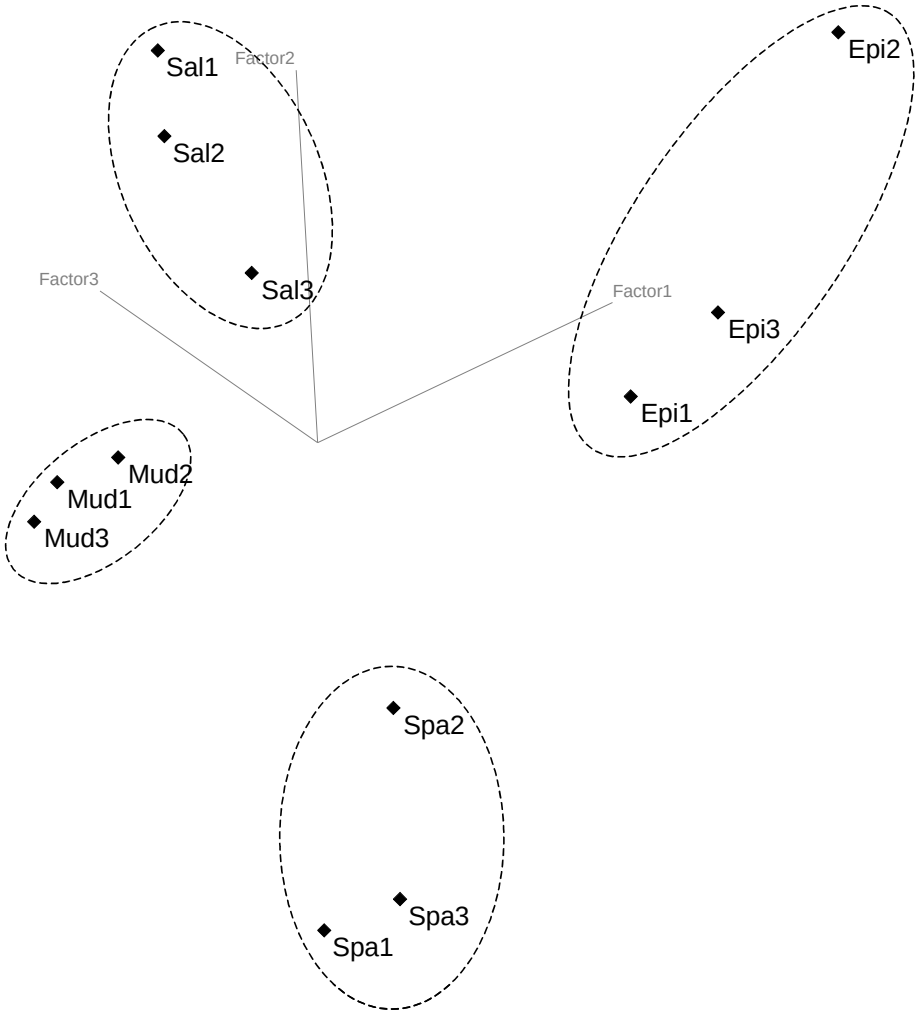

Figure 7. Principal Component Analysis reveals groupings among triplicate samples of top layers of sediment cores from the indicated vegetative zones. The axes of the plot are the first three principal component factors.

Table 1. Estimated rates of primary production in California marshes

Primary producer	Net primary production ($g\ C\ m^{-2}\ y^{-1}$)	Net primary production ($g\ DW\ m^{-2}\ y^{-1}$)	Maximum standing crop ($g\ DW\ m^{-2}$)	Reference
Marsh vegetation[1]				
Low marsh, 6-species			995.6	Callaway et al., 2003
Low marsh, 1-species			572.1	Callaway et al., 2003
Marsh vegetation[2]				
Low marsh	916-935			Zedler et al., 1980
High marsh	412-1046			Zedler et al., 1980
Low marsh[3]	2,858			Zedler et al., 1980
High marsh[3]	1,202			Zedler et al., 1980
Low marsh	70[3]	290		Onuf, 1987
High marsh	180[3]	730		Onuf, 1987
S. virginica			200-800	Onuf , 1987
Epipelic algae	130			Onuf, 1987
Submerged macrophytes	1300			Onuf, 1987
Phytoplankton	50			Onuf, 1987

[1] Planted; aboveground parts only
[2] Predominated by *Salicornia virginica*; aboveground parts only
[3] With freshwater input
[4] 1 g C ~ 0.25 g DW

Table 2. Factors reducing the utilization of a source of primary production by macroconsumers within a California coastal system (Mugu Lagoon; after Onuf 1987).

Factor	Phytoplankton	Epipelon	Submerged macrophytes	Emergent macrophytes
Live tissue nutritional quality	High	High	Moderate	Low
Leaching of live plant	High	Moderate	Moderate	Low
Leaching of dead plant	Very high	Very high	Moderate	Moderate
Export to coastal water	Moderate	Moderate	High	High
Export to upland	None	Slight	Slight	Moderate
Physical/temporal separation – Primary producer/consumer	None	None	Small	Large

Table 3. Multiple stable isotope ratios (pro mille) of primary producers and consumers collected from two California coastal wetlands. Three stable isotopes were used: carbon, nitrogen and sulfur (Tijuana Estuary and San Dieguito Lagoon; after Kwak and Zedler 1997). Mean values and standard errors. Information on biomagnification of THg and MeHg in food webs of Californian salt marshes is currently to be determined (TBD).

Species	Marsh Habitat	$\delta^{13}C \pm SD$	$\delta^{13}C \pm SD$	$\delta^{13}C \pm SD$	THg ± SD	MeHg ± SD
Primary producers						
Macrophytes						
Spartina foliosa	Low marsh	-15.1 ± 0.2	10.3 ± 0.3	11.5 ± 0.5	TBD	TBD
Salicornia virginica	High marsh	-26.7 ± 0.2	11.0 ± 1.2	12.3 ± 2.2	TBD	TBD
Microalgae						
Microcystis sp.	Marsh pool	-17.7	5.1	9.5	TBD	TBD
Macroalgae						
Rhizoclonium sp.	Mid marsh	-20.2	9.6	17.5	TBD	TBD
Consumers						
Birds						
L-F Clapper rail	Low marsh	-18.4 ± 0.2	17.9 ± 0.1	14.6 ± 1.2	TBD	TBD
Fish						
Arrow goby	Channel	-18.4 ± 0.2	17.9 ± 0.1	14.6 ± 1.2	TBD	TBD
Striped mullet	Channel	-16.1 ± 0.2	16.0 ± 0.2	7.4 ± 0.2	TBD	TBD
Invertebrates						
Mytilus edulis	Channel	-18.0	10.0	13.7	TBD	TBD
Orchestia traskiana	Mid marsh	-21.5	11.5	14.1	TBD	TBD

Table 4. Depth profiles of in situ redox potential, measured just outside the incubated cores. Mean values (SD; N=3), unless stated otherwise.

Marsh compartment	HAAF		China Camp	
	E_h (mV)	pH	E_h (mV)	pH
Non-vegetated sediment				
-2.5 cm	-114 (8)	7.1 (0)	-91	7.5
-5 cm	-202 (74)		-127	
-10 cm	-125 (1)		-112	
Epipelon-vegetated sediment				
-2.5 cm	-222	7.0	-114 (0)	7.0
Spartina root zone sediment				
-2.5 cm	-245 (48)	7.1 (0.3)	-248	7.0
-5 cm	-192 (68)		-104	
-10 cm	-242 (59)		-110	
Salicornia root zone sediment				
-2.5 cm	-183 (58)	7.1 (0.3)	-156	7.1
-5 cm	-127 (20)		-127	
-10 cm	-217 (93)		-144	

Table 5. Total Hg and MeHg levels in two existing tidal marshes bordering San Francisco Bay, in sediment, epipelic algae and marsh vegetation. Mean values (SD; sediment, N=9; roots, N≥1; stems, N≥1; leaves, N=3).

Marsh compartment	HAAF		China Camp	
	THg (ng g^{-1} DW)	MeHg (ng g^{-1} DW)	THg (ng g^{-1} DW)	MeHg (ng g^{-1} DW)
Non-vegetated sediment	378(89)	1.78(1.80)	327(17)	1.56(1.12)
Epipelon	296(51)	1.27(0.25)	288(12)	7.42(3.72)
Spartina foliosa				
Sediment	407(30)	1.35(1.42)	371(59)	2.22(1.29)
Roots (light)	260(62)	4.24(0.54)	175(32)	5.59(3.75)
Stems (light)	28(-)	2.65(-)	18(-)	1.08(-)
Leaves (light)	17(10)	0.68(0.36)	39(25)	0.90(0.35)
Salicornia virginica				
Sediment	314(42)	1.11(0.79)	304(36)	2.39(1.68)
Roots (light)	330(170)	3.03(1.22)	123(-)	2.28(-)
Stems (light)	114(-)	1.28(-)	203(-)	1.29(-)
Leaves (light)	24(12)	1.01(0.58)	18(5)	0.95(0.24)

Note: In HAAF, of the non-vegetated sediments, solids concentrations were 36.9% and loss on ignition (LOI) 19.6%; of the vegetated sediments, solids concentrations were 43.8% and LOI 16.4%.

Table 6. Total Hg and MeHg levels in sediment and marsh vegetation after 5-hour incubation in ambient light conditions and in darkness. Mean values (SD; sediment, N=18; roots, N≥4; stems, N≥1; leaves, N≥2).

Marsh compartment	THg ($ng\ g^{-1}$ DW)		MeHg ($ng\ g^{-1}$ DW)	
	Light	Dark	Light	Dark
Spartina foliosa				
Sediment	389 (49)	380(55)	1.79(1.39)	1.63(1.29)
Roots	217(64)	224(81)	4.92(2.51)	5.26(1.71)
Stems	205(-)	25(6)	4.75(-)	1.64(0.87)
Leaves	28(21)	13(6)	0.79(0.34)	0.55(0.24)
Salicornia virginica				
Sediment	310(38)	304(37)	1.75(1.44)	1.18(0.87)
Roots	278(173)	297(56)	2.84(1.06)	3.46(2.24)
Stems	158(62)	54(30)	1.28(0.01)	1.20(0.41)
Leaves	21(9)	38(20)	0.98(0.40)	1.02(0.19)

Table 7. Rates of methylmercury accumulation and methylation in non-vegetated and vegetated sediment in two existing tidal marshes. Mean values (SD; N=9).

Sediment	HAAF				China Camp			
	$Me^{199}Hg$ Accumulation rate (ng g^{-1}DW/12 hr)		Methylation rate (%Hg^{2+}/12 hr)		$Me^{199}Hg$ Accumulation rate (ng g^{-1}DW/12 hr)		Methylation rate (%Hg^{2+}/12 hr)	
	Light	Darkness	Light	Darkness				
Non-vegetated sediment	0.21(0.19)	0.13(0.10)	0.25(0.27)	0.12(0.09)	3.73(2.69)	4.97(4.39)	1.12(0.79)	1.43(1.13)
Epipelon-vegetated sediment	NA	NA	0.75(0.30)	0.54(0.13)	NA	NA	4.61(2.95)	6.07(1.70)
Spartina root zone sediment	0.26(0.33)	0.10(0.14)	0.22(0.28)	0.13(0.15)	0.19(0.12)	0.12(0.11)	0.23(0.16)	0.20(0.11)
Salicornia root zone sediment	0.30(0.30)	0.14(0.06)	0.36(0.21)	0.22(0.10)	0.10(0.07)	0.11(0.04)	0.23(0.09)	0.20(0.07)

Abbreviations: NA, not applicable.

Table 8. Rates of daily MeHg degradation rates in non-vegetated and vegetated sediment in two existing tidal marshes, in % $Me^{200}Hg$ degraded per day. Mean values (SD; sediment, N=9; epipelon-vegetated sediment, N=3).

Sediment	HAAF		China Camp	
	MeHg degradation rate (%$Me^{200}Hg$ degraded/day)		MeHg degradation rate (%$Me^{200}Hg$ degraded/day)	
	Light	Darkness	Light	Darkness
Non-vegetated sediment	37(22)	28(15)	26(37)	28(31)
Epipelon-vegetated sediment	35(6)	15(22)	71(18)	80(19)
Spartina root zone sediment	35(25)	52(25)	38(31)	43(31)
Salicornia root zone sediment	26(19)	19(13)	38(38)	31(22)

Table 9. Rates of methylation, demethylation, and methylation : demethylation ratio in the sediment of the existing marsh bordering the HAAF.

Sediment	THg [1]	MeHg [1]	Methylation rate [2,3]		Demethylation rate [4,5]		Meth.: Demeth. ratio
	(ng g^{-1} DW)	(ng g^{-1} DW)	(% Hg^{2+} per 12-h)	(ng g^{-1} DW per d)	(%$Me^{200}Hg$ degr. per d)	(ng g^{-1} DW per d)	
Non-vegetated sediment	378	1.78	0.19	1.44	33	0.59	2.45
Epipelon-vegetated sediment	296	1.27	0.65	3.85	25	0.32	12.12
Spartina root zone sediment	407	1.35	0.18	1.47	44	0.59	2.47
Salicornia root zone sediment	314	1.11	0.29	1.82	23	0.26	7.13

Note: [1], Mean light values HAAF (Table 6); [2], Average light and dark values HAAF (Table 7); [3], Based on the assumption that microbes use isotopic Hg^{2+} the same way as THg; [4], Average light and dark values HAAF (Table 8); [5], Based on the assumption that microbes use isotopic MeHg the same way as MeHg.

Table 10. Total microbial biomass in sediments, for which polar lipid fatty acids methyl ester (PLFAME) content is taken as a measure. Mean values (SD; N=3).

Sediment	Microbial biomass (pmole PLFAME g^{-1} DW)	
	HAAF	China Camp
Non-vegetated sediment		
-2.5 cm	4,022 (185)	22,884 (770)
-5 cm	2,564 (124)	14,333 (454)
-10 cm	2,172 (715)	20,609 (596)
Epipelon-vegetated sediment		
-2.5 cm	25,965 (382)	35,367 (639)
-5 cm	6,253 (-)	8,846 (-)
Spartina root zone sediment		
-2.5 cm	18,394 (217)	19,762 (838)
-5 cm	7,119 (174)	7,980 (127)
-10 cm	6,874 (-)	ND
Salicornia root zone sediment		
-2.5 cm	18,577 (328)	22,102 (338)
-5 cm	9,385 (201)	31,932 (993)
-10 cm	7,994 (348)	20,001 (772)

Note: ND, not determined

Table 11. Estimated mercury and methylmercury standing stocks of tidal marsh areas in the restored HAAF.

Compartment	Area HAAF	THg	MeHg	Mass	Mass	THg	THg	MeHg	MeHg
	(ha)	(ng g^{-1} DW)	(ng g^{-1} DW)	(kg DW ha^{-1})	(kg DW)	(g)	(% system)	(g)	(% system)
Year 2005									
Sediment (0->10 cm)[1]	203	378	1.78	400,000	$81.2x10^6$	30,693.6	100	144.5	100
Spartina veg.[1]		90	2.52	20,000	0	0	0		0
Salicornia veg.[1]		135	1.64	20,000	0	0	0		0
Total	203					30,693.6		144.5	
Year 2015									
Sediment (0->10 cm)[1]	203	378	1.78	400,000	$81.2x10^6$	30,693.6	98.6	144.5	94.3
Spartina veg.[1]	117	90	2.52	20,000	$2.34x10^6$	210.6	0.68	5.9	3.8
Salicornia veg.[1]	86	135	1.64	20,000	$1.72x10^6$	232.2	0.75	2.8	1.8
Total	203					31,136.4		153.3	
Year 2055									
Sediment (0->10 cm)[1]	203	378	1.78	400,000	$812x10^6$	30,693.6	98.2	144.5	95.6
Spartina veg.[1]	0	90	2.52	20,000	0	0	0	0	0
Salicornia veg.[1]	203	135	1.64	20,000	$4.06x10^6$	548.1	1.75	6.7	4.4
Total	203					31,241.7		151.2	

Note: [1], Sediment, average value Table 5. The following estimates have been used for dry mass contained in surficial sediment layers: 0-5-cm: 40 kg dry sediment m^{-2}; 0-10-cm: 20 kg dry sediment m^{-2}. Vegetation, average above- and belowground biomass Table 5; maximum standing crop 2 kg DW m^{-2}.

Table 12. Estimated potential methylmercury export of tidal marsh areas in the restored HAAF, using values this study.

Compartment	Area HAAF	Total mass	Methylation Rate[1]	Demethylation Rate[1]	Net MeHg Production Rate	Net MeHg Production Rate	MeHg Plant Decomp. Rate[3]	Total MeHg Potential Export to Bay
	(ha)	(kg DW)	(μg/kg DW/d)	(μg/kg DW/d)	(μg/kg DW/d)	(g/system/y)	(g/system/y)	(g/system/y)
Year 2005								
Sediment (0->5 cm)	203	40.6×10^6	1.436	0.587	0.849	12,581	0	
Potential export[2]						101	0	101
Year 2015								
Sediment (0->5 cm)	0	0	1.436	0.587	0.849	0		
Spartina-veg.sed.	117	23.4×10^6	1.465	0.594	0.871	7,441		
Salicornia-veg.sed.	86	17.2×10^6	1.821	0.255	1.566	9,831		
Spartina-veg.	117	2.34×10^6					2.95	
Salicornia-veg.	86	1.72×10^6					1.41	
Potential export[2]						138.6	4.36	143
Year 2055								
Sediment (0->5 cm)	0		1.436	0.587	0.849	0		
Spartina-veg.sed.	0		1.465	0.594	0.871	0		
Salicornia-veg.sed.	203	40.6×10^6	1.821	0.255	1.566	23,205		
Spartina-veg.	0						0	
Salicornia-veg.	203	4.06×10^6					4.36	
Potential export[2]						185.6	4.36	190

Note: [1], Data Table 9; [2], Export from surficial sediments estimated at 0.8% of net MeHg production per day. This estimate is derived as follows: the water-exchangeable fraction of THg is 0.35% (Brannon et al. 1980). MeHg is slightly more water-soluble than THg, i.e. 0.40%. MeHg is exposed two times per day to tidal waters; [3], Assumed that all aboveground standing crop of 1 kg DW m^{-2} senesces per year, and MeHg concentrations Table 11.

Table 13. Estimated potential methylmercury export of tidal marsh areas in the restored HAAF, using values Marvin Dipasquale 2003 for methylation and demethylation rates.

Compartment	Area HAAF	Total mass	Methylation Rate[1]	Demethylation Rate[1]	Net MeHg Production Rate	Net MeHg Production Rate	MeHg Plant Decomp. Rate[3]	Total MeHg Potential Export
	(ha)	(kg DW)	(μg/kg DW/d)	(μg/kg DW/d)	(μg/kg DW/d)	(g/system/y)	(g/system/y)	(g/system/y)
Year 2005								
Sediment (0->5 cm)	203	40.6×10^6	0.108	0.087	0.021	311.199	0	
Potential export[2]						2.5	0	2.5
Year 2015								
Sediment (0->5 cm)	0	0	1.44	0.087	0.021	0		
Spartina-veg.sed.	117	23.4×10^6	1.47	1.442	3.382	28,886		
Salicornia-veg.sed.	86	17.2×10^6	1.82	1.442	3.382	21,232		
Spartina-veg.	117	2.34×10^6					2.95	
Salicornia-veg.	86	1.72×10^6					1.41	
Potential export[2]						400.6	4.36	405
Year 2055								
Sediment (0->5 cm)	0		1.44	0.087	0.021	0		
Spartina-veg.sed.	0		1.47	1.442	3.382	0		
Salicornia-veg.sed.	203	40.6×10^6	1.82	1.442	3.382	50,118		
Spartina-veg.	0						0	
Salicornia-veg.	203	4.06×10^6					4.36	
Potential export[2]						400.6	4.36	405

Note: [1], Data Table 9; [2], Export from surficial sediments estimated at 0.8% of net MeHg production per day. This estimate is derived as follows: the water-exchangeable fraction of THg is 0.35% (Brannon et al. 1980). MeHg is slightly more water-soluble than THg, i.e. 0.40%. MeHg is exposed two times per day to tidal waters; [3], Assumed that all aboveground standing crop of 1 kg DW m^{-2} senesces per year, and MeHg concentrations Table 11.

Table 14. Estimated potential methylmercury production and export from tidal marsh areas in San Pablo Bay. Open water and salt marsh areas according to Goals Project (1999).

Compartment	Area	Mass	Mass	Net MeHg Production Rate	Net MeHg Production Rate	MeHg Plant Decomp. Rate	Total MeHg Potential Export	Export/ Production Bay
	(ha)	(kg DW/ha)	(kg DW)	(μg/kg DW/d)	(g/system/y)	(g/system/y)	(g/system/y)	
Year 2005								
Bay	102,870	200,000	$20{,}574 \times 10^6$	0.849	6,375,574			
Tidal marsh veg-sed.[1]	16,200	200,000	$3{,}240 \times 10^6$	1,566	1,851,952			
Tidal marsh-veg.[1]	16,200	20,000	324×10^6			348		
Tidal marsh export[1]							15,163	0.002
Total Baylands	119,070							
Target for future								
Bay	102,870	200,000	$20{,}574 \times 10^6$	0.849	6,375,574			
Tidal marsh veg-sed.[1]	42,525	200,000	$8{,}505 \times 10^6$	1,566	4,861,373			
Tidal marsh-veg.[1]	42,525	20,000	850.5×10^6			913		
Tidal marsh export[1]							39,804	0.006
Total Baylands	145,395							

Note: [1], Based on estimates for HAAF anno 2055, colonized completely by *S. virginica* (Table 1)

2- Spatial Distribution and Concentrations of Mercury Species in the Vegetated Marsh Zones of Salt Marshes Bordering the HAAF Wetland Restoration Site

SUMMARY

The purpose of this study was to determine a tentative relationship between marsh zones and THg and MeHg levels in the sediments, and assess the THg and MeHg concentrations in live and dead plant materials collected from these zones.

For this, a tentative relationship between marsh zonation and THg or MeHg concentrations in the sediment was explored by regrouping previously collected data on mercury species concentrations in surficial sediment cores according to vegetation zone, and calculating mean values for each zone. Furthermore, tissues from live plant shoots and of plant detritus were collected from as many zones as possible, and analyzed for mercury species. The following zones were distinguished: non-vegetated mudflats, *S. foliosa*-vegetated tidal marsh, *S. virginica*-vegetated upper marsh, and upland-seasonally flooded wetland.

The THg and MeHg levels in the surficial sediments of the marsh zones varied by zone. The mean THg concentrations in the surface sediments decreased in the order Low marsh>High marsh>Diked high marsh>Mudflat. No distinct effect of dry and wet season on THg concentration was noted. Mean THg concentrations, in ng g^{-1} DW, in the dry season were: Low marsh 346, High marsh 292, Diked high marsh 261, Mudflat 236.

Mean MeHg concentrations increased in the sediments of all zones during the wet season except in the mudflats. Mean MeHg concentrations, in ng g^{-1} DW, decreased in the order High marsh 7.29 >Low marsh 5.17 > Diked high marsh 1.82 > Mudflat 0.73.

In plant shoots, the mean concentrations of THg ranged from 14 to 25 ng g^{-1} DW, and of MeHg from 0.17 to 0.96 ng g^{-1} DW in *S. foliosa* and *S. virginica*. THg and MeHg levels in the plant shoots did not appear to be related to species or zone, but the number of locations sampled was low. The THg and MeHg levels in plant detritus were far higher than in live shoots, i.e., a factor of 5 to 8.

INTRODUCTION

Methylmercury (MeHg) is a concern in many wetland and aquatic systems. In a field survey of existing wetlands in the San Francisco Bay/Estuary system (Lee et al., 2000) found Hg accumulation in *Spartina foliosa*, *Salicornia virginica*, and other plant species in marine, estuarine and freshwater wetlands, suggesting that plants play a role in the cycling of Hg in

wetlands. Recent studies on the relationships between microbial assemblages and their interactions with saltmarsh plants have shown that MeHg concentrations in the rhizosphere of *Spartina alterniflora* can be lower than in the ambient sediments (King et al., 2001). In another recent study on Hg and MeHg cycling in freshwater floodplain margins, low MeHg concentrations (<0.5 ng $g^{-1,}$ i.e., <1% THg) were found in lake sediments, but far higher concentrations in the humic layer covering the sediments of the lake margins (Roulet et al., 2001). Maximum MeHg concentrations of 3-8 ng g^{-1}, or 2-5% of THg, occurred in the litter and organic layers of the inundated forest soils. Based on these results it was suggested that MeHg concentrations increase with organic carbon concentration. In a study on the effects of forest canopy on THg and MeHg fluxes in upland and wetland ecosystems in Ontario, Canada, the flux of THg and MeHg with litterfall was found to be substantial compared to throughfall and direct wet deposition, and it was suggested that the Hg in litterfall was derived from uptake from soil or directly by foliage (St. Louis et al., 2001).

The impacts of marsh plant communities on the production of MeHg in their rhizospheres, and the roles of these plant communities in the cycling of THg and MeHg in the marsh have to be quantified to serve as a basis for a management plan aimed at minimizing MeHg production in the wetland system.

PURPOSE

The purpose of this study was to determine a tentative relationship between marsh zones, non-vegetated and vegetated by dominant plant communities of salt marshes bordering the Hamilton Army Airfield (HAAF) Wetland Restoration Site (WRS) and THg and MeHg levels in the sediments, and assess the THg and MeHg concentrations in live and dead plant materials collected from these zones.

For this, a tentative relationship between marsh zonation and THg or MeHg concentrations in the sediment was explored by regrouping previously collected data on mercury species concentrations in surficial sediment cores according to vegetation zone, and calculating mean values for each zone. Furthermore, tissues from live plant shoots and of plant detritus were collected from as many zones as possible, and analyzed for mercury species. The following zones were distinguished: non-vegetated mudflats, *S. foliosa*-vegetated tidal marsh, *S. virginica*-vegetated upper marsh, and upland-seasonally flooded wetland.

METHODS AND MATERIALS

Regrouping of Previously Collected Sediment Core Data

Previously collected data on THg and MeHg concentrations in surficial sediment cores (McFarland et al., 2001; McFarland et al., 2003) were regrouped according to the vegetation zones distinguished for the entire study, and mean values for each zone were calculated, to explore a tentative relationship between marsh zone and THg or MeHg concentration in the sediment. For this regrouping, the following zones were distinguished: Non-vegetated mudflats, *S. foliosa*-vegetated tidal marsh, *S. virginica*-vegetated upper marsh, and upland-seasonally flooded wetland.

Site Selection for Plant Material Collection

Tissues from live plant shoots and from plant detritus were collected from as many zones as possible, and analyzed for mercury species. Sample sites were chosen to match selected sites at which sediments had been collected in September 2001 (McFarland et al., 2002) and being vegetated by representative higher plant communities. Photographs of sampling activities were reviewed to provide additional information in some cases. The plant samples were collected in June 2003. Sample station coordinates, provided in McFarland et al. (2002), were located using a global positioning unit, and plant communities and other station characteristics were noted. The tidal marshes around the San Francisco Bay are dominated by the native *Spartina foliosa* (Pacific cordgrass) and *Salicornia virginica* (Common Pickelweed; for description vegetation zones see Chapter 1, This Report).

Plant Tissue Collection

Plant tissue samples were collected from five locations (Table 1). Three locations were situated in the HAAF, one in the Bel Marin, and one in the China Camp wetland. At all locations shoot material of the dominant plant species was sampled, and at two locations detritus was also collected. The aboveground portion of each plant was cut approximately 5 cm above the soil surface with stainless steel shears. The cut tissue was immediately placed in Ziploc bags and stored in a cooler with dry ice. At the conclusion of the sampling day, the tissues were removed from the Ziploc bags and rinsed in distilled water to remove any dust or soil particles. The rinsed tissues were placed on paper towels to quickly remove excess water and then vacuum sealed in heavy-duty polyethylene bags. Each bag was labeled, placed back in the cooler and flash frozen with sufficient dry ice. Samples were shipped frozen to the ERDC where they were logged and placed in a freezer for continued preservation.

Analysis of Plant Tissues for Total and Methylmercury

Total Mercury

USEPA-method 7421 was used. The plant samples were thoroughly ground in a stainless steel mixer prior to the dissolution process. Approximately 0.2 g sample of the plant tissue was heated at 115º C with sulfuric acid and nitric acid for 1 hour or until the tissue dissolved. Subsequently, 50 mL water was carefully added to the acidic mixture followed by an excess of potassium permanganate. This mixture was heated at 95º C for 1 h. The excess potassium permanganate was reduced with hydroxylamine hydrochloride and sodium chloride solution. Mercury was determined using a CETAC M-6000A Atomic Absorption Mercury Analyzer. Typical reporting and method detection limits for this sample size are 0.025 and 0.005 ng g^{-1}, respectively.

Methylmercury

Methods were modified after Bloom (1989); Horvat et al. (1993); Hammerschmidt and Fitzgerald (2001); St.Louis et al. (2001). The plant material was blended using a stainless steel mixer. Approximately 0.2 g blended plant tissue was extracted and distilled from Teflon distillation vessels using a mix of H_2SO_4, KC1, H_2O and $CuSO_4$ as the extracting and distillation solution. Samples were distilled in a 130°C carbon block, assisted by a stream of nitrogen, until about 80% of the solution was collected in Teflon receiver bottles held just above freezing in a specially designed refrigerator. All of the connecting transfer lines for the distillation apparatus

are Teflon. 0.5 mL of 2 M acetate buffer was added to each sample, including standards and quality control samples, after the distillates were transferred to Erlenmeyer flask reaction vessels. 0.1 mL of 1% sodium tetraethyl borate was added to the reaction vessels and the ethylation process was allowed to proceed for 15 min.. At the end of the reaction period, volatile mercury compounds were purged from the reaction solution with nitrogen gas and the mercury compounds were collected on activated carbon column traps. The mercury compounds were purged from the activated carbon traps at 360° C and allowed to pass through a gas chromatograph with an OV-3 column held isothermal at 100° C. The effluent mercury compounds were pyrolyzed in a quartz column with quartz wool at approximately 800 ^{o}C and the resulting mercury detected with cold-vapor atomic fluorescence spectroscopy. The typical reporting limit for this sample size is 0.05ng g^{-1}.

RESULTS AND DISCUSSION

Total Mercury and Methylmercury Concentrations in Non-vegetated and Vegetated Sediments

Mean THg concentrations in the surface sediments decreased in the order Low marsh>High marsh>Diked high marsh>Mudflat (Fig. 1, Table 2). No distinct effect of dry and wet season on THg concentration was noted. Mean THg concentrations, in ng g^{-1} DW in the dry season were: Low marsh 346, High marsh 292, Diked high marsh 261, Mudflat 236.

Mean MeHg concentrations increased in the surface sediments of all zones during the wet season except in the mudflats (Fig. 2, Table 2). MeHg concentrations increased 449% in the upper marsh dominated by *S. virginica*, followed by the tidal zone dominated by *S. foliosa* (133%), upland zone (68.9%) and mudflat (-34.2%). Mean MeHg concentrations, in ng g^{-1} DW, decreased in the order High marsh 7.29 >Low marsh 5.17 > Diked high marsh 1.82 > Mudflat 0.73. High MeHg concentrations were found in the sediment of stations AF-36, AF-37 and BM-50. These sites were very dry in the dry season, but were covered by standing water and plant detritus during the wet season. Some of these conditions occurred also in the upper marsh in the wet season and in some other areas in the dry season.

Total Mercury and Methylmercury Concentrations in Plant Tissues

The mean THg concentrations ranged from 14 to 25 ng g^{-1} DW in the shoots of *S. foliosa* and *S. virginica* (Table 3). The mean MeHg concentrations ranged from 0.17 to 0.96 ng g^{-1} DW. The THg concentrations in the shoots were in the same order of magnitude of those reported in Chapter 1, This Report. However, the MeHg concentrations were far lower than reported in Chapter 1, i.e., they amounted to only about half of the values measured using an alternative analytical method. This underestimate in the current case may be due to problems encountered in analyzing the green plant tissues, where the fluorescence of the plant chlorophylls interfered with the fluorescence of the Hg.

Both the THg and MeHg concentrations in detritus greatly exceeded those in the plant shoots by a factor of 5 to 8 (Table 3). The concentrations of THg ranged from 236 ng g^{-1} DW on the high marsh to 114 ng g^{-1} DW in the diked marsh, and the concentrations of MeHg ranged from 7.09 ng g^{-1} DW on the high marsh to 16.32 ng g^{-1}DW on the diked marsh.

POINT OF CONTACT CHAPTER 2:

Richard A. Price
U.S. Army U.S. Army Engineer Research and Development Center, Environmental Laboratory, Vicksburg, Mississippi, USA
Ph: 601-634-3636; Email: richard.a.price@erdc.usace.army.mil

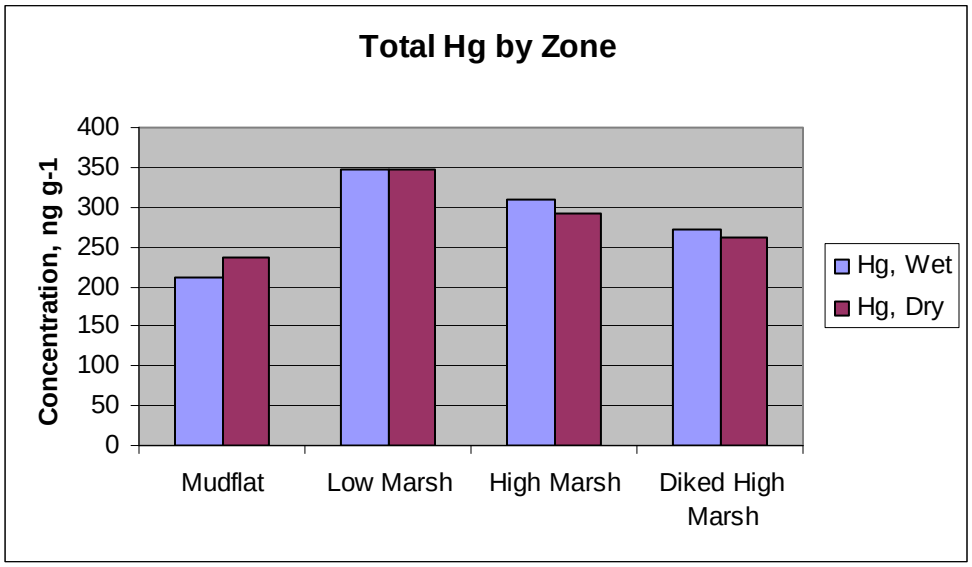

Figure 1. Total sediment Hg by vegetation zone.

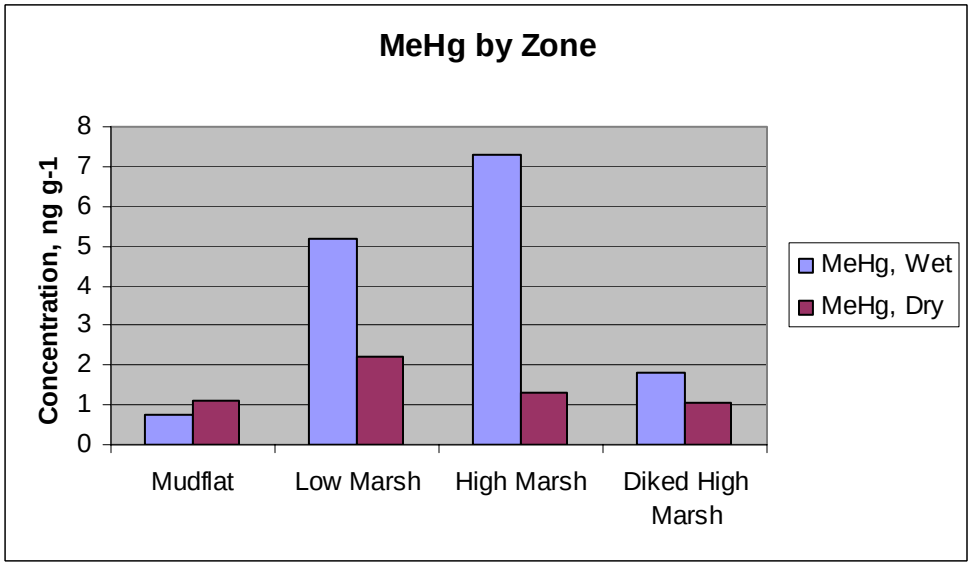

Figure 2. Sediment MeHg by vegetation zone.

Table 1. Sample stations in vegetation zones. Sample categories indicated.

Site/ Vegetation zone	HAAF	Bel Marin	China Camp
Low marsh	SM-10 Lat 38 03.116 Long 122 29.550 (*S. foliosa* shoots)		R-44 Lat 38 00.411 Long 122 28.758 (*S. foliosa* shoots) (*S. maritimus* shoots)
High marsh	SM-11 Lat 38 03.135 Long 122 29.637 (*S. virginica* shoots) SM-12 Lat 38 03.139 Long 122 29.723 (*S. virginica* shoots) (Detritus)		(*S. virginica* shoots)
Diked high marsh		BM-50 Lat 38 04.399 Long 122 29.085 (*S. virginica*) (Detritus)	

Table 2. Total Hg and MeHg characteristics in upper 2 cm of sediment in HAAF and China Camp (from McFarland et al., 2002).

Zone/ THg and MeHg	Mudflat		Low marsh		High marsh		Diked high marsh	
	Dry	Wet	Dry	Wet	Dry	Wet	Dry	Wet
Mean Hg, in ng g^{-1} DW (SD)	236 (231.5)	210.4 (200.4)	346 (100.6)	348 (92.4)	292 (75.6)	309 (122.8)	260.5 (78.8)	272 (73.4)
Maximum Hg, in ng g^{-1} DW	600	495	740	611	710	900	450	412
Minimum Hg, in ng g^{-1} DW	40	63.5	100	141	180	88.5	30	43
Mean MeHg, in mg kg^{-1} DW (SD)	1.11 (1.33)	0.731 (0.879)	2.21 (2.99)	5.17 (10.07)	1.33 (1.8)	7.29 (7.23)	1.08 (1.61)	1.82 (2.95)
Maximum MeHg, in ng g^{-1} DW	4.6	2.56	15	74.7	8.1	38.9	8.5	16.3
Minimum MeHg, in ng g^{-1} DW	0.05	0.018	0.05	0.34	0.05	0.05	0.033	0.03
MeHg, in % THg	0.471	0.347	0.64	1.48	0.454	2.36	0.41	0.67
MeHg wet season increase, in % dry season	NA	-34.20		133		449		68.90

Table 3. Total Hg and MeHg characteristics in plant tissues and detritus from HAAF, Bel Marin and China Camp. Samples collected on 12 June 2003. Mean values and standard deviations (N=5).

Site/ Vegetation zone	HAAF		Bel Marin		China Camp	
	THg (ng g^{-1}DW)	MeHg (ng g^{-1}DW)	THg (ng g^{-1} DW)	MeHg (ng g^{-1}DW)	THg (ng g^{-1} DW)	MeHg (ng g^{-1}DW)
Low marsh	SM-10				R-44	
S. foliosa shoots	16 (3)	0.17 (0.05)			14 (3)	0.41 (0.16)
S. maritimus shoots					16 (1)	0.23 (0.07)
S. virginica shoots					25 (2)	0.37 (0.09)
High marsh	SM-11					
S. virginica shoots	23 (5)	0.49 (0.18)				
	SM-12					
S. virginica shoots	28 (7)	0.96 (0.34)				
Detritus	236 (49)	7.04 (3.19)				
Diked high marsh			BM-50			
S. virginica shoots			25 (5)	1.33 (0.34)		
Detritus			114 (20)	16.32 (3.59)		

[This Page Intentionally Left Blank]

3- Geochemical Characterization of HAAF Sediment Profiles and Mercury Species Levels in Macrofauna

SUMMARY

This chapter details the results obtained from a field study conducted in June, 2003. The purpose of this effort was to measure total mercury (THg) and methylmercury (MeHg) levels in the sediment in relation to depth at intertidal sites at Hamilton Army Airfield (HAAF) and China Camp State Park (as a reference), as well as inland sites at HAAF and Bel Marin Creek. Other parameters important for the cycling of Hg and MeHg in sediments were also determined with the goal of establishing site-specific relationships between these parameters and THg and MeHg. Finally, Hg and MeHg were measured in macrofauna collected at the above-mentioned intertidal sites for the purpose of calculating site-specific biota-sediment bioaccumulation factors (BAFs).

For sediments, the highest MeHg concentrations were found in the upper 2.5 – 5.1 cm of the cores, and levels decreased with depth suggesting that conditions for the methylation of mercury are most favorable near the surface. THg levels increased with depth, correlating inversely with MeHg. The significance of this is unclear, but may suggest a net loss of mercury from the surface through volatilization or surface runoff/tidal transport of MeHg from the sediment surface. MeHg correlated directly with redox potential (E_h), total organic carbon (TOC), and phosphorus (P) suggesting that these parameters were associated with MeHg levels in HAAF marsh sediment. The predicted influence of E_h and pH on the bioavailability of mercury is consistent with the observed MeHg profile with more positive E_h values representing oxic conditions near the surface favoring mercury in the bioavailable Hg^0 state, and more negative E_h values (anoxic) at increasing depths favoring formation of non-bioavailable HgS.

For macrofauna, significant levels of THg and MeHg were detected in tissues of animals collected at intertidal sites at HAAF and China Camp, suggesting that both THg and MeHg are available for uptake. MeHg comprised on average 40 % of THg (range 20% to 70%), indicating that a significant portion of the invertebrate THg body burden is in the form of MeHg. Calculated BAFs (greater than 1) suggest that MeHg has a strong tendency toward bioaccumulation, and BAFs for MeHg ranged from about 3 to 50. Snails were the highest Hg bioaccumulators. Because the diet of these animals is composed largely by plant material, it is likely that MeHg in plants represents an important MeHg source for terrestrial trophic transfer.

INTRODUCTION

During the peak of the dry and wet seasons of 2002-2003 the surficial soils and sediments on the periphery of the HAAF Wetland Restoration site and at a nearby reference tidal salt marsh (China Camp) were sampled and analyzed for total mercury (THg) and methylmercury (MeHg)

(McFarland et al., 2002; McFarland et al., 2003a). THg surficial concentrations averaged 0.3 ng g^{-1} dry weight overall in both seasons and MeHg averaged 1.5 and 4.4 ng g^{-1} dry weight, dry and wet seasons, respectively. MeHg concentrations were highly variable in both seasons with sporadic occurrence of high outliers. Concentration distributions were strongly skewed toward the low end with median concentrations of MeHg equal to 0.6 and 1.9 ng g^{-1} dry weight (dry season, wet season) and with highest concentrations ranging to more than 20 ng g^{-1} dry weight in the wet season. MeHg concentration distributions at the western North Bay sites can be characterized as being typically in the order of 1-2 ng g^{-1} dry weight, but with infrequent ten-fold greater spikes, and overall about three-fold higher in the wet than in the dry season.

Increased MeHg concentrations were most pronounced in the area identified as "High Marsh" (i.e., McFarland et al., 2002). Samples at this location were taken close to the levee on the bay side of the former airfield. The uppermost reaches of the tertiary channels are in this location. Channel bottoms cut to depths up to 1 M through this part of the marsh. The flora in this area is predominated by pickleweed, interspersed with grasses. The area is above Mean High Water (MHW) and receives relatively more fresh water from storm runoff than salt water from tidal flux. There is little visible difference between the High and Mid-Marsh locations. High MeHg spikes were also found in the Mid-Marsh sampled in the wet season. Background information on tidal marsh structure and function is provided in Chapter 1, This Report.

PURPOSE

In FY03 a field study was conducted to:

(1) Measure total Hg and MeHg levels in the sediment in relation to depth at three intertidal sites at HAAF, one inland site at HAAF, one intertidal site at China Camp, and one site at the Bel Marin Creek
(2) Determine other parameters important for the cycling of Hg and MeHg in sediments
(3) Determine Hg and MeHg bioaccumulated in macrofauna.

SITE SELECTION FOR THE COLLECTION OF SEDIMENT CORES AND MACROFAUNA SPECIMENS

Five sites were selected for core sampling and analysis by depth section. THg/MeHg analyses of the wet season samples were not available for review before selection of the core sample sites, so knowledge of the areas showing highest seasonally affected potential for mercury methylation could not be used for this purpose. Instead, the sites were chosen based on results of the dry season analyses and on previous field studies of THg/MeHg levels in estuaries (Bartlett and Craig, 1981, Kannan et al., 1998). Selection of two intertidal sites at the HAAF "Bay Edge" location (SM-1 and SM-10) and a similar site at China Camp (R-44) was influenced by the relative abundance there of invertebrate biota at previous sample times. The highest THg concentrations were found at the HAAF Bay Edge sites, and rates of methylation were expected to be high at these sites because the redox cline was close to the surface. One sample site was selected at the Bel Marin Creek location (BM-50a) representing the lowest expected level of mercury contamination based on earlier studies. An additional site was sampled inland from the SM-10 location (designated SM-10U) in less wetted soil/sediment and provided the deepest core

obtainable with the collecting equipment used. Macrofauna (mussels, crabs, and snails) were collected at SM-1, SM-10, and R-44 for determination of THg and MeHg bioaccumulation. All samples were collected during the week of June 9-12, 2003. Stations were located using GPS and marked with stakes. The marked positions were used as reference points for the activities of all members of the research team in order to maximize comparability of results. Locations and brief descriptions are given in Table 1.

METHODS

Sediment Sampling

Five replicate samples were taken at site SM-1 within a rectangular zone extending ~ 3 m along the shoreline and approximately 2 m in width above the water's edge. At each of the five replicate sampling points (SM-1-1 through SM-1-5), 4–6 cores were collected within an area of approximately 1 m^2. Site SM-10 was sampled similarly to site SM-1. Sample SM-10U was collected approximately 30 m inland. No replicates were taken at SM-10U, and a modified sampling procedure was employed. One sample was taken at the Bel Marin Creek location (BM-50a) in a rectangular zone approximately 1 m in length along the edge of the channel and approximately 0.3 m in width from the water's edge inland. Four cores were collected. The China Camp site (R-44) was sampled similarly to the HAAF Bay Edge locations.

Core Sampling Procedure

At each site, samples were collected with a stainless steel 5 cm dia. x 30 cm core-sampling device. Clear plastic liners (with plastic eggshells at the bottom to prevent loss of the core when extracting the sampler from the ground) were inserted into the sampling device. A stainless steel head was attached to hold the liner and eggshell in place during the sampling process. The sampler was pushed into the sediment until the top was even with the sediment surface. The core was extracted by slowly withdrawing the sampler with the aid of a T-shaped handle on the top of the sampler. Cores collected in this manner typically measured 15-20 cm in length. The sampling procedure for SM-10U was modified to obtain a deeper core. The same sampler configuration as described above was employed. However, after extracting a single core from this sampling point, a second core was collected by reinserting the sampler into the hole created by removal of the first sample. In this manner, a depth profile of approximately 40 cm was achieved. The core liner containing the sample was immediately removed from the sampling device, labeled, capped, and frozen in a cooler with dry ice. Coolers were held overnight, repacked with dry ice as needed, and overnight express shipped to the ERDC Vicksburg Environmental Chemistry Laboratory. All samples were received frozen, and were stored frozen at -21°C until further processing.

Field Measurement of Core Redox Potential and pH

At each replicate site, a field depth profile for soil core oxidation/reduction potential (redox; E_h) and pH was performed. Modified core liners were fashioned with 1 cm diameter holes to allow an E_h or pH probe (SympHony probes, VWR International, West Chester, PA) to be inserted into freshly collected core samples. The core to be profiled was collected using one of these liners. The liner with core in place was then removed from the sampler and placed horizontally on a paper towel on the ground. Multiple probes were simultaneously pushed

through the holes in the side of the core liner into the core, and E_h /pH was recorded as soon as the meter stabilized (typically less than 1 minute). In this manner E_h then pH readings were taken at 2.5 cm intervals the full length of the core sample. Typically, all E_h /pH readings for a given core were collected within a 10-minute time period. Five such depth profiles were taken at SM-1, SM-10, and China Camp(Figures 1-3); one was taken at Bel Marin (Fig.4). An E_h /pH depth profile was not obtained on the core collected at SM-10U. To ensure proper function, E_h /pH probes and meters (Beckman 255 meter, Beckman Coulter, Fullerton, CA) were checked frequently (~ hourly) using standard solutions (VWR International, West Chester, PA). A "poised" solution was used as the E_h probe/meter calibration standard. E_h values were calculated from measured mV readings of Pt-electrodes and corrected for the potential of the reference AgCl by adding 200 mV (Light, 1972) to the instrument reading.

Invertebrate Sampling

Invertebrate specimens were collected at three sites: SM-1, SM-10, and R-44. Collections were made by hand over the period 10-12 June, 2003. Three species were found in sufficient abundance for analysis. The ribbed mussel, *Geukensia* (= *Modiolus*) *demissa*, and yellow shore crab *Hemigrapsus oregonensis*, were found at all three locations. Mudsnails *Nassarius* (= *Ilyanassa*) *obsoletus* (Fig.12) were found only associated with a small tidal creek at SM-1. Five pooled samples of approximately 50 g wet-weight (excluding shell weight of molluscs) were collected for each species. Samples were collected in 4 oz screw-top glass jars, frozen on dry ice as with sediment samples, and transported to the ERDC Omaha facility for analysis of total THg and MeHg.

Sample Preparation for Analysis

Frozen cores were manipulated in a glove box under nitrogen (Labconco, Kansas City, MO) continuously monitored with the aid of a probe and meter (Extech Instruments, Model 407510) to ensure internal atmospheric oxygen levels remained below 1%.Frozen cores were sectioned using a PVC pipe cutter at 2.5 cm intervals along the entire length of the core. In this manner each core yielded six subsamples reflecting the depth profile of the core. Subsamples of corresponding depths for each replicate core taken at a given sampling point were composited. Plant stems and rocks were removed as much as possible from the samples. After compositing was completed, samples were refrozen on dry ice to minimize the potential loss of MeHg from the sample. Composite samples were then submitted for determination of MeHg, THg, total organic carbon (TOC), acid volatile sulfide with simultaneously extractable metal (mercury; AVS/SEM), total metals (aluminum, cesium, iron, lithium, manganese, phosphorus, selenium), particle size distribution (PSD), and clay mineralogy. Procedures for these analyses are described below. Frozen mussels and clams were partially thawed, shucked, and prepared for mercury analyses as described previously (Reference 2). Crabs were analyzed with exoskeleton. A 10-15 mg aliquot of each pooled sample was taken for separate lipid determination (Van Handel, 1985).

Lipid Analysis in Invertebrate Tissues

Samples were weighed (10-50 mg) into a microcentrifuge tube then chilled in 1 mL of chloroform/methanol (1:1 v/v) for 1 hr. The mixture was then transferred to a ground glass homogenizing tube with 3 ml of chloroform/methanol and homogenized thoroughly. The homogenate was then centrifuged at 3000 rpm for 5 min. Three separate aliquots (0.25 mL each)

were transferred to individual test tubes. Volume of the remaining extract was determined and recorded. Standards were prepared by adding 0, 10, 25, 50, 100, 150, 200, and 250 ul of 1 mg/ml soybean oil to 13 x 100 mm tubes (in triplicate). Solvent was evaporated from samples and standards on a dry heating block. Concentrated sulfuric acid (100 uL) was added to each tube followed by heating on a dry block at 100˚C for 10 min. After cooling, vanillin reagent (2.4 mL/tube) was added followed by vortexing to mix. An aliquot (250 uL) of each sample/standard was transferred to a 96-well plate and absorbance measured at 490 nm to determine lipid content.

Total Hg Determination in Sediments and Invertebrate Tissues

THg analysis of all samples was based on EPA Method 7471A (EPA, 1992c). Briefly, sediment samples were dried at 105°C and ground with a mortar and pestle in preparation for analysis. For each dried sample, a 1.0 g aliquot was digested in a BOD bottle with concentrated hydrochloric acid and concentrated nitric acid for 15 min at room temperature. Each sample was then heated for 1 hr with 99 mL reagent water and 15 mL 5% (w/v) potassium permanganate at 95°C. Samples were allowed to cool, after which 10 mL sodium chloride-hydroxylamine hydrochloride solution (144 g NaCl and 144 g $NH_2OH{\cdot}HCl$ in 1 L reagent water) was added. An aliquot of the digestate was mixed with 10% (w/v) stannous chloride in 7% (v/v) hydrochloric acid solution and injected onto a CETAC M6000A mercury analyzer equipped with a long path cell. Sample absorption was monitored at 254 nm.

Methylmercury Determination in Sediments and Invertebrate Tissues

MeHg concentrations in all samples were determined in an acidic aqueous medium using sample distillation and cold trapping prior to derivatization with sodium tetraethylborate. Volatile organomercury compounds wee then separated and detected by gas chromatography and atomic fluorescence (Demuth and Heumann, 2001). MeHg determinations were performed under clean room conditions by the procedure described previously (McFarland et al., 2002). Briefly, approximately 0.25 g sediment was weighed into a Teflon container (100 mL volume) containing 60 mL 0.4% HCl and 200 µL 1% APDC (pyrrolidine carbodithioic acid, ammonium salt, 97%). The sample was distilled at 130°C for 3.5 to 3.7 hr under 60 mL min^{-1} flow of high purity nitrogen in a laminar flow hood. The distillate was collected and transferred to a 250 mL Erlenmeyer flask and the volume adjusted to approximately 100 mL with Barnstead Nanopure water. The flask was topped with a four-way valve glass stopcock. Ethylation of the mercury species was initiated and allowed to proceed (with valves closed) 20 minutes by addition of 2 M sodium acetate buffer and 1% sodium tetraethylborate (in 2% KOH). High purity nitrogen was then bubbled through the reaction mixture for 20 minutes, and organomercury species were collected in a quartz tube packed with 3 g Carbotrap 20/40 mesh graphitized carbon black. The quartz tube was then inserted into a tubular heating jacket heated to 350°C for 2 min under a flow of ultra high purity argon which proceeded through a 1 m U-shaped glass column (2 mm ID, 0.25 in OD) with 3% OV-17 on Chromasorb WHP 80/100 mesh packing fitted into a HP 5890 gas chromatography oven held at 100°C, and flow was directed to a quartz pyrolysis tube held at approximately 700°C. Pyrolysis products were observed by using a Tekran Model 2500 CVAFS Mercury Detector. Analog data were collected on a Shimadzu C-R4A Chromatopac integrator.

Total Metals Determination in Sediments and Invertebrate Tissues

Soil sub-samples were dried and weighed (1.0 g) into glass digestion vessels. The samples were digested according to EPA Method 3050B (EPA, 1992a) using the hotplate technique. Once digested, the corresponding solutions were filtered, diluted as necessary, and spiked with Yittrium internal standard for metals analysis by ICP-AES using EPA Method 6010B (EPA, 1992b). The instrument used was a Perkin Elmer Optima 3000DV equipped with a cyclonic spray chamber and cross flow nebulizer. Nebulizer gas flow was set to 0.8 mL/min according to manufacturer's suggestions and optimization experiments; a plasma power of 1320 W was used. Pre- and post-digestion analytical spikes were added for quality control for all analytical batches in addition to using laboratory control standards.

Determination of Acid Volatile Sulfide and Simultaneously Extractable Mercury in Sediments

AVS-SEM (Hg) in the sediment was determined using the diffusion method of Leonard et al. (1996). The soil sub-sample was placed in a sealed 500 mL glass bottle with 50 mL of deionized water to which an aliquot of hydrochloric acid was added to make the final acid concentration 1 M. The evolved sulfide gas was collected in a 30 mL vial containing 0.25 M sodium hydroxide inside the sealed 500 mL container. Sulfide was measured in the sodium hydroxide capture solution using standard colorimetric techniques. The colorimetric method (Lachat Instruments, Hach Corporation, Loveland, CO) uses methylene blue color formation to detect dissolved sulfide. Metals extracted from the soil sample were analyzed by ICP-AES, except for mercury, which was determined by cold vapor atomic fluorescence as described above, after the hydrochloric acid solution was filtered to 0.45 μm.

Determination of Total Organic Carbon in Sediments

Total organic carbon was determined through conversion of organic carbon in a sample to carbon dioxide (CO_2) by high temperature combustion. The CO_2 formed was measured directly by a linearized non-dispersive infrared detector. The method was based on EPA Method 9060 (EPA, 1986). Briefly, 1-2 grams of wet sample was placed in a porcelain dish and concentrated nitric acid was added drop-wise until any observed effervescence ceased. The sample was then placed in an oven at 75^{o}C until dry (15 minutes minimum). The dried sample was ground using a mortar and pestle. Samples were analyzed using a Dohrmann 183 Boat Sampling Module and a Dohrmann DC-190 High Temperature TOC Analyzer. The instrument was calibrated using a blank and a 10,000 ppm carbon standard (4.25 g potassium hydrogen phthalate [Sigma-Aldrich, Milwaukee, WI] in 200 mL organic-free reagent grade water) according to the instrument manufacturer's instructions. A second source standard (Environmental Resource Associates, Arvada, CO) was analyzed following calibration as a quality control measure. Continuing calibration verification (CCV) standards were used to check the validity of the calibration after every 10 samples. All samples were analyzed in quadruplicate and the average result reported.

Determination of Particle Size Distribution in Sediments

Particle size distributions of HAAF soil/sediment cores were determined using the hydrometer method of Day (1956) as modified by Patrick (1958). Particles were separated into size fractions of >50μm (sand), 50-2μm (silt), and <2μm (clay) by suspension of 40g dry material in 1 L of a dispersing solution (sodium metaphosphate at pH 8.3). An ASTM

hydrometer (152H) placed in the suspension was read at specified sedimentation times for the various size fractions based on Stokes equation. Results were reported in percentage of sand, silt and clay.

Identification of Clay Minerals in Sediments

Clay mineral identification was determined using X-Ray diffraction of randomly-oriented packed powders. A Philips PW1800 Automated Powder Diffractometer system was utilized to collect X-ray diffraction (XRD) patterns employing standard techniques for phase identification. The run conditions included Cu K_α radiation and scanning from 2 to 65º2θ with collection of the diffraction patterns accomplished using the PC-based, Windows version of Datascan, and analysis of the patterns using the Jade program (both from Materials Data, Inc.). In preparation for XRD analysis, a portion of the sample was ground in a mortar and pestle to pass a 45-μm mesh sieve (No. 325). Bulk sample random powder mounts were analyzed using XRD to determine the mineral constituents present in each sample. To determine the type of phyllosilicates present, oriented samples of the <4 μm size fraction of each sample were prepared and XRD patterns were obtained. These samples were then placed in an ethylene glycol atmosphere overnight at room temperature, and an X-ray diffraction pattern was collected for each sample. Samples showing expansion of the crystal structure after exposure to an ethylene glycol atmosphere compared to air-dried pattern indicate expandable smectitic clays. Comparisons of patterns obtained before and after exposure to ethylene glycol were used to determine the amount of expandable clay present. Quantitative determinations of whole-rock mineral amounts were done utilizing integrated peak areas (derived from peak-decomposition/profile-fitting methods) and empirical reference intensity ratio (RIR) factors determined specifically for the diffractometer used in data collection. The total phyllosilicate (clay and mica) abundance of the samples was determined on the whole-rock XRD patterns using combined {001} and {hkl} clay mineral reflections and suitable empirical RIR factors.

Statistical Analysis

Statistical analyses were performed using SAS procedures (SAS Institute, Inc. 2001) and SigmaStat, version 3.0 (SPSS, Inc., Chicago, IL). Parametric comparison test assumptions were checked for violations using the Shapiro-Wilk's test for normality of residuals, and a modification of Hartley's *F*-max test for equality of variances (Shoemaker 2003). Site data failing the normality assumption were compared using the nonparametric Kruskal-Wallis test. Site data passing the normality test were compared using *t*-tests for equal or unequal variances. A significance level of 0.05 was used for all statistical tests. Non-detects were substituted as one-half detection limit prior to analysis. Figures were produced using SigmaPlot, version 8.0 (SPSS, Inc., Chicago, IL).

RESULTS AND DISCUSSION

Total Mercury and Methylmercury Levels in Sediments

THg and MeHg in Relation to Depth within the Sediment

The THg concentrations did not differ greatly between the primary sample sites, SM-1 and SM-10 at HAAF, and R-44 at China Camp, but they increased with depth within the

sediment (Table 2, Fig.2). The MeHg concentrations were highly variable (SDs as large as the means), higher in the first 5.1 cm layers at SM-1 and SM-10, but lower in the deeper layers (Table 2, Fig.2). MeHg constituted about one percent of THg down to almost 10.2 cm depth (Table 2). The THg concentrations were far lower at Bel Marin than at both other sites, i.e., almost one-half to two-thirds, and MeHg was well above 1% in all depth sections -except the 5.1 cm- 7.6 cm section (Table 2). The methylation of mercury is apparently higher at Bel Marin than at both other sites, consistent with earlier observations (McFarland et al., 2002; McFarland et al., 2003a). SM-10U was sampled to explore a depth profile at a higher elevation of the marsh. This core was sectioned using visually distinct horizons as a criterion (Table 3). It was found that in this core the highest MeHg concentrations occurred deeper in the sediment, i.e., at 17.8 to 40.6 cm, than at the other sites.

Other Parameters Important for the Cycling of THg and MeHg in Sediments

Sediment Quality Characteristics

Sediment quality characteristics for HAAF (SM-1 and SM-10) and China Camp (R-44) are summarized in Table 4. Additional data is tabulated for sediment quality (HAAF SM-10U and Bel Marin BM-50a) in Appendix - Chapter 3 (Table 1), and for clay mineralogy (all sites) in Appendix - Chapter 3 (Tables 11-15).

The concentrations and depth profiles of organic carbon were similar at HAAF (SM-1 and SM-10; Table 4). Surficial sediment layers were usually relatively richer in sand and organic matter, and deeper layers were more compacted and contained relatively more silt and clay. The sulfide (AVS) concentration and redox potential were inversely related to depth. The redox cline occurred within 2.5 to 5.1 cm of the surface at SM-1 and at 3.8 to 10.2 cm at SM-10 (Fig.1). The redox potential barely changed below the cline at HAAF. At the higher elevation site, SM-10U, redox potential and pH were not measured. The AVS concentration was measured and found to be elevated, i.e., 1600 ug g^{-1}, deeper than 30.5 cm below the sediment surface, the same depth at which a dark color was observed indicating a reducing environment (Appendix - Chapter 3, Table 1; Table 3). The sediments at China Camp were less organic and more sulfidic near the surface (Table 4) compared to those at HAAF (SM-1 and SM-10), and the fines concentration was very low (<1%). The redox cline in these sediments ranged from 5.1 to 12.7 cm below the surface (Fig.3). The sediment at Bel Marin was the least organic with TOC <2% (Appendix - Chapter 3, Table 1), and it was more oxic with the redox cline occurring at about 17.8 cm (Fig.4). AVS was below detection at the sediment surface, but about 1100 ug g^{-1} at a depth of 12.7-15.2 cm.

Major and Trace Elements

Results for analysis of major and trace elements are summarized in the Appendix - Chapter 3, Table 2 (SM-1, SM-10, R-44) and Appendix - Chapter 3, Table 2 (BM-50a, SM-10U). Aluminum (Al) and iron (Fe) were detected as major elements at all sites. The levels of these elements increased with depth at HAAF (SM-1, SM-10, SM-10U), but did not show this relationship at HAAF (R-44) and Bel Marin (BM-50a). Trace elements included cesium (Cs), lithium (Li), manganese (Mn), phosphorus (P), and selenium (Se). The concentrations increased in the order of Se<Cs<Li<Mn<P at all three sites at depths. The Se and Cs concentrations

remained constant at all depth profiles at all sites. The Mn concentration showed a tendency to increase with depth at two sites, i.e. SM-10 and R-44, but remained constant at all depths at tow other sites, i.e., SM-1 and BM-50a. The Mn concentration was a factor of ten higher in the surficial sediment at SM-10U than at SM-10. The Li concentration increased with depth at HAAF (SM-1, SM-10, SM-10U), but remained constant at all depths at China Camp (R-44) and Bel Marin (BM-50a). The phosphorus concentration generally decreased with depth. Within HAAF, it was approximately two times higher at the higher elevation site, SM-10.

Significant Relationships Between MeHg and Other Parameters and Depth Within the Sediment

The tentative relationships between MeHg concentrations and other parameters, and depth within the sediment at HAAF (SM-1 and SM-10) and China Camp (R-44) were explored using statistics. A non-parametric statistical test (Tukey's on Ranks) was employed, because unequal variances were observed in some cases. Statistically significant relationships were established among THg, MeHg, P, Mn, TOC, E_h, and pH. Data tables showing these relationships are located in the Appendix – Chapter 3, Tables 4 – 10, respectively.

For THg, significant differences were observed across the depth profile of SM-1, but not SM-10 and R-44. For MeHg and P, significant differences were observed across the depth profile of SM-10, but not SM-1 and R-44. For Mn, significant differences were observed across the depth profile of SM-10 and R-44, but not SM-1. For TOC, E_h, and pH, significant differences were observed across the depth profile of all three.

The parameters described in the preceding paragraph also showed statistically significant correlation (Spearman Rank Order Correlation; $P < 0.050$) with changes in MeHg concentration (Figures 2 – 6). When measurements from SM-1, SM-10, and R-44 were combined as a single group, MeHg correlated positively with P (Fig.3), TOC (Fig.4), and E_h (Fig.5) and negatively with THg (Fig.2) and Mn (Appendix – Chapter 3, Fig.1). Correlations performed on a per site basis were not as clear cut. THg showed a negative correlation with changes in MeHg concentrations for the depth profile of SM-1, but not SM -10 and R-44 (Fig.2). Both P (Fig.3) and %TOC (Fig.4) showed a strong positive correlation with changes in MeHg concentrations at SM-1 and SM-10, but not R-44. SM-10 and R-44, but not SM-1, showed negative correlations between Mn and MeHg (Appendix – Chapter 3, Fig.1). E_h showed a strong positive correlation with changes in MeHg concentrations for SM-1 and SM-10, but not R-44 (Fig.5). A negative correlation between pH and MeHg was observed for SM-1, but not SM-10 and R-44 (Fig.6).

SM-10 was the only site with statistically significant differences along its depth profile for MeHg. Significant differences for P, TOC, and E_h were also seen at SM-10, and this further reinforces correlations between MeHg and these parameters at this site (Figures 3, 4, and 5, respectively). Parallel correlations for these same parameters at SM-1 (Figures 3, 4, and 5, respectively) provide additional support to the observation that these three parameters are associated with MeHg in intertidal sediments at HAAF.

The correlation observed between P and MeHg may be related to sediment phosphate serving as a nutrient for sediment microorganisms responsible for mercury methylation. Organic carbon also provides a carbon substrate for microorganisms and in a similar manner might support production of MeHg. Additionally, MeHg is known to associate with organic carbon, and correlations between MeHg and TOC may be related to organic carbon's contribution to a favorable environment for retention of MeHg. In situ pH data indicated sediment was most acidic at the surface, consistent with a predicted elevation in organic acid content resulting from

microbial degradation of sediment organic carbon (Marvin-DiPasquale et al., 2003). Others have reported elevated mercury methylation rates at low pH in freshwater systems (Winfrey and Rudd, 1990).

Highest levels of MeHg were observed in highly oxygenated upper sediment strata as indicated by positive E_h readings (Fig.5). Under oxic conditions, Fe and Mn form oxyhydroxides that may bind MeHg. All three metals were detected at significant concentrations (Appendix – Chapter 3, Table 2) in sediment core samples, and may have exerted a sorptive influence that contributed to elevated surface MeHg. Sulfate reducing bacteria (SRB) are the primary producers of MeHg in sediment, and these strict anaerobes inhabit an E_h range of –100 mV to +100 mV (Bartlett and Craig, 1981) suggesting methylation would be most favored at depths below 5.1 centimeters. However, SRB activity may be elevated in the oxygenated root zones where they occupy anaerobic "microzones" (Marvin-DiPasquale et al., 2003). Given the dense *S. foliosa* vegetation found in areas sampled for this study, such an explanation is certainly plausible and would account for elevated MeHg at the surface. E_h and pH also influence mercury speciation as indicated in Fig.7. Data collected at Hamilton (SM-1 and SM-10) and China Camp (R-44) suggests that mercury would be expected to exist in its elemental form (Hg^0) at the surface but as HgS at lower depths. HgS is insoluble and would not be available to microorganisms while Hg^0 would be available for conversion to MeHg. The diagram depicted in Fig.7 is based on measurements taken under laboratory conditions, but if assumptions of the model are valid at Hamilton, then E_h-pH influences on mercury bioavailability could help explain elevated surface levels of MeHg.

Total Mercury and Methylmercury Levels in Macrofauna

The highest concentration of THg (100.9 ng g^{-1} wet weight) was found in snails from HAAF site SM-1 (Table 5). THg in snails from SM-1 was significantly higher than in mussels from SM-10 and crabs from R-44, and THg in mussels from R-44 was significantly higher than in mussels from SM-10 (Fig.9). THg concentrations in crabs (Table 5) were approximately equal at all sites ranging from 18.1 ng g^{-1} (R-44) to 21.3 ng g^{-1} (SM-10). THg concentrations in mussels (Table 5) varied among sites with concentrations ranging from 15.7 ng g^{-1} (SM-10) to 29.3 ng g^{-1} (R-44).

The highest concentration of MeHg (39.5 ng g^{-1}) was found in snails from SM-1 (Table 5). MeHg in snails from SM-1 was significantly higher than in mussels from SM-1 and crabs from R-44 (Fig.9). MeHg concentrations in crabs and mussels varied among sites with the highest crab MeHg concentrations (14.2 ng g^{-1}) at SM-10 while highest mussel MeHg concentrations (16 ng g^{-1}) were found at the reference site (R-44). MeHg as a percentage of THg (Table 5) ranged from 19.9 % (R-44) to 67.4 % (SM-10) for crabs, and 20.5 % (SM-1) to 53.8 % (R-44) for mussels; for snails, it was 39.9 % (SM-1).

THg and MeHg tissue/sediment bioaccumulation factors (BAF) were calculated as the ratio of dry weight tissue concentrations (Table 5; Figures 10 and 11) divided by dry weight sediment concentrations at the surface (0 – 2.5 cm) for THg or MeHg at a given site (Table 2). Macrofauna and sediments were collected during the same time period (June 9-12, 2003). BAFs for MeHg were highest with snails (BAF = 47.0; Table 5) and were statistically greater than crabs from R-44 (Fig.10). BAF values greater than 1 generally indicate a tendency towards bioaccumulation, and all MeHg BAFs were greater than 1 (lowest MeHg BAF was 3.3; Table 5) indicating an elevated bioaccumulation potential for MeHg in invertebrates at HAAF and China Camp. BAFs for THg were highest for SM-1 snails (1.2; Table 5) and were statistically greater

than in mussels from SM-10 and crabs from R-44 (Fig.10). The THg BAF for snails exceeded 1, but this is probably due to the fact that ~ 40 % of THg was actually MeHg (Table 5). In fact, if MeHg is factored out the THg values for snail tissue [reduced by 40% from 401 ng g^{-1} (Table 5) to 241 ng g^{-1}] and sediment [reduced by 1% from 330 ng g^{-1} (Table 2) to 327 ng g^{-1}], the BAF drops to 0.74. Considering this and the fact that all other THg BAFs were less than 1, it is reasonable to conclude that THg (representing all detectable mercury species) was generally associated with the sediment and bioaccumulation potential for THg, as a whole, is relatively low.

THg and MeHg levels for snails (SM-1) were about five times higher than crabs or mussels collected at all sites. The elevated BAFs for snails concurs with the observations of Gardner et al. (1978) who found concentrations of THg in salt marsh snails *Littorina irrorata* that formed the basis of BAFs as much as ten-fold higher than found in other invertebrates. Mussels are filter feeders and would be expected to absorb THg and MeHg associated with suspended particulate matter in bay water. Crabs are omnivores, feeding on detritus of plant and/or animal origin. Snails feed largely on plant tissue, and since tissue levels and BAFs were significantly elevated for both THg and MeHg in snails, it may be that plants represent an important source of MeHg for terrestrial trophic transfer pathways. Furthermore, since plants comprise the majority of biomass at HAAF and China Camp, their total contribution to MeHg input for the local ecosystem could be significant. Additionally, plant detritus washed into the bay with the change in tides could be an important source of MeHg input for the San Pablo Bay ecosystem.

This work raises several important questions to address in the near future. Are MeHg profiles (and related parameters) similar in other topographically distinct areas (mudflats, upland areas, etc.)? What are the impacts of seasonal variability on MeHg profiles? Is MeHg in surface sediment or detritus mobile with respect to tidal flux or storm runoff? Is there a net loss of Hg from HAAF sediments to the surrounding environment? If plants are a major component of MeHg trophic transfer pathways at HAAF, can the critical variables controlling the magnitude of their impact be identified and managed?

POINT OF CONTACT CHAPTER 3:

Robert P. Jones
U.S. Army U.S. Army Engineer Research and Development Center, Environmental Laboratory, Vicksburg, Mississippi, USA
Ph: 601-634-4098; Email: robert.p.jones@erdc.usace.army.mil

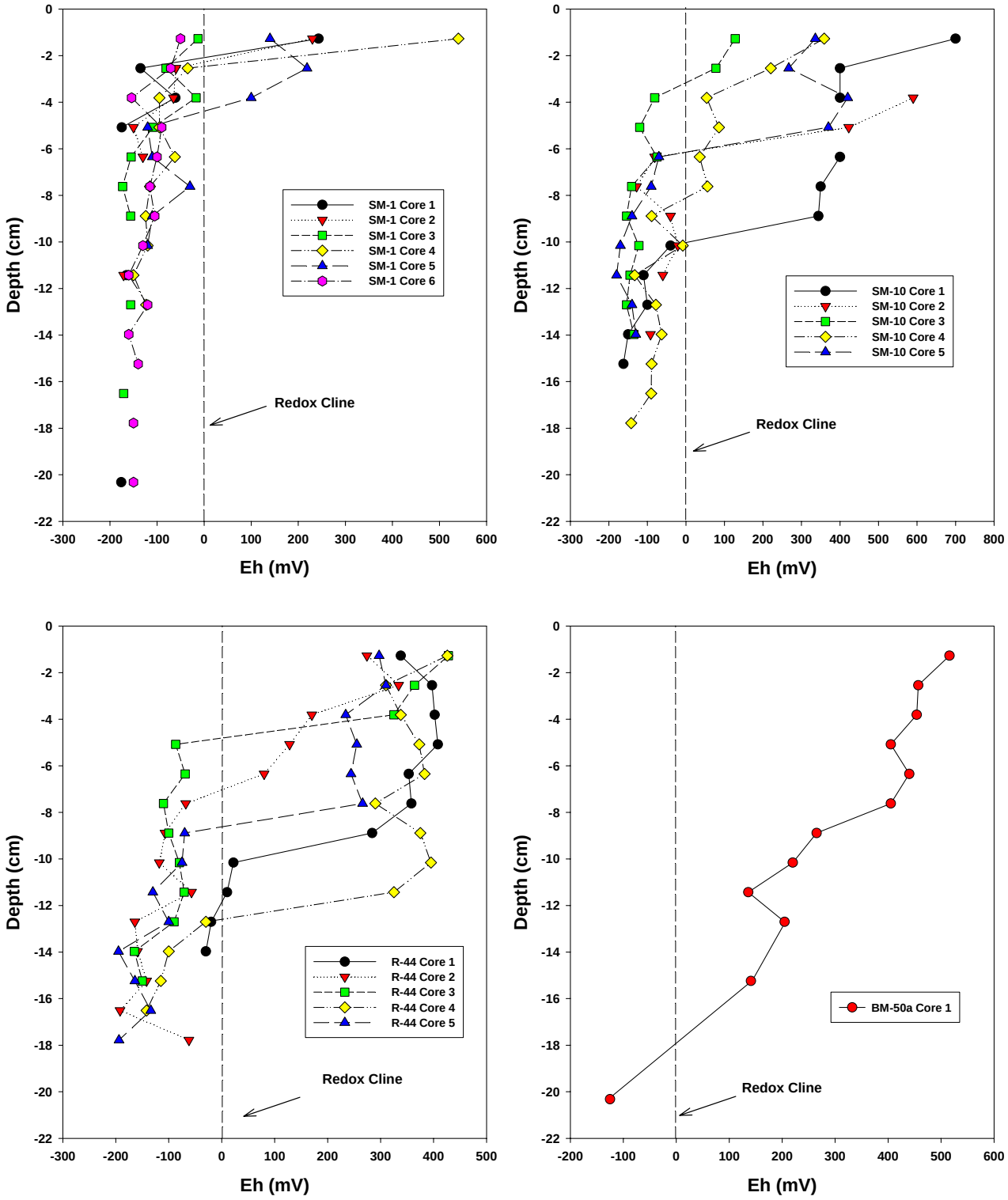

Figure 1. Depth profile of in situ redox potential measurements in sections of replicate cores taken at HAAF Bay Edge (SM-1, SM-10), China Camp (R-44), and Bel Marin (BM-50a). Vertical dashed line is redox cline.

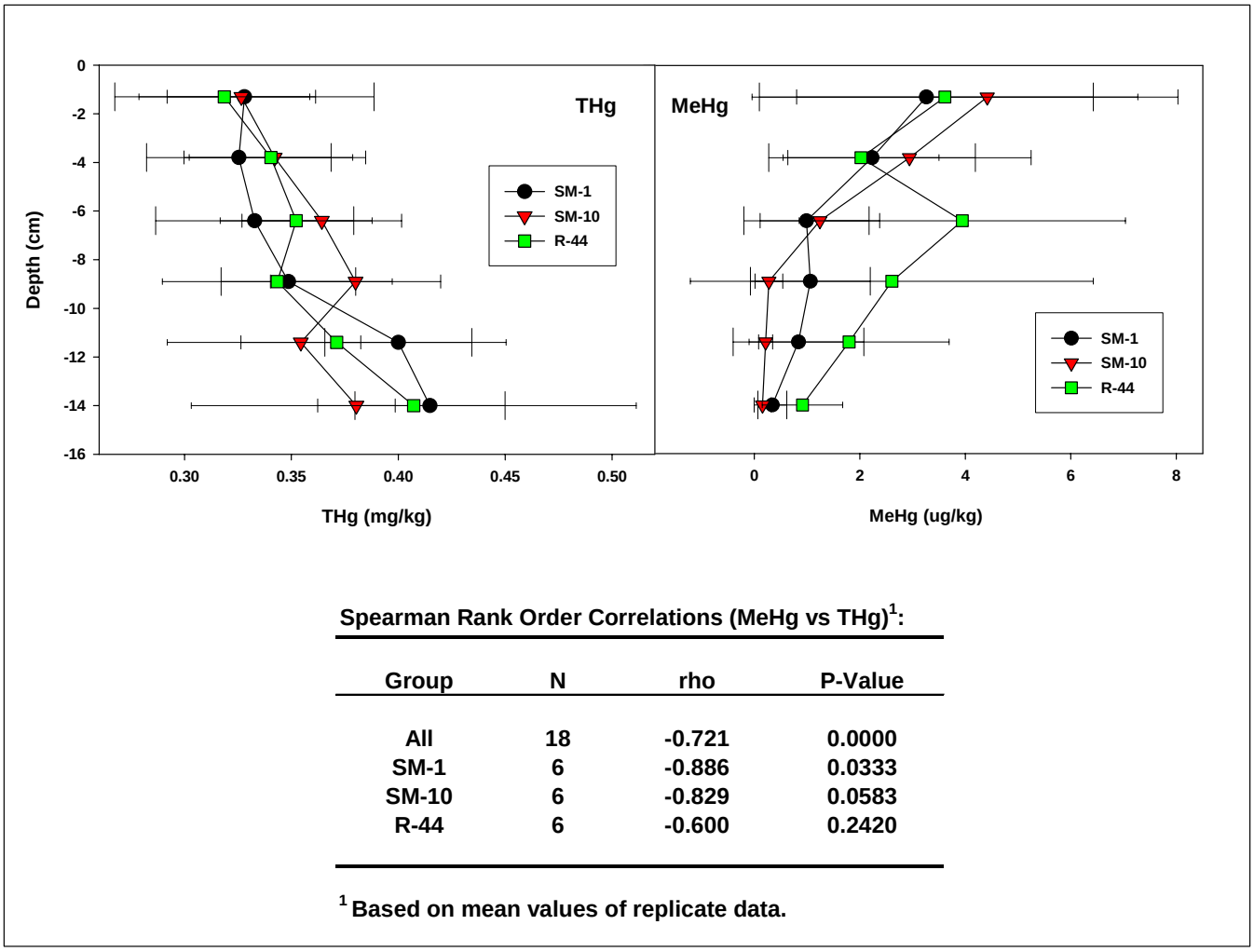

Spearman Rank Order Correlations (MeHg vs THg)[1]:

Group	N	rho	P-Value
All	18	-0.721	0.0000
SM-1	6	-0.886	0.0333
SM-10	6	-0.829	0.0583
R-44	6	-0.600	0.2420

[1] Based on mean values of replicate data.

Figure 2. Depth profile comparisons and correlations for THg and MeHg in cores collected at HAAF (SM-1, SM-10) and China Camp (R-44). Mean values and SD (N=5).

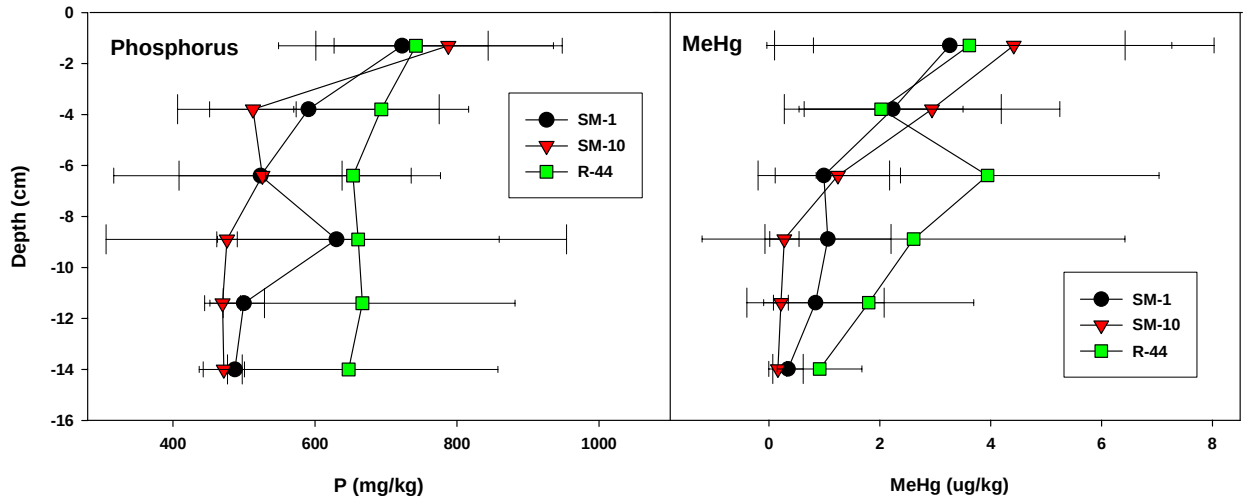

Spearman Rank Order Correlations (MeHg vs P)[1]:

Group	N	rho	P-Value
All	18	0.785	0.0000
SM-1	6	0.943	0.0167
SM-10	6	0.886	0.0333
R-44	6	0.257	0.6580

[1] Based on mean values of replicate data.

Figure 3. Depth profile comparisons and correlations for phosphorus (P) and MeHg in cores collected at HAAF (SM-1, SM-10) and China Camp (R-44). Mean values and SD (N=5).

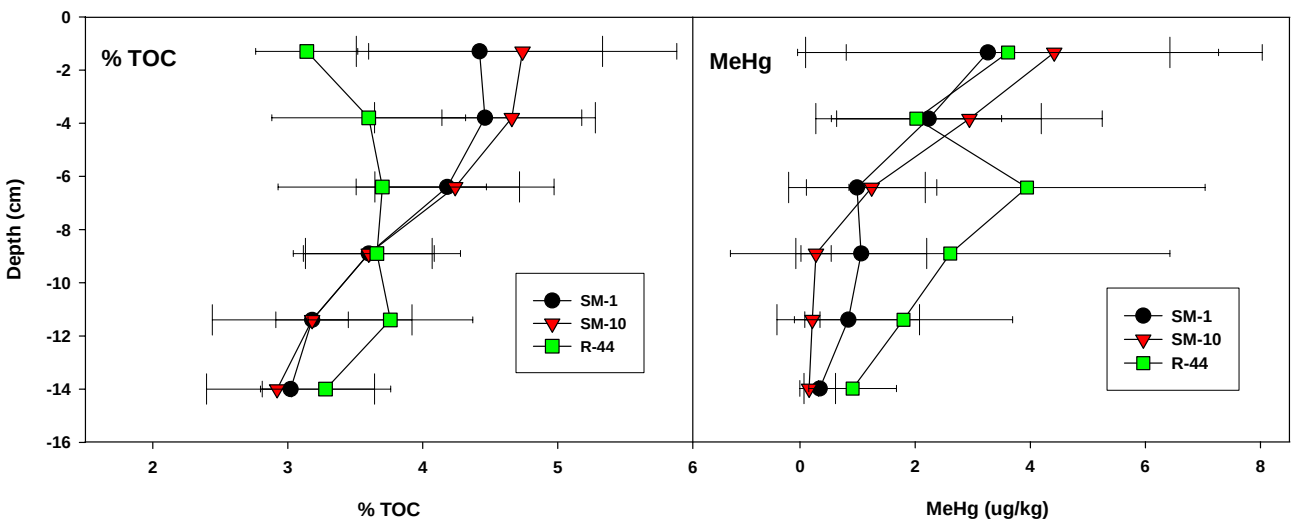

Spearman Rank Order Correlations (MeHg vs % TOC)[1]:

Group	N	rho	P-Value
All	18	0.639	0.0043
SM-1	6	0.886	0.0333
SM-10	6	1.000	0.0028
R-44	6	0.029	1.0000

[1] Based on mean values of replicate data.

Figure 4. Depth profile comparisons and correlations for Total Organic Carbon (%) and MeHg in cores collected at HAAF (SM-1, SM-10) and China Camp (R-44). Mean values and SD (N=5).

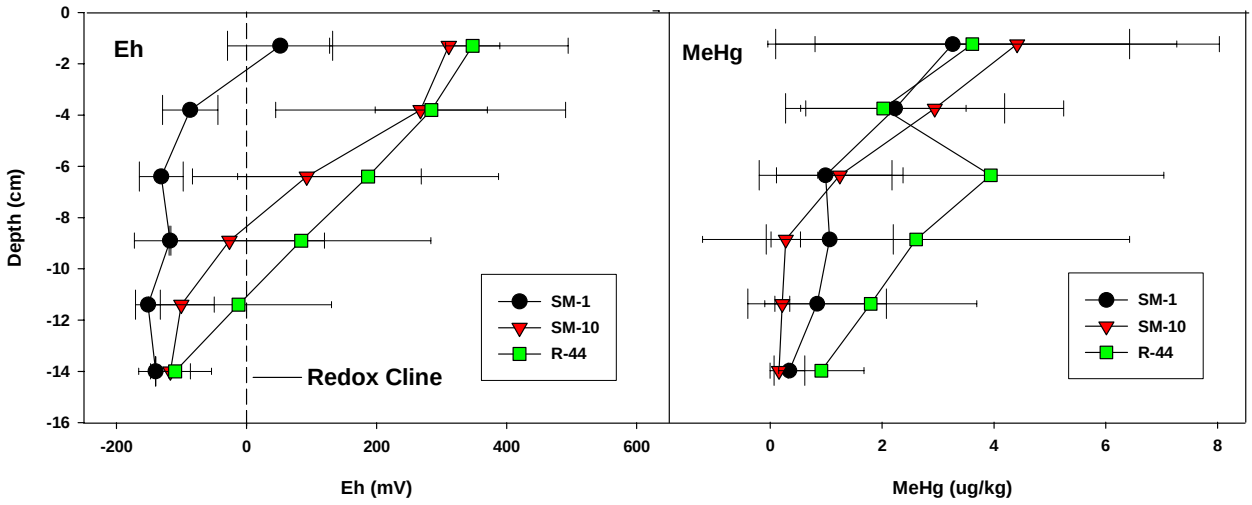

Spearman Rank Order Correlations (MeHg vs Eh)[1]:

Group	N	rho	P-Value
All	18	0.775	0.0000
SM-1	6	0.943	0.0167
SM-10	6	1.000	0.0028
R-44	6	0.714	0.1360

[1] Based on mean values of replicate data.

Figure 5. Depth profile comparisons and correlations for Redox Potential (Eh) and MeHg in cores collected at HAAF (SM-1, SM-10) and China Camp (R-44). Mean values and SD (N=5).

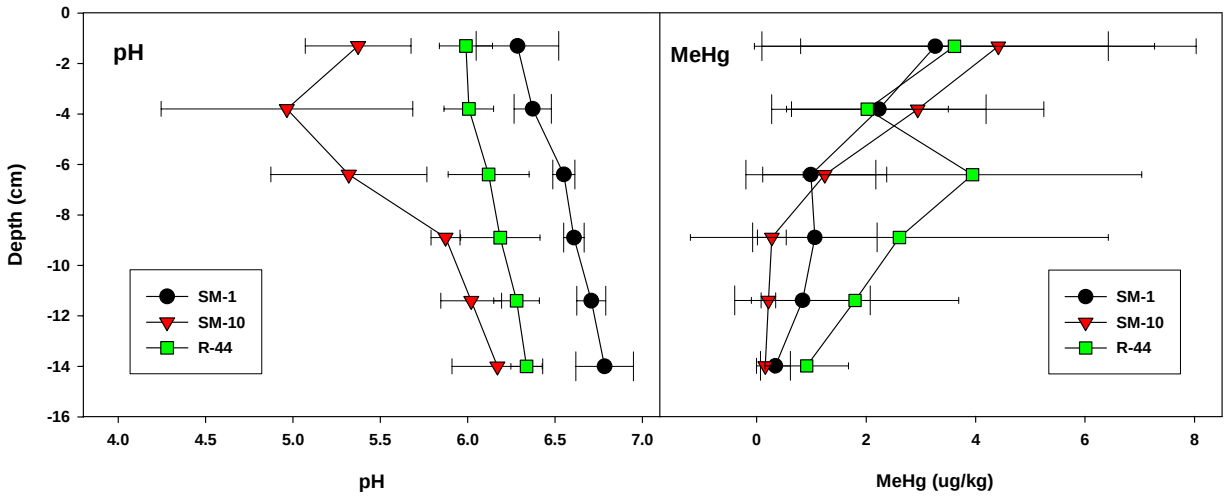

Spearman Rank Order Correlations (MeHg vs pH)[1]:

Group	N	rho	P-Value
All	18	-0.342	0.1610
SM-1	6	-0.943	0.0167
SM-10	6	-0.829	0.0583
R-44	6	-0.714	0.1360

[1] Based on mean values of replicate data.

Figure 6. Depth profile comparisons and correlations for pH and MeHg in cores collected at HAAF (SM-1, SM-10) and China Camp (R-44). Mean values and SD (N=5).

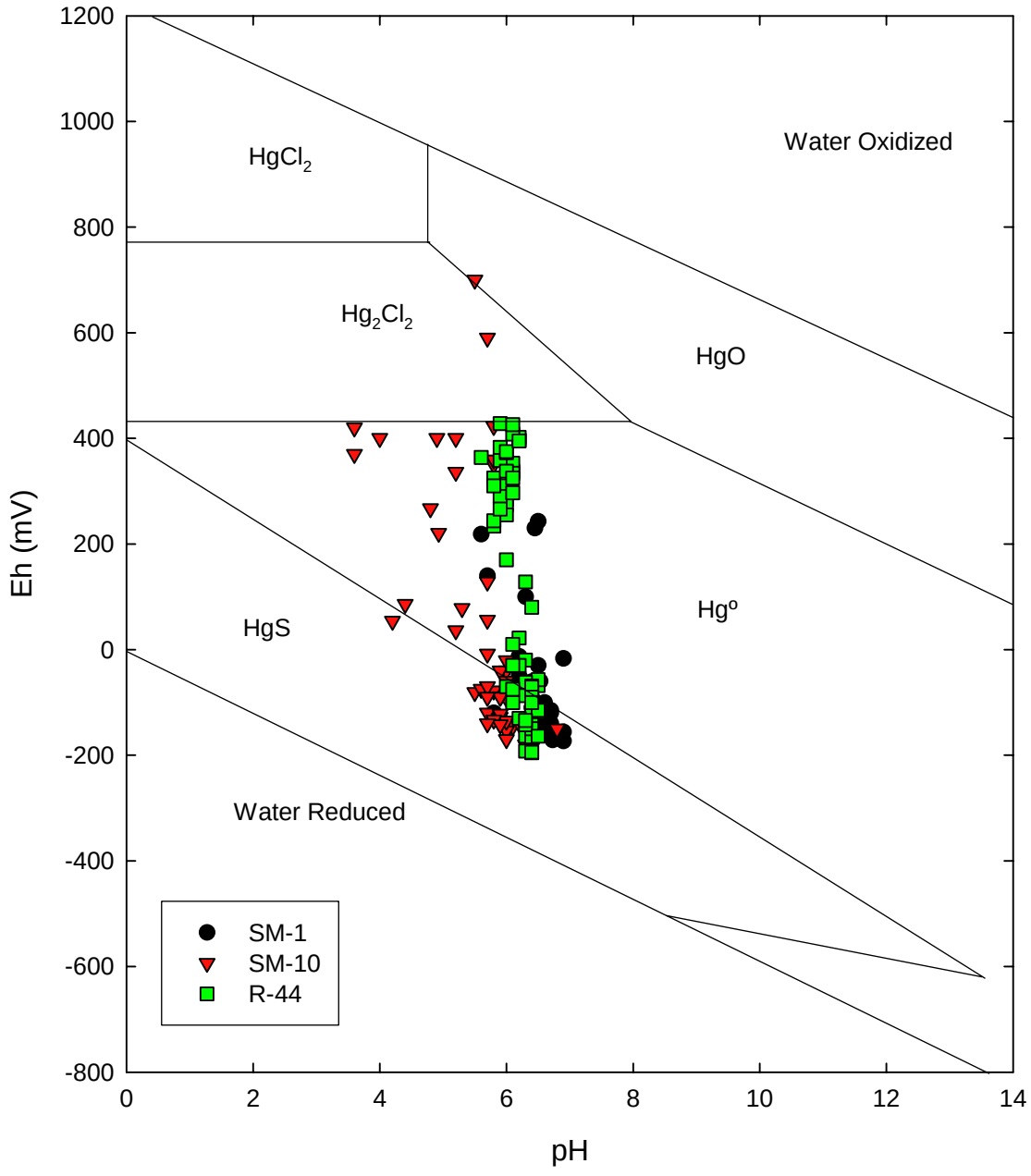

Figure 7. Eh-pH diagram (Mills 1997) populated with data from samples collected at HAAF (SM-1, SM-10) and China Camp (R-44).

Figure 8a. *Geukensia demissa*.

Figure 8b. *Hemigrapsus oregonensis*.

Figure 8c. *Nassarius obsoletus*.

Figure 8. Invertebrate organisms collected at HAAF and China Camp. Mussels (5a), crabs (5b), and snails (5c).

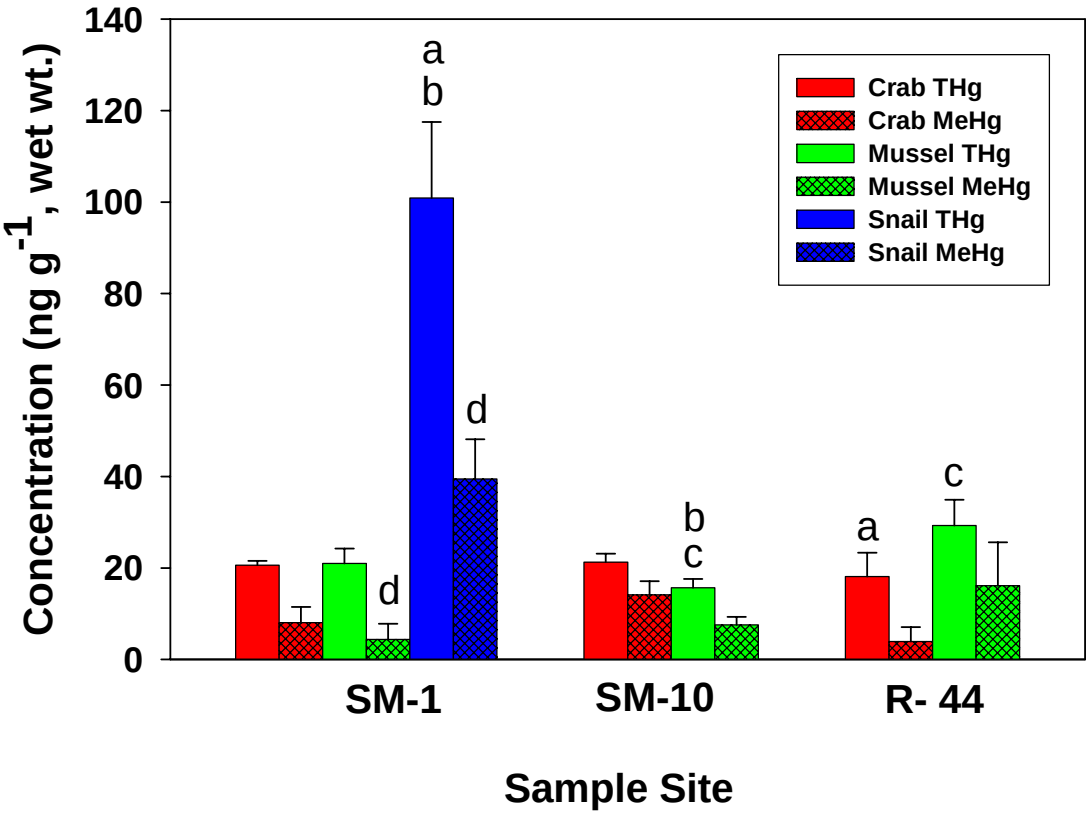

Figure 9. Tissue concentrations of THg and MeHg in invertebrates collected at HAAF (SM-1, SM-10) and China Camp (R-44). Mean values and SD (N=5). Matched letters indicate results were significantly different by Kruskal-Wallis One Way ANOVA on Ranks with Dunn's post hoc test ($P < 0.05$).

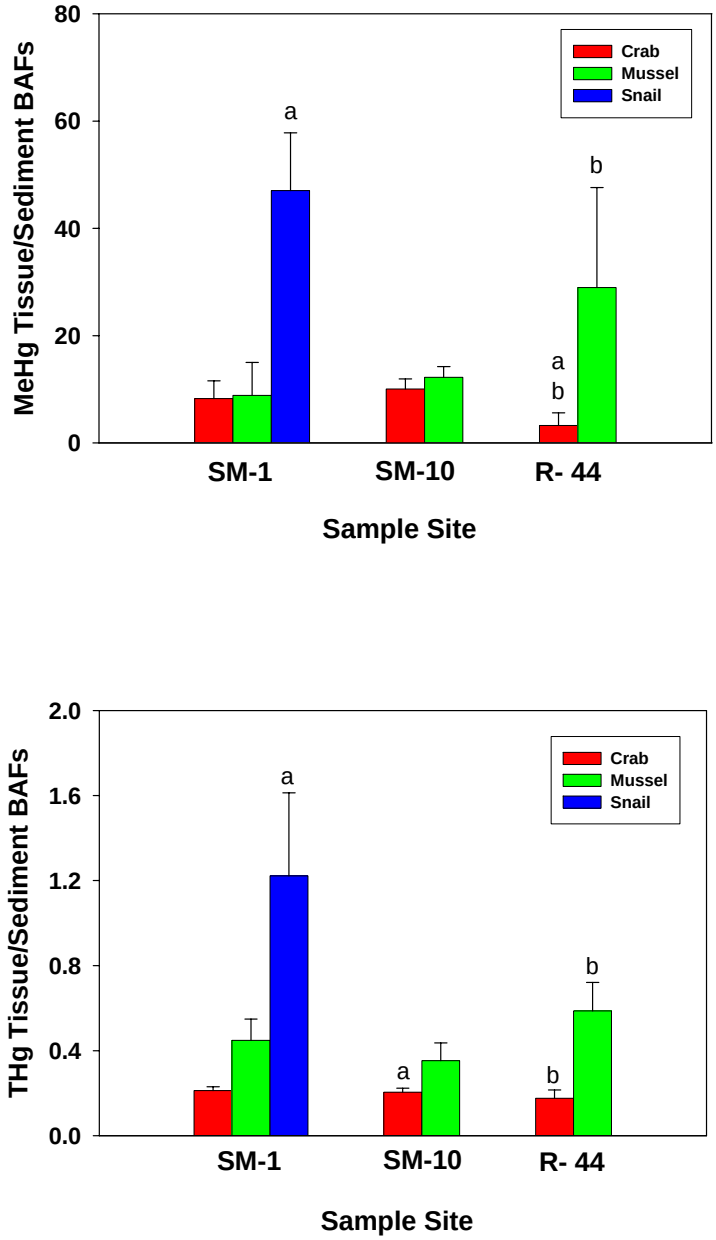

Figure 10. Bioaccumulation Factors (BAFs) for MeHg (upper) and THg (lower) in invertebrates collected at HAAF (SM-1, SM-10) and China Camp (R-44). Mean values and SD (N=5). Matched letters indicate results were significantly different by Kruskal-Wallis One Way ANOVA on Ranks with Dunn's post hoc test ($P < 0.05$).

Table 1. Sample stations in vegetation zones.

Site/ Vegetation zone	HAAF	Bel Marin	China Camp
Low marsh	SM-1 Lat. (N) 38° 02.904 Long. (W) 122° 29.613 (*S. foliosa* dominated) SM-10 Lat. (N) 38° 03.116 Long. (W) 122° 29.550 (*S. foliosa* dominated)		R-44 Lat. (N) 38° 00.411 Long. (W) 122° 28.758 (*S. foliosa* transitioning into *S. virginica*)
Mid marsh	SM-10U Lat./Long Not measured (10 m inland from SM-10) (*S. virginica* dominated with abundant detritus)		
Diked high marsh		BM-50a Lat. (N) 38° 03.116 Long. (W) 122° 29.550 (pump station creek edge) (*S. virginica* dominated)	

Table 2. Total Hg and MeHg levels in HAAF Bay Edge (SM-1, SM-10; N = 5), China Camp (R-44; N = 5), Bel Marin (BM-50a; N = 1), and HAAF Inland (SM-10U; N = 1) soil/sediment cores. Mean (SD).

Depth (cm)	THg (ng g^{-1})	MeHg (ng g^{-1})	MeHg (%)[1]
SM-1			
0 - 2.5	330 (61)	3.3 (3.2)	0.92 (1.1)
2.5 - 5.1	330 (43)	2.2 (2.0)	0.62 (0.69)
5.1 - 7.6	330 (46)	0.99 (1.2)	0.30 (0.32)
7.6 - 10.2	350 (32)	1.1 (1.1)	0.28 (0.37)
10.2 - 12.7	400 (34)	0.84 (1.2)	0.20 (0.31)
12.7 - 15.2	420 (35)	0.34 (0.27)	0.50 (1.0)
SM-10			
0 - 2.5	330 (35)	4.4 (3.6)	1.3 (0.93)
2.5 - 5.1	340 (43)	2.9 (2.3)	0.69 (0.62)
5.1 - 7.6	360 (37)	1.2 (1.1)	0.30 (0.32)
7.6 - 10.2	380 (40)	0.28 (0.26)	0.07 (0.07)
10.2 - 12.7	350 (28)	0.22 (0.13)	0.07 (0.04)
12.7 - 15.2	380 (18)	0.16 (0.16)	0.04 (0.04)
R-44			
0 - 2.5	320 (40)	3.6 (3.7)	1.2 (1.3)
2.5 - 5.1	340 (38)	2.0 (1.5)	0.63 (0.47)
5.1 - 7.6	350 (36)	3.9 (3.1)	1.1 (0.89)
7.6 - 10.2	340 (54)	2.6 (3.8)	0.79 (1.1)
10.2 - 12.7	370 (79)	1.8 (1.9)	0.54 (0.64)
12.7 - 15.2	410 (100)	0.91 (0.76)	0.25 (1.2)
SM-10U			
0 – 7.6	480	1.7	0.6
7.6 – 10.2	710	0.79	0.11
10.2 –14.0	500	0.9	0.18
14.0 – 17.8	530	1.4	0.27
17.8 – 24.1	550	13	2.3
24.1 – 30.5	500	6.9	1.4
30.5 – 40.6	510	3.1	0.61
BM-50a			
0 - 2.5	190	2.2	1.1
2.5 - 5.1	190	2.4	1.2
5.1 - 7.6	190	0.8	0.41
7.6 - 10.2	170	2	1.2
10.2 - 12.7	170	2.4	1.5
12.7 - 15.2	160	2.6	1.6

Table 3. Appearance of seven visually different depth sections of upland Salt Marsh core sample (SM-10U).

Depth (cm)	Observed appearance
0 – 7.6	Loose plant detritus
7.6 – 10.2	Compacted plant detritus
10.2 –14.0	Red and light gray compacted material
14.0 – 17.8	Light gray compacted material
17.8 – 24.1	Medium gray compacted material
24.1 – 30.5	Dark gray compacted material
30.5 – 40.6	Dark gray compacted material with black flecks

Table 4. Sediment quality characteristics of HAAF (SM-1, SM-10) and China Camp (R-44) soil/sediment cores. Mean (SD).

Depth Section (cm)	Eh (mV)	AVS (µg/g)	TOC (%)	Sand (%)	Silt (%)	Clay (%)	Fines (%)
SM-1							
0 - 2.5	180 (210)	51 (83)	4.4 (0.9)	61 (29)	21 (24)	18 (6)	0.39 (0.29)
2.5 - 5.1	- 49 (86)	110 (150)	4.5 (0.8)	51 (30)	30 (24)	20 (7)	0.50 (0.30)
5.1 - 7.6	-110 (35)	20 (19)	4.2 (0.5)	44 (26)	35[2] (24)	21[2] (3)	0.56[2] (0.26)
7.6 - 10.2	-110 (59)	140 (150)	3.6 (0.5)	57 (30)	23 (25)	19 (5)	0.43 (0.30)
10.2 - 12.7	-160 (9)	150 (220)	3.2 (0.7)	50 (30)	25 (25)	26 (3)	0.50 (0.26)
12.7 - 15.2	-160[1]	230 (210)	2.7 (0.6)	31 (21)	36 (19)	33 (8)	0.69 (0.21)
SM-10							
0 - 2.5	380 (240)	30 (30)	4.7 (1.1)	31 (11)	53 (8)	16 (5)	0.69 (0.11)
2.5 - 5.1	280 (280)	24 (27)	4.7 (0.5)	32 (11)	53 (9)	15 (3)	0.68 (0.11)
5.1 - 7.6	42 (210)	51 (74)	4.2 (0.7)	25 (11)	60 (8)	16 (4)	0.75 (0.11)
7.6 - 10.2	-16 (210)	66 (64)	3.6 (0.5)	15[2](1)	69[2] (2)	16 (1)	0.85[2] (0.01)
10.2 - 12.7	-130 (45)	70 (28)	3.3 (0.2)	13[2] (6)	67[2] (7)	21 (2)	0.87[2] (0.06)
12.7 - 15.2	-110 (36)	89 (63)	2.9 (0.1)	12[2] (3)	65[2] (3)	23 (3)	0.88[2] (0.03)
R-44							
0 - 2.5	350 (72)	120 (240)	3.1 (0.4)	12 (9)	58 (6)	31 (9)	0.89 (0.09)
2.5 - 5.1	290 (92)	50 (90)	3.6 (0.7)	20 (8)	53 (8)	27 (9)	0.80 (0.08)
5.1 - 7.6	200 (190)	120 (210)	3.7 (0.8)	14 (10)	52 (9)	35 (9)	0.86 (0.10)
7.6 - 10.2	76 (230)	140 (280)	3.7 (0.6)	5.4 (3.2)	56 (4)	42 (8)	0.95 (0.03)
10.2 - 12.7	15 (180)	51 (54)	3.8 (0.6)	7.2 (2.8)	56 (6)	37 (6)	0.93 (0.03)
12.7 - 15.2	-130 (66)	35 (23)	3.3 (0.5)	4.4(3.5)	56 (5)	40 (5)	0.96 (0.03)

[1] Not Replicated.

[2] N = 4. All others, N = 5

Table 5. THg, MeHg, percent MeHg and bioaccumulation factors (BAF) in benthic invertebrates collected at HAAF (SM-1, SM-10) and China Camp (R-44) sites - June 2003.

Invertebrate	THg (ng g^{-1} wet wt.)	MeHg (ng g^{-1} wet wt.)	MeHg[1] (%)	THg (ng g^{-1} dry wt.)	MeHg (ng g^{-1} dry wt.)	THg BAF[2]	MeHg BAF[2]
SM-1							
Crab	20.6 (0.9)	8.0 (3.4)	67.3 (17.0)	69.6 (5.8)	26.9 (10.7)	0.21 (0.02)	8.2 (3.3)
Mussel	21.0 (3.2)	4.4 (3.4)	20.5 (13.9)	147 (33)	28.9 (20.0)	0.45 (0.10)	8.8 (6.1)
Snail	100.9 (16.6)	39.5 (8.7)	39.9 (11.0)	401 (128)	153 (35)	1.2 (0.4)	46.0 (10.8)
SM-10							
Crab	21.3 (1.8)	14.2 (2.9)	67.4 (17.0)	67.0 (6.0)	44.5 (8.2)	0.2 (0.02)	10.1 (1.9)
Mussel	15.7 (1.9)	7.5 (1.8)	49.0 (12.9)	115 (27)	54.0 (8.8)	0.35 (0.08)	12.3 (2.0)
R-44							
Crab	18.1 (5.2)	3.9 (32)	19.9 (10.3)	56.0 (12.7)	11.8 (8.6)	0.18 (0.04)	3.3 (2.4)
Mussel	29.3 (5.7)	16.0 (9.4)	53.8 (30.9)	187 (43)	105 (67)	0.58 (0.13)	29.2 (18.6)

[1] Values represent percent MeHg as a percentage of THg.

[2] BAFs calculated as the ratio of tissue dry weight concentration divided by the surface (0 - 2.5 cm) sediment dry weight concentration from Table 2.

4 - Bioavailability of Mercury to Benthic Invertebrates: Characterization and Remediation Effects in HAAF Wetland Sediments

SUMMARY

Many studies have identified the potential adverse effects, bioaccumulation and biomagnification of Hg. As such, it is imperative that the bioavailability of Hg, and in particular the MeHg species, be ascertained as part of any assessment of environmental and human risk. The study incorporated two research goals, (1) to establish baseline bioaccumulation of Hg and MeHg in a representative and locally abundant benthic organism, the bent nosed clam *Macoma nasuta*, and (2) whether Hg uptake might be reduced by the addition of Hg-sorbing materials into the sediment. In the bioaccumulation experiment we measured the uptake and elimination of THg and MeHg in *M. nasuta* exposed to HAAF Bay Edge (SM-1 and SM-10) and the reference site China Camp State Park (R44) cores. A similar pattern of THg temporal bioaccumulation and similar final THg body burden at termination of the uptake phase of the experiment suggest that the bioavailability of THg was similar at all sites. The uptake phase was characterized by a rapid increase in body burden followed by a slower increase whereas during the elimination phase a rapid decrease in body burden was followed by a slower decrease. Overall, the bioaccumulation study indicated that the elimination of Hg is very slow in benthic clams, as the apparent steady state body burden was not reached following a 56-d exposure. The body burdens of the experimentally exposed clams were only approximately half of those recorded in clams inhabiting Bay Edge sediments, further suggesting that longer exposure periods longer than 56-d are needed for THg to approach apparent steady-state in clam tissues. The tissue MeHg concentrations varied considerably between replicates throughout the exposure hampering the observation of temporal changes in body burden during the uptake and elimination phases of the bioaccumulation experiment.

In the remediation study, sediment from the SM-10 site was used to test the effects of granular activated carbon (GAC) and sulfonated Kraft lignin on speciation and bioaccumulation of THg and MeHg in 56-d exposures using *M. nasuta*. Results were mixed but promising. GAC significantly decreased the bioaccumulation of spiked MeHg, and MeHg methylated from spiked Hg^{2+}, despite the higher concentration of those substances in the amended sediment, while it did not affect the bioaccumulation of legacy $Me^{202}Hg$. We suggest that GAC was more effective in reducing the uptake of spiked Hg species, since these were more labile and hence were freer to associate with GAC particles. In contrast, ambient Hg is more likely to be in closer association with sediment ligands, and hence would be more refractile and less available for contact with GAC. We suggest that further experiments should contact sediment with GAC for periods longer than 16 days, to address efficacy of GAC on ambient Hg availability. Sulfonated Kraft lignin was extremely soluble in seawater, suggesting a short theoretical contact time with Hg in

the sediments and raising issues of transportation of any lignin-sorbed Hg out of the system. Therefore, lignin was eliminated as a viable sorption candidate.

INTRODUCTION

Hg is one of the most studied trace elements, due to its high toxicity to both humans and animals, its association with historical and recent anthropogenic activities, and its disposition for biomagnification in food webs as MeHg (Chan et al., 2003). Hg contamination has been recognized as a serious problem in San Francisco Bay for many years, predominantly as a result of gold and silver mining activities in the coastal mountain ranges since the mid 1800s (Alpers and Hunerlach, 2000).

Many studies have identified the potential for bioaccumulation of Hg, and that the retention of MeHg within organism tissue and high trophic transfer efficiency results in significant potential for Hg biomagnification within food webs. As such, it is imperative that the bioavailability of Hg, and in particular the MeHg species, be ascertained as part of characterization of Hg risk assessment. This study investigated the bioaccumulation of Hg and MeHg in a representative and locally abundant benthic organism, the bent nosed clam *Macoma nasuta*.

In addition, this study addressed whether the Hg and MeHg bioavailability might be reduced by the addition of Hg-sorbing material. Recent studies have demonstrated that low-density carbonaceous particles can reduce contaminant aqueous availability in sediments (e.g. Zimmerman et al., 2004, Millward et al., 2004). In addition, activated carbon has been shown to be an effective sorbent of Hg in the elemental (USEPA 1997), ionic (Calgon Corp. unpubl.) and methyl forms (Victor Magar, Battelle, pers. comm.). Sulfonated Kraft lignin is a byproduct of the paper industry, characterized by a high density of Hg-reactive sulfur groups, suggesting potential for sorption of ionic Hg. We investigated whether the addition of such materials reduce the bioavailability of Hg to *M. nasuta* due to the repartitioning of Hg species onto these strong sorbents from more labile phases.

OBJECTIVES

The objectives of this study were to (1) describe the bioaccumulation of Hg to a representative sediment-dwelling intertidal invertebrate, and (2) explore the utility of Hg-sorbent addition as an *in situ* remediation technique.

APPROACH

In the bioaccumulation experiment we measured the uptake and elimination of THg and MeHg in the sediment-dwelling bivalve *Macoma nasuta* to establish site-specific patterns of bioaccumulation of those contaminants. In the remediation experiment, we tested the efficacy of two potential sorbents, granular activated carbon (GAC) and sulfonated Kraft lignin, in reducing the bioavailability of THg and MeHg to *M. nasuta*. The latter experiment was expected to

provide baseline information for potential THg and MeHg remediation strategies for HAAF sediments.

Study Site

Sediment samples were collected from three tidal wetland sites: two locations at the HAAF Bay Edge (SM-1 and SM-10), with a high potential for Hg methylation, and one reference location at the China Camp State Park (R44; McFarland et al., 2002; Chapters 1 and 3, This Report).

Sample Collection

Sediment samples were collected on 10-12 July 2003**.** Methods for the collection, transportation and storage of sediments for both studies were designed to prevent the methylation of Hg in the sediment prior to the initiation of the experiment (Ullrich et al., 2001). For the bioaccumulation experiment, sediment cores (10.2 cm diameter, 20.3 cm height) were collected at the three field sites using schedule 40 PVC piping. Twenty-four cores containing undisturbed surficial sediment were taken from each sampling location. Sediment cores were capped immediately, flash-frozen and transported to Vicksburg, MS, packed with dry ice. Sediment cores were stored at 4º C for < 4 days before use. For the remediation experiment, surficial sediments were collected in 4-L buckets from site SM-10 only.

Experimental Organism

The estuarine, sediment-dwelling clam, *Macoma nasuta,* was used in all experiments. This bivalve inhabits shallow mud to muddy-sand substrates and occurs from Alaska to Southern California. The species has been recorded from the San Francisco Bay sediments, and fills a niche similar to that of *M. balthica*, a clam common in the intertidal sediments in San Pablo Bay. *Macoma nasuta* is a facultative deposit feeder, capable of suspension filter feeding and selective deposit feeding, and typically burrows down to a depth of 15 cm. Its siphons are separated: the inhalant siphon takes up detritus and organic matter directly from either the overlying water or from the substrate, while the exhalant siphon deposits the indigestible particles and sediment on the sediment surface. The clams were purchased from a commercial vendor (Aquatic Research Organisms, Hampton, NH), who collected them from an unknown location and shipped them overnight to the Environmental Laboratory in Vicksburg, MS. Upon arrival, clams were acclimated to 15 °C in 25-‰ artificial seawater over a period of 2-3 h.

Sediment Exposures

The bioavailability of Hg and the effects of remediation strategies upon bioavailability, were assessed by measuring bioaccumulation and kinetics of THg and MeHg in *M. nasuta* using methods based on standard bioaccumulation test protocols (USEPA, 1989)**.**

Bioaccumulation Experiment

The uptake and elimination of THg and MeHg were investigated in *M. nasuta* exposed to intact sediment cores collected from the SM-1, SM-10 and China Camp R-44 sites. Time-series-sediment exposures were conducted using HAAF sediments from the three locations to establish site-specific patterns of bioaccumulation. Each core was submerged in an upright position in one 4-L plastic container containing 25‰ artificial seawater (2:3 ratio mixture of Forty Fathoms

Crystal Sea®, Baltimore, MD, and Instant Ocean®, OH), on 16 June, i.e., 5-6 days following sediment collection. Cores were maintained at 15°C in a temperature-controlled water bath under constant aeration using air stones. Five clams were sampled for tissue analysis prior to use in the experiment (day 0). After 48 h, one clam was added to each core. The water in each container was renewed three times weekly and no supplemental food source was provided. To determine the uptake rate, clams were sampled after 2, 7, 14, 28, and 56 d of exposure, with three replicates per time point. At day 56, the remaining clams were transferred to approximately 300 g WW of laboratory-control sediment from Sequim Bay, WA (pre-sieved to < 0.3 mm, 57 ± 1 ng g^{-1} DW THg), in 1-L beakers. Clams were sampled after 7, 14, and 28 days of exposure to control sediment to determine elimination rates. Tissues were removed from the clam shells, rinsed, blotted dry, wet weighed and stored at –80°C for subsequent chemical analysis. Sediment samples were taken from the top 2 cm of 3 replicate exposure beakers for each sediment treatment at experiment initiation, and analyzed for THg, MeHg, total organic carbon (TOC), acid-volatile sulfide (AVS) and simultaneously extractable metals.

Remediation of Hg Bioavailability Experiment

Sediment from the SM-10 site was used to test the effects of granular activated carbon (GAC) and sulfonated Kraft lignin on speciation and bioaccumulation of THg and MeHg, using methods derived from similar sorbent remediation trials (Zimmerman et. al., submitted; Millward et. al. submitted). GAC is a heat-activated carbon substrate of both high surface area and high affinity for non-polar and ionic compounds, and has been suggested as a viable sorbent for the removal of contaminants from gaseous, aqueous and sediment phases (Millward et al, submitted). GAC has a proven ability as a sorbent for Hg in the elemental (USEPA, 1997), ionic (Calgon Carbon Corp., Pittsburgh, PA. unpubl.) and methyl forms (V. Magar, Battelle, 2003, pers. comm.).

The addition of a sorbent as an in-situ treatment for contaminated sediments is under evaluation in laboratory and field trials, both as an introduced additive and as part of an active cap (Zimmerman et al, submitted, Millward et al, submitted, Magar pers. com). The addition of sorbent materials is expected to repartition the contaminants from the sediment and pore water phases onto the more strongly binding sorbent matrix, thereby reducing the availability flux into pore water and bioaccumulation into organisms. Experimental trials conducted at our laboratory in collaboration with Stanford University, have shown that GAC reduces PCB concentrations in pore water by 92% and PCB bioaccumulation by up to 87% after 6 months of contact (Millward et al. submitted). Other trials have shown that a GAC cap reduces flux of aqueous MeHg by 96% after 14 days. In addition, up to 58% of MeHg and 62% of THg can repartition from the sediment onto the sorbent after 4 months of contact (Magar, pers. comm.). These data suggest that GAC addition to contaminated sediments warrants consideration as a remediation strategy to reduce the availability of Hg for uptake into organisms and for methylation by microbes.

The surface sediments collected at HAAF site SM-10 were homogenized and sampled in triplicate for THg and MeHg. Sediments were divided into three portions, one was amended with 3.4% (by DW) GAC, one was amended with 3.4% (by DW) sulfonated Kraft lignin, and the third portion served as an untreated control. After amendment, the sediments were mixed thoroughly with an impeller for approx. 4 h, placed in sealed glass containers and rolled at room temperature for 16 d. Sediments were then sampled for total THg and methyl MeHg. After sub-sampling, sediments were divided into 7 replicate beakers, with approximately 150g (DW) of

sediment in each beaker. Replicates were covered with water (25‰ artificial sea water), aerated gently and the sediments were allowed to settle for 24h. Adult *M. nasuta* (range 6.1 – 7.2 g whole wet weight) were added to each beaker, and were maintained at 15 °C for 56 days. Water was renewed three times a week, and no supplemental food was provided.

In addition, we addressed the effects of GAC and lignin on the pool sizes of THg and MeHg. After sediment amendment and 16-d mixing, 500g aliquots (dry weight) of each sediment were spiked with a cocktail of ^{199}Hg(II): Me^{200}Hg isotope cocktail, sufficient to add 15-ng/g ^{199}Hg(II) and 150-pg/g Me^{200}Hg (for details method, see Chapter 1, This Report). Sediment sub-samples were taken to determine the initial ^{199}Hg(II): methyl ^{200}Hg ratio and frozen at -80°C until further analysis. The remaining sediment was divided into three 1-L beakers and used in the *M. nasuta* exposures described above. After 56 d, 3 animals were harvested from each treatment, and the tissue and sediment samples were frozen prior to analysis for THg, MeHg, and stable Hg isotopes. Results of the stable isotope experiment were used to quantify the impacts of GAC and lignin amendment on the bioaccumulation of ambient Hg, ambient MeHg, spiked MeHg and newly methylated Hg.

Chemical Analyses

Clam tissue and sediments were extracted and analyzed for THg using the USEPA Method 7471A cold-vapor technique (USEPA, 1994). MeHg concentrations in sediment and tissue samples were determined using sample distillation and cold trapping prior to derivatization with sodium tetraethylborate. The volatile ethylated compound was then separated and detected by gas chromatography and atomic fluorescence (Demuth and Heumann, 2001). MeHg determinations were performed under clean room conditions by the procedure described previously (McFarland et al., 2002). Total organic carbon content of sediments was measured using an Astro 2100 TOC analyzer (Zellweger Analytics, League City, TX, USA). Acid-volatile sulfide and simultaneously extractable metals were measured using the diffusion method of Leonard et al. (1996).

RESULTS AND DISCUSSION

Bioaccumulation Experiment

Sediment Chemistry

Preliminary analyses of the intact sediment cores collected from SM-1, SM-10 and R-44 sites revealed that concentrations of THg, MeHg, TOC and simultaneously extractable metals were similar at the three sites (Table 1). However, concentrations of acid-volatile sulfide (AVS) in the top 2 cm at SM-1 and SM-10 were low. In contrast, AVS was relatively high in the China Camp sediment, and was in excess of the concentrations of simultaneously extractable metals and total inorganic Hg, suggesting that most metals would be present as insoluble sulfides in reducing conditions. Bay Edge sediments offered a less sulfidic environment, probably due to the higher porosity of these sediments linked to the lower silt content (Chapter 3, This Report) and visually apparent deeper redox potential discontinuities compared to the China Camp sediment. The lower sediment sulfide concentrations at the Bay Edge sites would suggest only partial binding of metals into insoluble sulfides (although the extremely high affinity of Hg^{2+} for S^{2-} would lead to preferential HgS formation should any sulfide become present), suggesting that

excess inorganic Hg at Bay Edge was available for methylation and bioaccumulation at the time of sampling.

Bioaccumulation

Detectable levels of THg and MeHg were present in the clams before exposure (THg 14 ng g^{-1}, MeHg 8 ng g^{-1} wet weight). A similar pattern of THg temporal bioaccumulation and similar final THg body burden at termination of the uptake phase of the experiment (Fig.1) suggest that the bioavailability of THg was similar at all sites, despite the presence of excess sulfide measured at R-44, but not at Bay Edge sites SM-1 and SM-10. We conclude that any HgS formation at R-44 resulting from the reducing conditions at this site did not affect Hg bioavailability. Tissue MeHg concentrations varied considerably between replicates throughout the exposure (9 - 17 ng g^{-1} for SM-1, 13 - 18 ng g^{-1} for SM-10, and 13 – 21 ng g^{-1} for R-44, data are not shown) hampering the observation of temporal changes in body burden during the uptake and elimination phases of the bioaccumulation experiment.

THg uptake and elimination kinetics did not conform to single compartment kinetics at all sites. The uptake and elimination of THg appeared to be biphasic processes. The uptake process was characterized by a rapid (< 7 d) uptake phase to 14 – 18 ng g^{-1} wet weight above background, followed by a slower uptake phase to 52 – 57 ng g^{-1} THg above background. Similarly, elimination was characterized by a rapid (< 14 d) loss of 29 – 33 ng g^{-1} of day 56 residues, followed by a slower elimination phase after day 14. One plausible explanation for the rapid initial uptake (and elimination) is the ingestion (and egestion) of contaminated sediment. Simple calculations indicate that the initial rapid increase in body burden during the uptake phase could be explained by the ingestion of approximately 30 mg dry weight sediment, and that the rapid decrease in body burden during the initial rapid elimination phase could be explained by the ingestion of approximately 60 mg dry weight sediment. While we were unable to find literature references to *Macoma* gut volumes, it is plausible that the flux of ingested sediment accounts for the rapid 'uptake' and 'elimination' phases of THg accumulated. Uncertainty regarding the impact of ingested material on body burden analyses prevents us from establishing uptake and elimination kinetics. Nevertheless, the bioaccumulation data indicated that the elimination of Hg is very slow in these organisms, as the apparent steady state body burden was not reached following a 56-d exposure. The final body burdens of the experimentally exposed clams were only 55-59% of those recorded in *Modiolus* sp. clams collected at a range of sites at Hamilton in 2001 (McFarland et al., 2002), further suggesting that long exposure periods are needed for THg to approach apparent steady-state in this species.

Remediation of Hg Bioavailability Experiment

Effect of GAC and Lignin on Sediment MeHg

The addition of GAC did not affect the THg concentration in sediment, as expected (Fig. 2). However, ambient MeHg concentrations in the sediment was substantially higher in the GAC-amended treatment (1.34 ± 0.07 ng g^{-1}) compared to the non-amended treatment (0.85 ± 0.04 ng g^{-1}) (Fig. 2). The concentration of spiked MeHg ($Me^{200}Hg$ and of $Me^{199}Hg$) were also higher in GAC-treated sediments (Fig. 2). Presently we cannot explain this increase, but will monitor this phenomenon in future studies.

The addition of GAC did not significantly affect the bioaccumulation of legacy $Me^{202}Hg$ in this experiment (Fig. 3). However, as noted above, the legacy $Me^{202}Hg$ concentration was elevated in the GAC treatment, resulting in higher MeHg exposure. Biota accumulation factor (BAF, concentration of a substance in an aquatic organism divided by the concentration of the substance in the sediment) were determined to quantify Hg and MeHg bioavailability in the laboratory exposures. The $Me^{202}Hg$ BAF for the GAC treatment was 46% lower than that for the untreated sediment (Fig. 4) indicating a decrease in the bioavailability of ambient MeHg BAF in the presence of GAC.

The presence of GAC decreased the bioaccumulation of $Me^{200}Hg$ by 63% and of $Me^{199}Hg$ by 85%, despite the increased concentration of MeHg in GAC-amended treatments. Therefore, the addition of GAC followed by a 16-d contact period caused decreases in bioaccumulation from the more labile Hg pools, added as a $Me^{200}Hg$ spike and newly methylated from the ^{199}Hg spike by an order of magnitude. GAC reduced the $Me^{200}Hg$ BAF by 89% and $Me^{199}Hg$ BAF by 93% demonstrating substantial effectiveness of GAC in reducing the bioavailability of spiked or newly formed MeHg. GAC was less effective in reducing the bioavailability of legacy $Me^{202}Hg$, as the corresponding BAF was reduced by only 46%.

Results from this study agree with results obtained from previous work with the effects of GAC on fate of MeHg (Magar. pers.com) reporting that the effects of GAC emerged far more rapidly for the more labile aqueous phase than for the more recalcitrant, sediment-associated MeHg. This is almost certainly due to the slow and partial release of MeHg from a solid into the dissolved phase, from where it is available for repartitioning onto the sorbent-active-surface. Such desorption-rate-limiting processes have been observed in sorbent studies with PCB-contaminated sediments (Millward et al. submitted, Zimmerman et al. submitted). If this is the case, then contact periods longer than 16 days should be used to address the longer-term efficacy of GAC on legacy Hg availability.

Sulfonated Kraft lignin was extremely soluble in sea water, suggesting a short theoretical contact time with Hg in the sediments and raising issues of transportation of any lignin-sorbed Hg out of the system. Therefore lignin was eliminated as a viable sorption candidate.

POINT OF CONTACT CHAPTER 4:

Rod N. Millward
Applied Research Associates, Inc.,
c/o U.S. Army U.S. Army Engineer Research and Development Center,
Environmental Laboratory, Vicksburg, Mississippi, USA
Ph: 601-634-3669; Email: roderic.n.millward@erdc.usace.army.mil

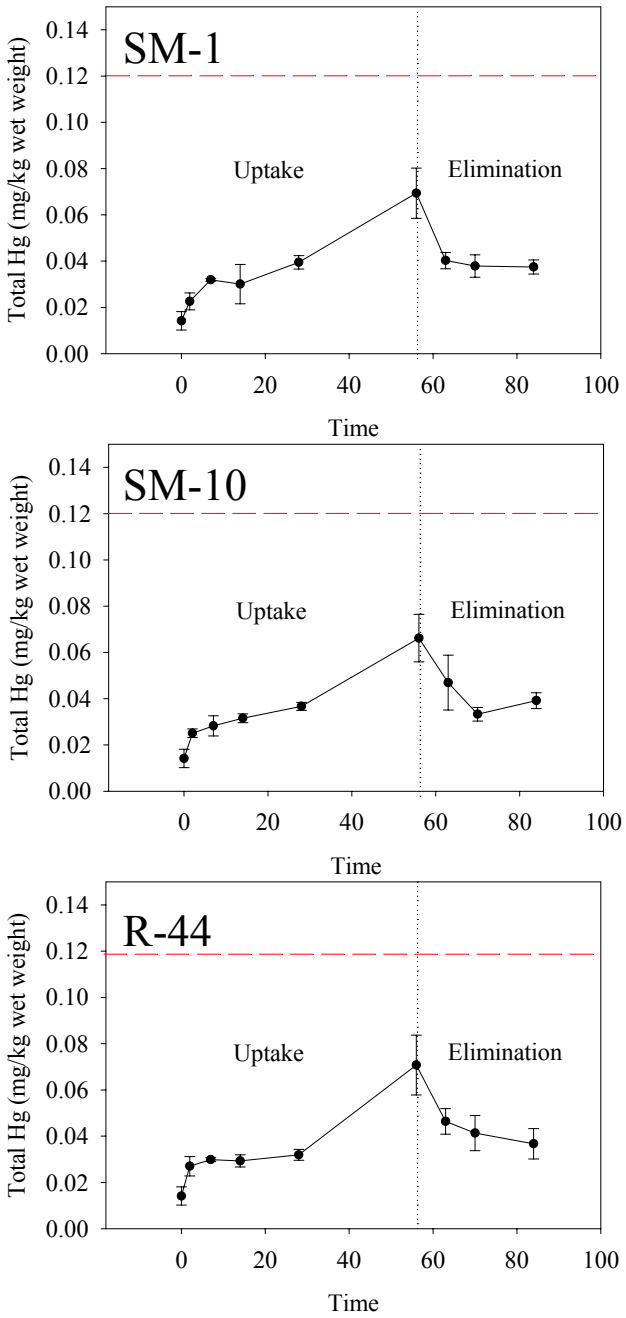

Figure 1. Uptake and elimination of THg from *Macoma nasuta* exposed to SM-1, SM-10 and R-44 sediments. Dashed line indicates the body burden in field-collected *Modiolus* sp. (0.12 ng kg^{-1}, McFarland et al., 2002).

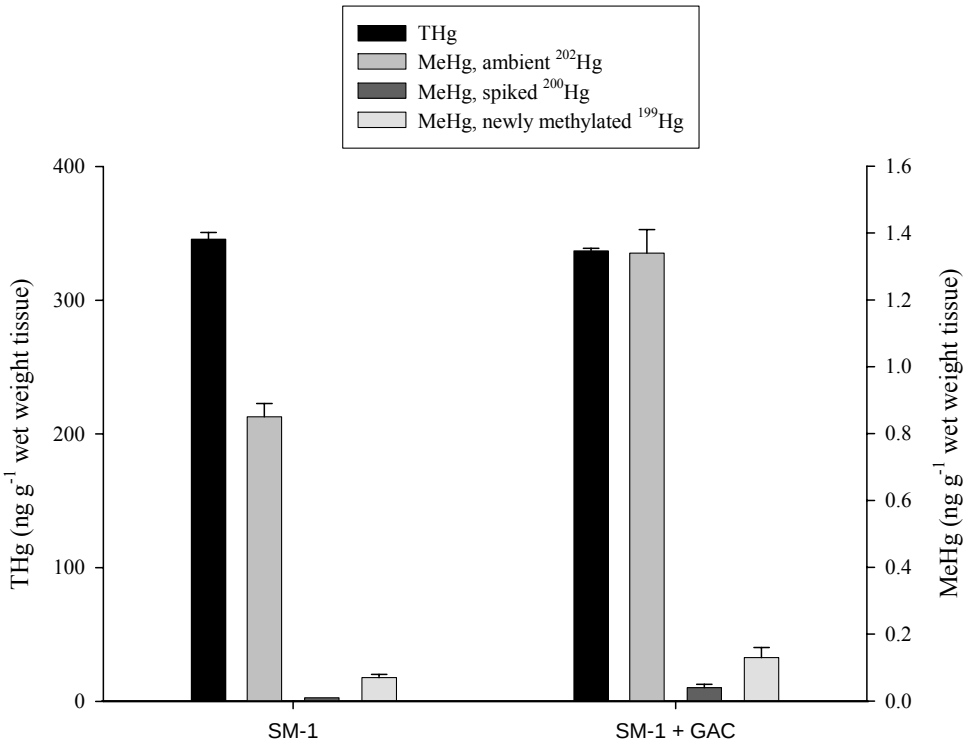

Figure 2. Effect of granular activated carbon on sediment pool sizes of legacy ^{202}Hg, spiked Me^{200}Hg and newly methylated ^{199}Hg.

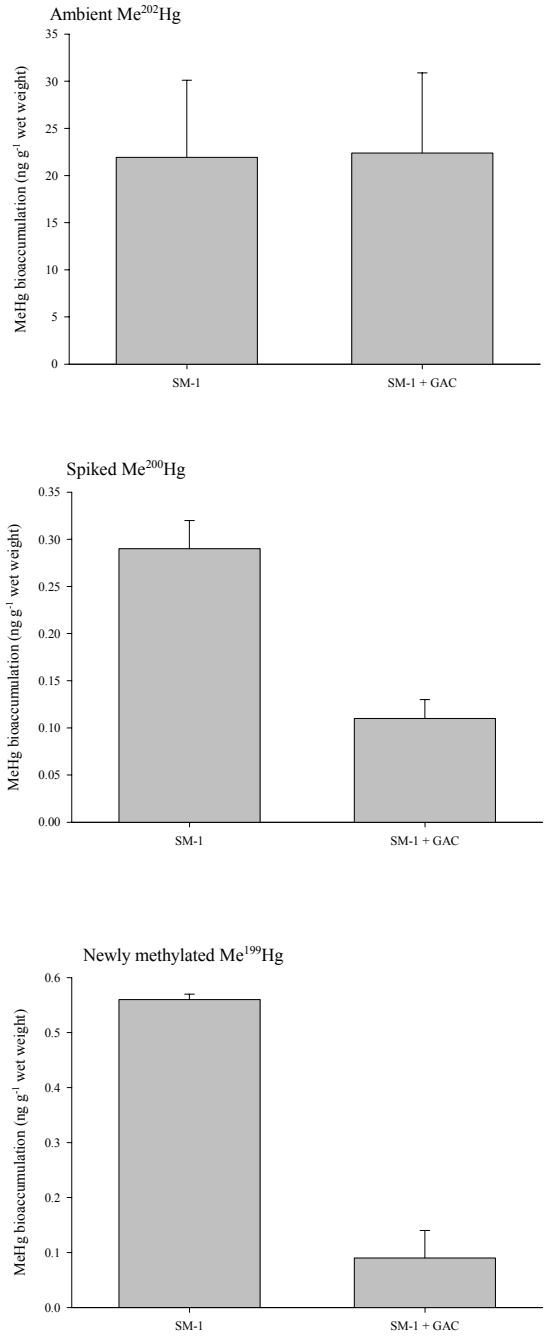

Figure 3. Effect of granular activated carbon on bioaccumulation of legacy ^{202}Hg, spiked $Me^{200}Hg$ and newly methylated ^{199}Hg.

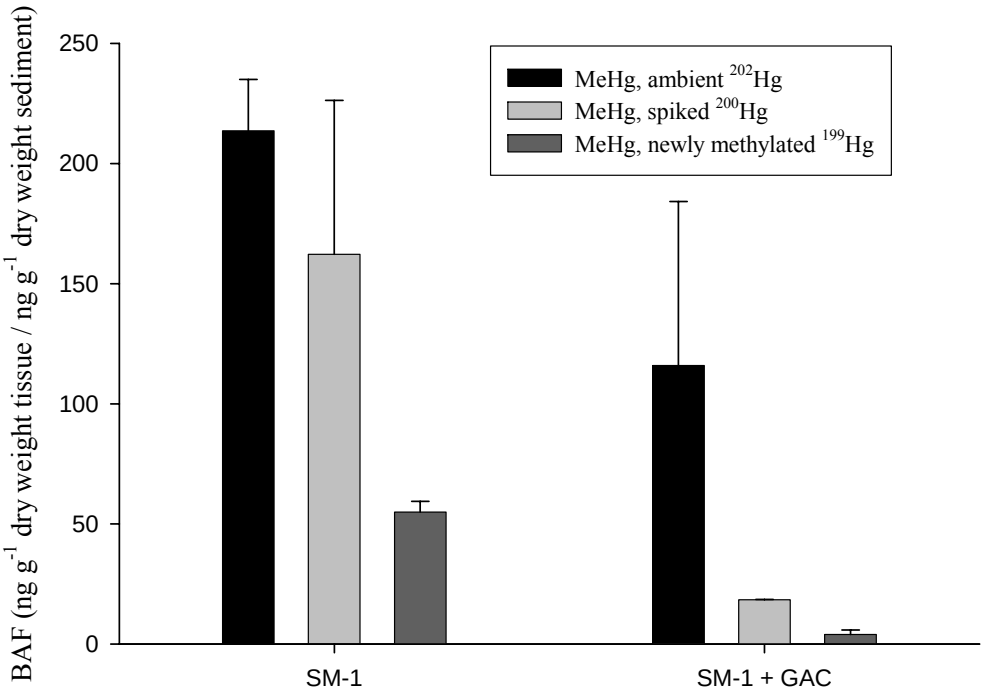

Figure 4. Effect of granular activated carbon on biota accumulation factor (BAF) for legacy ^{202}Hg, spiked $Me^{200}Hg$ and newly methylated ^{199}Hg.

Table 1. Chemical analyses of sediment from SM-1, SM-10 and China Camp (R-44). SEM = simultaneously extracted metal; AVS = acid volatile sulfide, TOC = total organic carbon.

Site	Hg ($ng\ g^{-1}$)	Methyl Hg ($ng\ g^{-1}$)	AVS ($ng\ g^{-1}$)	SEM_{Cu} ($ng\ g^{-1}$)	SEM_{Pb} ($ng\ g^{-1}$)	SEM_{Cd} ($ng\ g^{-1}$)	SEM_{Zn} ($ng\ g^{-1}$)	SEM_{Ni} ($ng\ g^{-1}$)	TOC (%)
SM-1	269	0.74	0	497	109	18	990	368	1.4
SM-10	266	1.00	101	483	107	19	975	382	1.5
R-44	270	1.54	5099	441	100	19	900	307	1.6

5- Integrating Physical, Chemical and Biological Processes that Drive Mercury and Methylmercury Cycling in San Pablo Bay Salt Marshes into a Screening-Level Model

SUMMARY

The *Questions and Decisions* ™ (QnD): screening model system was created to provide an effective tool to incorporate ecosystem and management issues into a user-friendly framework. The QnD model links the spatial components within GIS files to the prevalent abiotic, climatic, and biotic interactions in an ecosystem. QnD has a simple design and can be upgraded easily. This modeling approach has been applied to the Hamilton Army Airfield wetland restoration project (QnD:HAAF). The purpose of the current QnD:HAAF version 1.0 is to integrate the field and laboratory data detailed in the preceding chapters of this report. QnD:HAAF is being applied in an iterative, interactive, manner to identify critical abiotic and biotic drivers of salt marsh mercury and methylmercury cycling and guide subsequent work on HAAF and San Francisco Bay salt marshes. It is planned to also incorporate and link scientific, economic and social issues in a manner that enables the evaluation of their relative impacts through scenario projections. As further learning occurs, those drivers that are shown to be important can be explored and subsequently expanded, those judged unimportant be discarded. Whereas these changes would require substantial code rewriting of other models, they are rapidly made in QnD.

The QnD:HAAF v1.0 is composed by four spatial areas (High *Salicornia*-vegetated Marsh, Mid *Spartina*-vegetated Marsh, Mud Flat, and Sub Tidal), three drivers (day-time light, dry and wet season, and tide-dependent redox potential), and two processes (methylation and demethylation). Biota are represented by typical plant and animal species.

Although QnD:HAAF v1.0 development is based for only 10 percent on concepts and literature data, and for 90 percent on data measured in one year only, i.e. 2003, the model results have generated several interesting points for discussion and further exploration.Two fourteen-day scenario's were simulated, i.e., one scenario representing the wet season (Feb 1 –14, 2004) and one scenario representing the dry season (June 1 – 14, 2003). Simulated MeHg levels in biota indicated a significant bioaccumulation potential from lower to higher trophic levels, regardless of season. Elevation was an important factor influencing net MeHg production. Simulated MeHg concentrations in the sediment greatly exceeded the measured levels while simulated methylation and demethylation rates were in the same order of magnitude as measured values.. The difference between the simulated and measured mercury levels in the sediment and biota can provide a first estimate of the magnitude of the HAAF mercury export term. Validation of the value of the HAAF mercury export term and the processes by which this export is realized is the focus of current work plans.

INTRODUCTION

Stakeholders involved in wetland restoration activities on the former Hamilton Army Air Field (HAAF) aim at restoring San Pablo Bay wetland habitat, while minimizing conditions for methylmercury production and its subsequent trophic transfer to San Francisco Bay fisheries. However, sufficiently detailed information on environmental mercury levels at HAAF are lacking. That is, we lack a mechanistic understanding of the factors that control these levels and the means to use this information in ecosystem models supporting environmental management decisions. In this chapter an approach is outlined that integrates information from the other four chapters of this report, into a tool that directly links the environmental information in such a way that practical management decisions related to design, construction and maintenance of coastal wetland areas can be based on the simulation results.

The *Questions and Decisions* ™ (QnD) screening model system was created to provide an effective tool to incorporate ecosystem, management, economics and socio-political issues into a user-friendly framework. The QnD model links the spatial components within geographic information system (GIS) files to the prevalent abiotic, climatic, and biotic interactions in an ecosystem. QnD has a simple design and can be upgraded easily. It facilitates the use of our developing dataset as a basis for screening-level predictions for (1) other coastal wetland sites, and (2) "scaling up" for landscape-scale simulations. QnD:HAAF is being applied in an iterative, interactive manner to identify critical abiotic and biotic drivers of salt marsh mercury and methylmercury cycling and guide subsequent work on HAAF and San Francisco Bay salt marshes. Scientific, economic and social issues will also be incorporated and linked in a manner that enables the evaluation of their relative impacts through scenario projections. As further learning occurs, those drivers that are shown to be important can be explored and subsequently expanded, those judged unimportant be discarded. Whereas these major structural changes would require substantial code rewriting of other models (e.g., Mercury Cycling Model; Hudson et al., 1994), these changes are rapidly made in QnD. QnD achieves modeling nimbleness by keeping compartments, processes and interactions conceptually simple. Thus, the QnD:HAAF system can serve as a 'capstone' for integrating monitoring results into a more management-focused model.

The current version (v1.0) of QnD:HAAF is focused on exploring consensus technical questions formulated at the CALFED Stakeholders' Workshop on Mercury in San Francisco Bay held 8-9 October 2002 at Moss Point Landing.
These included:

1. What are the present levels of MeHg in SF Bay wetlands with respect to biota and sub-habitats, and location within the Bay?
2. What are the rates of MeHg production?
3. What factors control MeHg production? Can these be managed?
4. Are some wetlands larger mercury exporters than others?
5. Can we model/predict the effects of wetland restoration on MeHg production and export?

QnD:HAAF MODEL DESCRIPTION

The various objects used in the initial version of QnD:HAAF are presented in Fig.1. These objects (Chemicals, Organisms and Drivers) exist within a 'virtual' landscape of spatial areas and habitats. The Chemical and Organism objects participate in specific processes that cause changes in the ecosystem. For example: within a High Marsh (spatial area object), a crab

(organism object) may take MeHg up from the sediment (chemical object). An extended description of the model, including the data with which it was calibrated originally, is presented in Appendix Chapter 5.

Four Spatial Areas

While QnD can simulate ecosystem components and processes for an entire map of linked spatial areas, the initial version of QnD:HAAF utilizes four stylized wetland areas (Fig. 2). This spatial simplification allows the use of the data of initial feasibility studies with simplified modeling concepts, instead of attempting to fit a complex model to an ecosystem in which no data have been collected. In QnD:HAAF, the selected scale of each spatial area is 10 x 10 m (100 m^2), all mass data are on a dry weight basis, and all simulated data are on a m^2 basis.

The "High Marsh" area represents *Salicornia virginica* (pickle weed)-dominated areas that are rarely flooded. The "Mid Marsh" area represents *Spartina foliosa* (cord grass)-dominated areas that are partially flooded as a part of the daily tidal cycle. The third spatial area represents the "Mud Flat" zone that is partially submerged. The fourth spatial area represents the "Sub Tidal" zone that is completely submerged. The elevation of each spatial area is kept constant. High Marsh was kept at 3.0 feet (1 m) above Mean High Water (MHW), Mid Marsh at 1.0 foot (0.333 m), Mud Flat at 0.5 foot (0.167 m) and Sub Tidal at –1.0 feet (-0.333 m). Each spatial area has resident biota listed in Fig. 2.

Habitats

Habitats exist within, and occupy a fraction of each spatial area. The habitats are assumed to be homogeneous and harbor different combinations of biota and chemicals. In the initial version of QnD:HAAF, no specialized habitats within the spatial areas are distinguished, *i.e.* one "default" habitat occupies 100% of the spatial area . In upgrades, a plant- and a non-plant influenced habitat within each spatial area may be introduced. The latter upgrade would allow QnD to simulate the effects of depositing dredged material on a vegetated area. This management action may convert a portion of a vegetated wetland temporarily into a mud flat with altered mercury dynamics.

Environmental Drivers and Time Scales

Three environmental drivers were selected to link processes at time scales varying from current (on site measured methylation and demethylation rates in light versus in darkness, cf. Chapter 1, This Report) to seasonal (wet versus dry season data on THg and MeHg concentrations in the sediment, cf. MacFarland et al., 2003). An on-line tide simulator for the bay area was used to provide initial estimates of tidal water levels for selected time periods on an hourly basis (http://tbone.biol.sc.edu/tide/sitesel.html). Values pertaining to the mouth of the Petaluma River were selected, since these were considered as representative for the nearby HAAF. In general, SI units are used. The only exception is water depth, where feet are used for easy import of water level data from the on-line tide simulator.

For initial QnD:HAAF v1.0 testing, two hourly time series were constructed, representing a dry season, i.e. 1 – 14 June 2003, and a wet season, i.e., 1 – 14 February 2004), respectively. QnD:HAAF v1.0 utilizes a default time step of one hour, and can model results can, thus, easily be converted into daily values by multiplication with a factor of 24.

Tidal and Redox Processes

Water depth on each spatial area is calculated by subtracting its' local elevation hourly from tidal water level. If the calculated local water depth has a positive sign, then the spatial area is considered as being submerged and susceptible to decreasing oxygen diffusion. Vice versa, if the calculated local water depth has a negative sign, then the spatial area is considered as extending above the water level and thus susceptible to oxygen diffusion from the ambient air. The cumulative numbers of hours under and above the water level, respectively, are used to calculate the hourly change in redox potential (mV). The hourly change in redox potential is then added to the cumulative redox potential for each spatial zone.

Mercury Dynamics

Two chemical mercury pools are assumed to exist and available for transformation: total mercury (THg) and methylmercury (MeHg) (Fig. 1). Both pools are assumed to reside in the surficial 5-cm sediment layer and its associated pore water. The pools change in mass per unit area (ng m^{-2}), but have an associated, calculated, concentration (ng g^{-1}). The pools are considered as fully active, i.e., the whole THg pool is available for conversion into the MeHg pool, and vice versa. THg is transformed into MeHg as a function of time of year (dry or wet season), redox potential (dependent on tidal movements) and time of day (light or dark conditions). The values assigned to the pools of mercury are defined by the analytical procedures used to measure THg and MeHg. We assume that all THg and MeHg is reactive, but are aware that this is an overestimate since only a fraction may be reactive and/or is bioavailable. However, it is currently not known what and how large the reactive and bioavailable fractions are.

Mercury Methylation

The methylation process is presented in Fig. 3. In the model, methylation is affected by redox potential, tidal water movements, season, and light/dark conditions. The calculations of water depth and redox potential, prerequisites for the calculation of methylation, have been described in the Appendix Chapter 5.

The base THg methylation rates have been derived from the rates measured in the field in 2003, under dry season, daylight, and aerobic conditions (Chapter 1, This Report). A description of the effects of season, daylight, and redox potential on methylation is given in Appendix Chapter 5.

In the model, the amount of Hg methylated hourly in each spatial area is calculated as a percentage of the total available, inorganic Hg^{2+} pool (TotalHg), and follows equation (3):

$$MeHg_n = BaseRate_{meth} \times Season(month) \times \mathrm{Re}dox_m(hours) \times Light_m(daylight) \times TotalHg \quad (3)$$

where $BaseRate_{meth}$ = THg methylation (ng MeHg methylated ng^{-1} Hg^{2+} hr^{-1}),
Season(month) = seasonal, month-specific, effect on methylation rate (-),
$Redox_m$(hours) = redox potential effect on methylation rate, depending on the cumulative number of hours under water or extending above the water level (-),

$Light_m$(daylight) = daylight effect on methylation rate depending on time of day (-),
TotalHg = size Hg^{2+} pool (ng DW)

Methylmercury Demethylation

The demethylation process is represented in Fig. 4. MeHg is demethylated and returns as Hg to the active Hg^{2+} pool following a simplified, first-order, rate equation (DTMC /SRWP, 2002), which is affected by redox potential, tidal water movements, season, and light/dark conditions.

The base MeHg demethylation rates have been derived from the rates measured in the field in 2003, under dry season, daylight, and oxic conditions (Chapter 1, This Report). A description of the effects of season, daylight, and redox potential on methylation is given in Appendix Chapter 5.

In the model, the amount of MeHg demethylated hourly in each spatial area is calculated as a percentage of the MeHg pool, and follows equation (4):

$$demethHg_t = BaseRate_{Demeth} \times \mathrm{Re}dox_d(hours) \times Light_d(daylight) \times MeHg_t \qquad (4)$$

where $BaseRate_{demeth}$ = MeHg demethylation rate (ng MeHg demethylated ng^{-1} MeHg hr^{-1}),
$Redox_d$ (hours) = redox potential effect on demethylation rate depending on the cumulative number of hours under water or extending above the water level (-),
$Light_d$ (daylight)= daylight effect on demethylation rate depending on time of day (-),
MeHg = size MeHg pool (ng DW)

Simple MeHg Export From Sediments

In QnD:HAAF, MeHg is exported from the sediments at a constant rate as described in Chapter 1, This Report-Table 12. It is assumed that 0.8 percent of the resident MeHg load in the sediment is exported per day, i.e., 0.0333 percent per hour. This amount of MeHg exported enters into a general pool that quantifies the potential MeHg export to the bay.

Biota

Selected organisms are included in the QnD:HAAF model, i.e., plants, invertebrates and one vertebrate animal (a bird). Two emergent macrophytic plant species and one microalgal group are represented in the current version of QnD:HAAF. *Salicornia virginica* (Pickle weed) and *Spartina foliosa* (Cord grass) are simulated at the simplest level as an established standing crop with constant biomass over the two-week simulation. Plant MeHg load (ng) and potential contribution to export were assumed to be the primary data of interest in these simulations. The epipelon (algae living on the sediments) are also potential contributors to the export of MeHg. The values on plant biomass, THg and MeHg concentrations to calibrate the model are reported in Chapter 1, This Report. The following wetland invertebrates are modeled as potentially resident in all four spatial areas, but with population size and –biomass being spatial area-specific: Ribbed Mussel (*Geukensia Demissa*), Yellow Shore Crab (*Hemigrapsus Oregonensis*)

and the Eastern Mud Snail (*Iyanassa obsoleta*). These animals have been identified in HAAF field samples (Chapter 1, This Report). For exploring the trophic transfer and bioaugmentation of MeHg to higher levels in the food chain, the California Clapper Rail (*Rallus longirostris obsoletus*) is included as potentially resident in all four spatial areas. For the time being, it is assumed that biota do not migrate between spatial areas.

Biomass-related Processes

In this QnD:HAAF version the relationships between consumers and their food sources are formulated as a predator-prey relationship (Fig. 5). According to this approach, when a mud snail grazes epipelon, the mud snail would be a predator and the epipelon would be a prey. The uptake of prey biomass by the predator is calculated using equation (6):

$$Intake_{pred} = Biom_{pred} \times DemandRate_{prey} \quad (6)$$

where $Intake_{pred}$ = amount of prey biomass ingested by a specific predator (g DW),
$Biom_{pred}$ = predator biomass (g DW),
$DemandRate_{prey}$ = amount of prey required per unit weight of the predator (g DW prey per g DW predator)

The biomass of the prey is transferred from the prey pool to the predator pool ($Intake_{pred}$). If the prey pool is smaller than the demand of the predator, all available prey biomass is transferred to the predator. The predators and prey demand rates are listed in Appendix Chapter 5.

Biomass Loss

Long-term changes in biomass due to growth and respiration are not included. The biomass of plants (*Salicornia*, *Spartina* and epipelon) and ribbed mussels is assumed to be constant within the two-week simulation period. However, for animals that consume prey organisms (mud snails, shore crabs and clapper rails) and, thus, would increase in biomass, a mass-loss rate is introduced that is set equal to the biomass uptake rate to enable the simulation of trophic transfer of MeHg. The mass loss rates are listed in the Appendix Chapter 5.

Uptake of MeHg Directly from Sediment

In QnD:HAAF, all biota have uptake and loss processes that allow them to potentially bioaccumulate and release MeHg. This methodology is in accordance with DTMC/ SRWP (2002), recommending an initial simplified approach, followed by a detailed bioenergetic approach once MeHg data become available on higher trophic levels. Data on uptake and bioaccumulation of MeHg from soil, sediment, and pore water are still extremely scarce in the literature, and they are, therefore, largely estimated from most recent research reported in the Chapters 1, 2, 3, and 4 of This Report, and from (Mason et al., 1996; Rogers, 1995; Barber, 2001).

Uptake of MeHg from sediment is represented in Fig. 6, and calculated using equation (7):

$$MeHgIntake_{sed} = Biomass \times Transfer_{sed} \times Sat(MeHg_{conc}) \quad (7)$$

where $MeHgIntake_{sed}$ = uptake of MeHg from sediment (ng),
Biomass = biomass organism (g DW),
$Transfer_{sed}$ = potential MeHg transfer rate from sediment into organism (ng g^{-1} organism-DW),
$Sat(MeHg_{conc})$ = relative function that reduces MeHg uptake to 0.0 when the species-characteristic initial (equilibrium) MeHg concentrations are reached.

MeHg will only be taken up from the sediment when the MeHg concentration in the organism is below the concentration measured in the field, since the latter is assumed to be in equilibrium with the environment. One potential MeHg transfer rate from sediment into organism is used for all organisms. This $Transfer_{sed}$ value (0.14042 ng MeHg g^{-1} DW hr^{-1}) was measured in preliminary uptake experiments with Hg^{2+} on a *Macoma* species that filters sediment (Chapter 4, This Report). It is planned to include more species-characteristic uptake/transfer rates when these become available.

Uptake of MeHg from Grazing or Predation by Predator

Uptake of MeHg by ingestion of biotic food sources is represented in Fig. 10, and is calculated using equation (8). This equation has been formulated after Rogers (1994).

$$MeHgIntake_{prey} = Biomass_{pred} \times \Pr eyConsumed \times MeHg_{prey} \qquad (8)$$

where $MeHgIntake_{prey}$ = uptake of MeHg from ingesting a prey (ng),
$Biomass_{pred}$ = biomass predator (g DW),
Prey Consumed = biomass prey consumed (g prey-DW),
$MeHg_{prey}$ = MeHg concentration prey (ng g^{-1} prey-DW)

MeHg Loss From Biota

All macrophytes lose 50 percent of their biomass per year (estimate Chapter 1, This Report), and, based on this estimate they would also lose that fraction of the MeHg contained in the plant biomass. In QnD:HAAF all plants, i.e. macrophytes and epipelon, are modeled as losing 50 percent of the MeHg contained in their maximum standing crop per year, i.e., 5.7078x 10^{-3} percent hr^{-1}. All animals, including the ribbed mussels with constant biomass, are assumed to release 10 percent of their resident MeHg load per day, i.e., 0.4167 percent hr^{-1}. The latter value is based on a study on elimination of THg and MeHg by the zooplankter Daphnia magna feeding on phytoplankton (Tsui and Wang, 2004). This amount of MeHg released enters into a general pool that quantifies the potential MeHg export to the bay.

QnD:HAAF V1.0 MODEL RESULTS

Two fourteen-day scenario's were simulated using QnD, i.e., one scenario representing the wet season (Feb 1 –14, 2004) and one scenario representing the dry season (June 1 – 14, 2003). The results for all spatial areas, i.e., *Salicornia* Marsh, *Spartina* Marsh, Mud Flat and SubTidal, are presented separately, and expressed per m^2 to facilitate comparison between areas. *In situ*, however, the spatial areas differ in size.

The relative size of all successive pools has a large impact on the amount of MeHg transported throughout the system. Each pool size is at least two or three orders of magnitude larger than those of the subsequent pools. For example, within the *Salicornia* Marsh the THg pool of the sediment (≈ 8.9 x 10^6 ng m^{-2}) is far larger than the MeHg pool of the sediment (≈ 38000 ng m^{-2}), which, in turn, is larger than the MeHg pools in plants (≈ 5000 ng m^{-2} to 430 ng m^{-2}), which are larger than most MeHg pools in other biota (≈ 58 ng m^{-2} to 0.8 ng m^{-2}). The effect of these unequal pool sizes is that rates are usually unlimited, except in cases where the prey demand of the predator is not met. Given the two-week simulations, prey levels were always large enough to meet predator demands. The THg pool is assumed to be large enough to make it a non-limiting source for methylation and the MeHg pool large enough to be non-limiting for uptake into organisms. However, seasonal and environmental drivers control and alter the methylation and demethylation rates, while trophic transfer of MeHg occurs at constant rates, depending on organism.

Mercury Dynamics in Spatial Areas

Comparison of Simulated and Measured Methylation Rates

An important means to build confidence in the capabilities of QnD:HAAF to generate results that reflect what is happening in the ecosystems of interest, is to compare simulated results with measured values. Below several cases are illustrated.

The QnD model was used to simulate methylation and demethylation rates in the *Salicornia*-vegetated High Marsh spatial area over a two-week period. The simulated values were compared with values measured in a *Salicornia*-vegetated High marsh along San Francisco Bay by Marvin-DiPasquale et al. (2003). The simulated methylation and demethylation rates of 7.85 and 7.37 ng g^{-1} DW day^{-1}, respectively, were similar to the rates described by Marvin-DiPasquale et al. (2003). A more detailed analysis and comparison of methylation and demethylation rates described in This Report and those measured by Marvin-DiPasquale et al. (2003) is given in Chapter 1, This Report.

As with any modeling effort, more comparisons of simulated values with measured ones will increase the confidence of a model's performance.

Comparison of Simulated MeHg Concentrations and Transfer Rates Under Wet and Dry Season Conditions

The MeHg concentrations simulated over a two-week period in the four spatial areas under wet and dry season conditions are presented in Fig. 8. The MeHg concentrations in the sediment increased far more during the wet season than during the dry season. Increases were several orders of magnitude larger in vegetated sediments than in non-vegetated sediments (note the differences in scale of the vertical axes in Fig. 8), and dynamic patterns of MeHg concentrations differed greatly between spatial areas. The increase in MeHg concentration in the

wet season is due to the increasing seasonal effect on methylation rate (described in Appendix Chapter 5, Table 3). The simulated MeHg concentrations in the *Salicornia* marsh were 32 ng g^{-1} DW in the wet season and 4 ng g^{-1} in the dry season. The concentrations in the *Spartina* marsh and Mud Flat varied more dynamically under the influence of tidal activity and the inherent changes in redox potential. The concentrations in the *Spartina* marsh varied from 10 to 23 ng g^{-1} in the wet season, and from 1.5 to 3 ng g^{-1} in the dry season. The concentrations in the Mud Flat varied from 14.5 ng g^{-1} in the wet season to 6 ng g^{-1}in the dry season. MeHg in the SubTidal area increased slowly in both seasons, but somewhat more rapidly in the wet than in the dry season (3.5 versus 2.5 ng g^{-1} DW, respectively). Explanations for the differences in levels and dynamic patterns of MeHg concentrations can easily be explored using QnD:HAAF, since the model enables rapid data capture and visualization of temporal behavior of the processes and factors believed to drive MeHg concentrations, i.e. methylation, demethylation processes and on-site hourly water depth and redox potential.

In Fig. 9 the simulated methylation and demethylation rates are presented that lead to the MeHg concentrations in the spatial areas shown in Fig. 8. Also in this case, the increasing effect of the wet season is apparent (Appendix Chapter 5, Table 3). The regular, short-term (12 hour) cyclical fluctuations in methylation and demethylation rates are caused by daylight effects (Appendix Chapter 5, Tables 4 and 6). The methylation and demethylation rates in the *Salicornia* marsh and SubTidal spatial areas show regularly cycling, consistent equilibrium rates. The methylation and demethylation rates in the *Spartina* marsh and Mud Flat spatial areas show irregular humps in activity, caused by effects of tidal inundation and redox (Appendix Chapter 5, Figs 6 and 8). The two humps in MeHg transfer in the Spartina marsh, i.e. after 0-80 and 180-250 hrs (Fig. 9), are reflected clearly in the MeHg concentrations (Fig. 8), since the methylation rates are higher than the demethylation rates on a sediment-dry weight basis (sediments contain 100 x more THg than MeHg). The hump in MeHg transfer in the Mud Flat, i.e. after 80-200 hrs (Fig. 9), is barely visible by affecting the MeHg concentrations (Fig. 8), since the methylation and demethylation rates are in the same order of magnitude during this period in this spatial area. The methylation and demethylation rates do not reach equilibria during the two-week simulated period in the *Spartina* marsh and Mud Flat spatial areas.

Mercury Dynamics in Biota

QnD:HAAF simulation results indicated a significant bioaccumulation potential of MeHg from lower to higher trophic levels, regardless of season. The dynamics in bioaccumulation potential depend on the size of the available MeHg pools in the sediment and are greatly affected by the MeHg body burdens of the biota in each of the four spatial areas.

Mercury Dynamics in Plants

At this stage of QnD:HAAF development, the biomass and initial MeHg levels in all plants (*Salicornia*, *Spartina* and Epipelon) were kept at measured levels and did not change, because they were only measured at one point in time. This was done to keep initial model development simple. However, macrophytes and algae play important roles in the food webs in Californian coastal wetlands, as pointed out in Chapter 1-Tidal marsh vegetation zones, and these relationships have to be investigated further. Thus, based on this simplified assumption, *Salicornia* and *Spartina* had little influence on the overall MeHg dynamics within the sediment and in animals. Simulated uptake of MeHg by the plants was only to replace what was lost via simple export.

Mercury Dynamics in Animals

At this stage of QnD:HAAF development, the simulations were started from biomass and initial MeHg levels in all animals (mussels, snails, shore crabs, and clapper rails) measured at one point in time (Chapter 1, This Report; Appendix Chapter 5, Table 8). Simulation results conducted for the dry and wet seasons showed that the MeHg pools in the various spatial areas were large enough to allow unlimited uptake and bioaccumulation of MeHg in animals.

Simulation results on sediment-dwelling animals with a high biomass, such as the ribbed mussel in the Mud Flat and Sub Tidal spatial areas, indicated that these animals exhibit a stable uptake and retention of MeHg because their biomass is high and losses from predation by clapper rails and crabs are small. This can be explained from the fact, that most potential losses of MeHg from these animals, ranging from 0.43 in the High Marsh spatial area to 14.9 ng m^{-2} day^{-1} in the Sub Tidal spatial area, were regained through uptake of MeHg through the ingestion of sediment. Given the current assumptions of QnD:HAAF, ribbed mussels and epipelon may play similar roles as mid-level organisms in the food chain transfer of MeHg. These preliminary judgments are based on the assumptions of large, initial biomass levels with no short-term changes in biomass. Once biomass growth and mortality are simulated, these dynamics may give different conclusions.

Simulation results on sediment-dwelling animals with a lower biomass than mussels, such as eastern mud snails (0.1 to 1.0 g DW m^{-2}), showed that these animals are more sensitive to predation by crabs and clapper rails, since their biomass decreased in both seasons over the two-week period. The snails are different from mussels in that they bioaccumulate MeHg directly from sediment and by consuming epipelon. Because sediment and epipelon pools are large, the uptake of MeHg by snails was unlimited. The MeHg concentration in snails remained, therefore, close to the initial level of 7.9 ng MeHg g^{-1}. In addition, because of the low biomass and MeHg body burdens, the potential loss of MeHg from these animals (0.036 to 0.36 ng m^{-2} day^{-1}) was also small compared to exports from other MeHg sources.

Yellow shore crabs have a biomass in the same order of magnitude as eastern mud snails, a relatively lower MeHg body burden et equilibrium, but provide a significant resource for predators higher in the food chain. Simulation results indicated that the biomass of the crabs decreased substantially and in all spatial areas in both seasons over the two-week period due to the assumed biomass loss and predation by clapper rails. The MeHg concentration in crabs decreased slightly, i.e. 1.72 to 1.68 ng g^{-1} over the simulation period since the MeHg loss rate decreased the MeHg loads of the crabs. In exploratory sensitivity analysis simulations, biomass and MeHg concentrations of the crabs were more sensitive to assumed biomass loss than to direct MeHg loss from biomass- probably since the MeHg concentration at equilibrium was extremely low.

The clapper rail is considered as a ‘capstone’ species. It has the lowest biomass of all animals considered in HAAF-QnD, and the initial MeHg concentration was set purposely low to explore the bioaccumulation of MeHg. Simulated results indicated, that under the initial diet and MeHg assumptions clapper rails may bioaccumulate MeHg to substantial levels within an ecosystem such as HAAF. All clapper rail MeHg concentrations increased from 0.3 to 12 ng g^{-1} almost entirely through their diet of snails, crabs and mussels. As stated earlier, the rate of bioaccumulation for individuals depends on diet, biomass loss, MeHg loss as well as habitat utilization.

Export

Potential export of MeHg is considerable in all spatial areas. In QnD:HAAF, 'potential export' encompasses all potential MeHg export pathways, i.e. export with tidal movements and by volatilization. Simulated results show a large difference in export spatial areas and seasons (Fig. 10). In the wet season, the *Salicornia* Marsh had the highest potential for export (300 ng m^{-2} hr^{-1}) and the least contact with tidal waters. In the dry season the same *Salicornia* Marsh had a far lower export potential
(38 ng m^{-2} hr^{-1}).

By scaling the sizes of the spatial areas up to an area with the size of the future HAAF tidal wetland, i.e. 203 ha, insights were gained into the consequences of wetlands such as the HAAF-wetland for the MeHg TMDLs in San Pablo Bay. The calculation of the conversion factor used for scaling up is presented below:

1 ng MeHg m^{-2} hr^{-1} = 1 * 10^{-12} * 10^{4} * 24 * 365 kg MeHg ha^{-1} yr^{-1}
or 8.76 * 10^{-5} kg MeHg yr^{-1}

Net export potential would be expected to range from 5.3 to 0.4 kg MeHg yr^{-1} (Table 1). These values generated by dynamic simulation are 3 to 10 times higher than those derived from relatively simple, back-of-the envelope, calculations using static measured values, as presented in Chapter 1, This Report-Table 12. It is common knowledge that dynamic simulations generally yield higher production and export values for ecosystems than calculations based on values collected at only one point in time or on values collected with a very low frequency. However, for the current HAAF case and for other wetland restoration and creation plans it would be prudent to narrow the range of potential MeHg export and fate, effects and consequences for the food chain of MeHg further down.

Initial Answers to Questions Raised at the CALFED Stakeholders Workshop 8-9 October 2002 at Moss Point Landing

What are the Present Levels of MeHg in SF Bay Wetlands with Respect to Biota and sub-habitats?

MeHg levels in biota were simulated in such a way that they could not exceed the equilibrium concentrations measured in the field samples. The QnD:HAAF simulation results indicated a significant bioaccumulation potential of MeHg from lower to higher trophic levels, regardless of season. Simulations were greatly inhibited by the lack of available data on food chain structure, components, and MeHg accumulated in the biota.

The initial, measured (Chapter 1, This Report), MeHg concentrations in the sediments ranged from 1.1 to 1.8 ng MeHg g^{-1} DW. The simulated MeHg levels in the four sub-habitats, represented by spatial zones in QnD:HAAF, showed dynamics that depended on season and redox levels. MeHg concentrations increased over the two-week simulation period in all areas and both seasons to levels vastly exceeding the measured levels.

What Are the Rates of MeHg Production?

The simulated methylation and demethylation rates ranged from 100 to 20,000 ng m^{-2} hr^{-1}, depending on environmental conditions. For these simulations measured field data and

estimated effects of daylight, redox potential via tidal movements, and season were used as a basis. The fluctuations in methylation and demethylation due to the effect of time of day were regular, and the effect was similar in all spatial areas. Within areas that were frequently flooded and exposed to air, the redox potential became an important driver. The four spatial zones exhibited methylation rates that varied considerably with the tidal movements, because of the assumed 90-percent decreased methylation under air-exposed conditions. Methylation was assumed to be increased by a factor of 9 during the wet season compared to methylation in the dry season, and, this therefore, directly affected net MeHg production and pool size. The first simulation results compare favorably with the scarce values published for similar marsh areas. However, more monitoring data are required on the variation in net MeHg production in spatial zones and locations within the bay, for higher confidence in the potential of the QnD:HAAF model.

What Factors Control MeHg Production? Can These be Managed?

At this point in our understanding and modeling, most factors that are believed to control MeHg production and bioaccumulation are not easily managed. The primary management option with known influence is elevation. The importance of elevation is illustrated by the large differences in simulated methylation and demethylation rates in the *Spartina* Marsh and the Mud Flat areas that only differ 0.5 foot in elevation. Since net MeHg production is a microbial process, factors influencing this process deserve further attention to be explored.

Are Some Wetlands Larger Mercury Exporters than Others?

The current version of QnD:HAAF does not offer a detailed description of export in terms of THg and MeHg movement with tides or volatilization. All exported MeHg is deposited into one 'potential export' pool. However, simulated export from the four spatial zones proved to be vastly different. Consequently, based on these simulations it is to be expected that wetlands predominated by a relatively large share of *Salicornia* Marsh and *Spartina* Marsh may produce a relatively high contribution to the MeHg TMDL in the Bay. Moreover, wetlands in which the spatial zones are changing because of recent restoration may have export regimes that differ from those in established wetlands.

Simulated export greatly exceeds the export estimated from simple calculations using static values measured in the dry season, as presented in Chapter 1, Table 12. Ddynamic simulations generally yield higher production and export values for ecosystems than calculations based on values collected at only one point in time or on values collected with a very low frequency. However, for the current HAAF case and for other wetland restoration and creation plans it would be prudent to narrow the discrepancy between simulated and measured export further down.

Can we Model/Predict the Effects of Wetland Restoration on MeHg Production and Export?

Models exist as testing platforms of concepts and measured data. The predictive power of models usually grows with the confidence of the users in the concepts and data on which the models are based, and in the model results that reflect phenomena users can observe. QnD:HAAF v1.0 development is based for 10 percent on concepts and literature data and for 90 percent on data measured in 2003. Even with this very limited first year data set, the model results have generated several interesting points for discussion and further exploration.

THE WAY FORWARD: RECOMMENDATIONS FOR RESEARCH

From comparisons of simulated and measured data, we conclude that:

- large discrepancies exist between the simulated MeHg concentrations in the sediments of the spatial areas distinguished and the measured MeHg concentrations
- large discrepancies exist between the simulated export of MeHg from wetlands and the MeHg export calculated from measured values, causing uncertainties in the contribution of wetlands to the MeHg TMDL of the Bay
- large uncertainty exists on how the most important factors controlling net MeHg production influence this microbially-mediated process
- a large data gap exists on the MeHg concentrations in sediments of various locations within the Bay
- a large data gap exists on food chain structure, components, and MeHg accumulated in the biota of San Francisco Bay wetlands.

We recommend to direct future research and modeling efforts into collecting data through monitoring and experimental studies to fill the data gaps, and increase our understanding of ecosystem functioning and the reasons for discrepancies between simulated and measured data.

POINT OF CONTACT CHAPTER 5:

Gregory A. Kiker
U.S. Army U.S. Army Engineer Research and Development Center, Environmental Laboratory, Vicksburg, Mississippi, USA
Ph: 601-634-4578; Email: gregory.a.kiker@erdc.usace.army.mil

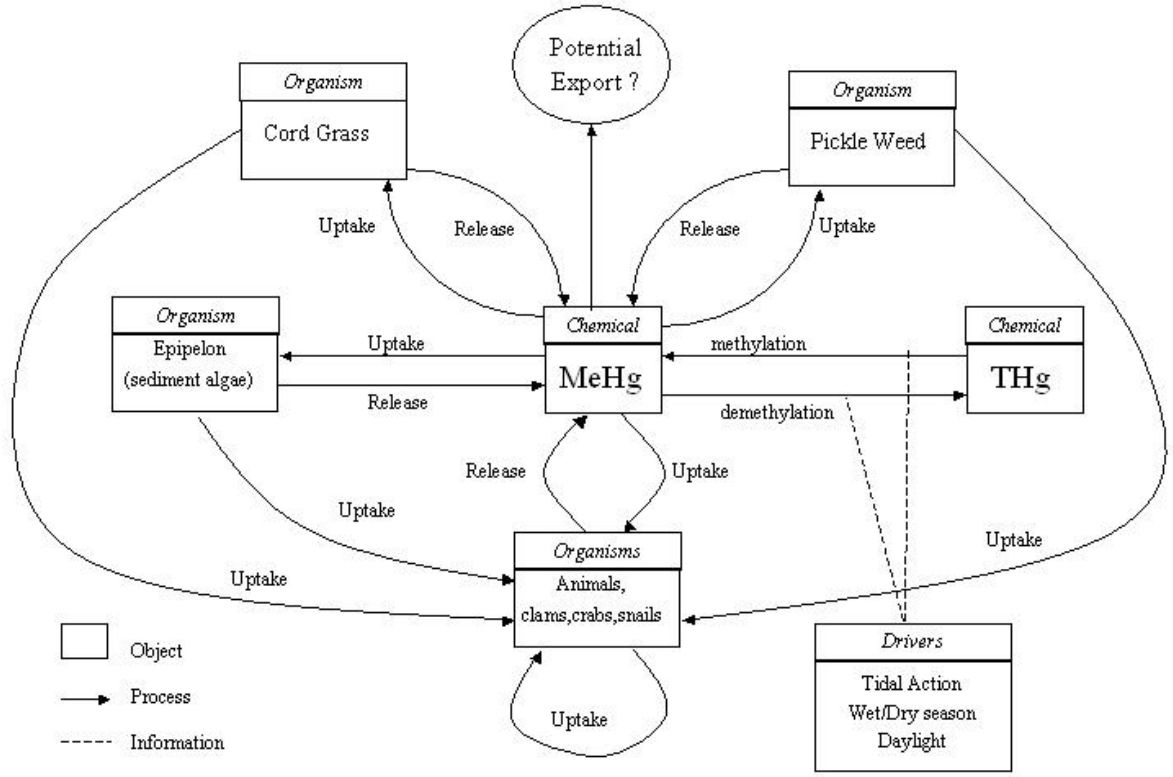

Figure 1. Overview of QnD:HAAF components, drivers and processes.

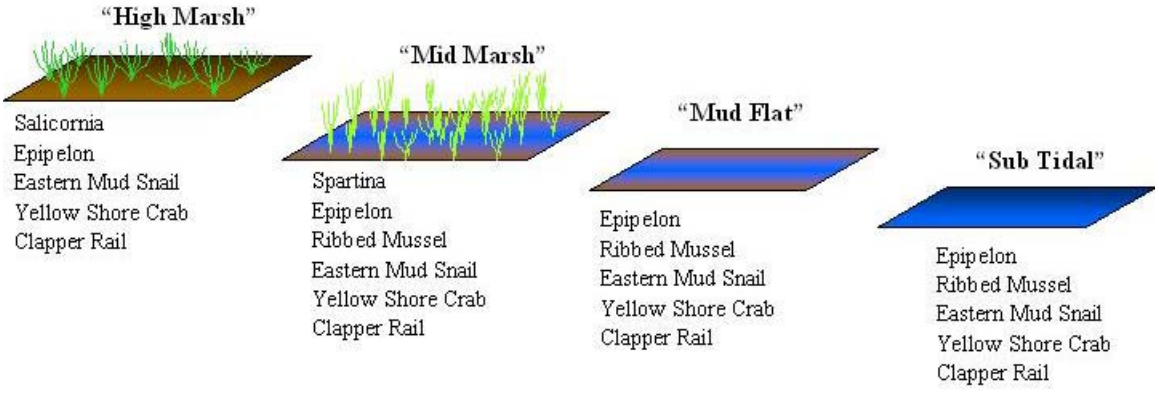

Figure 2. Spatial units and organisms within QnD:HAAF version 1.0.

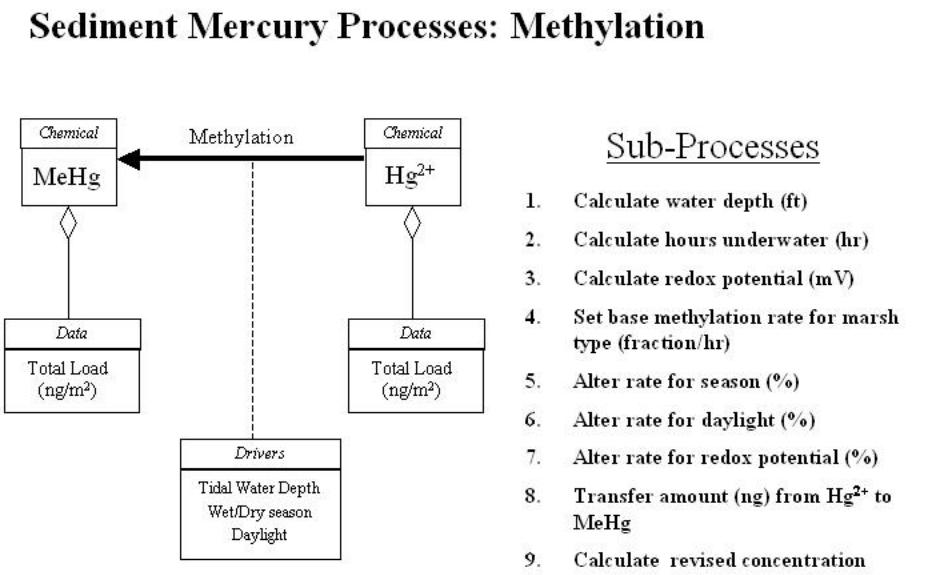

Figure 3. Overview of the QnD:HAAF mercury methylation process.

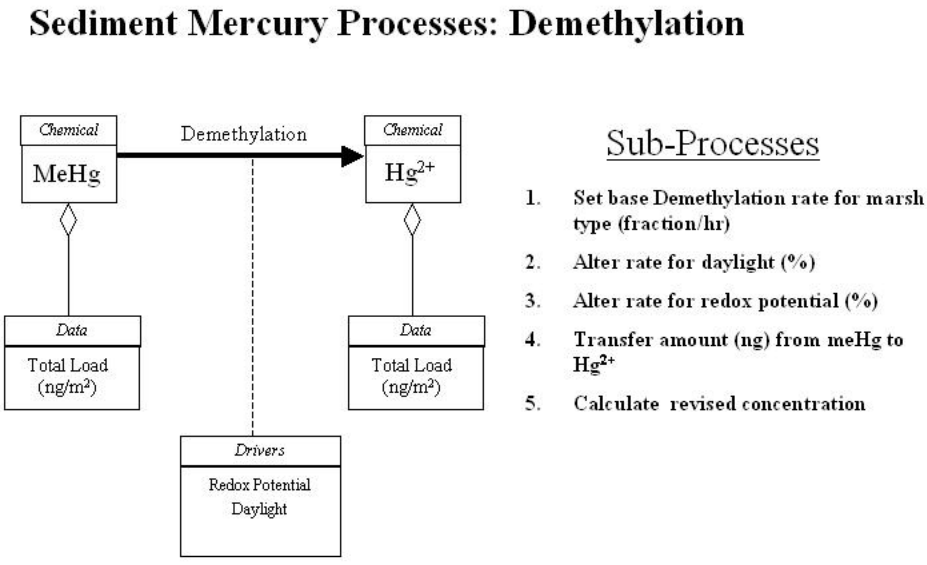

Figure 4. Overview of the QnD:HAAF mercury demethylation process.

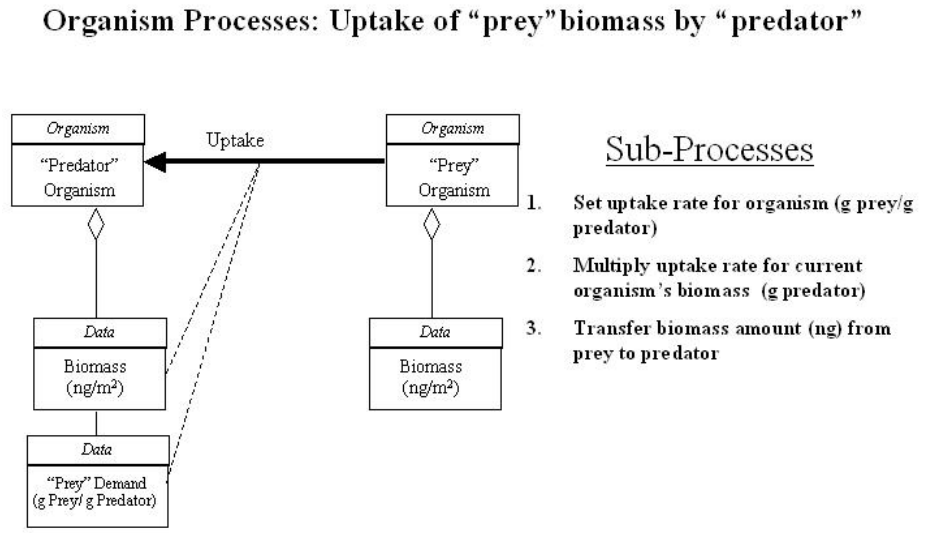

Figure 5. Overview of the QnD:HAAF biomass intake process.

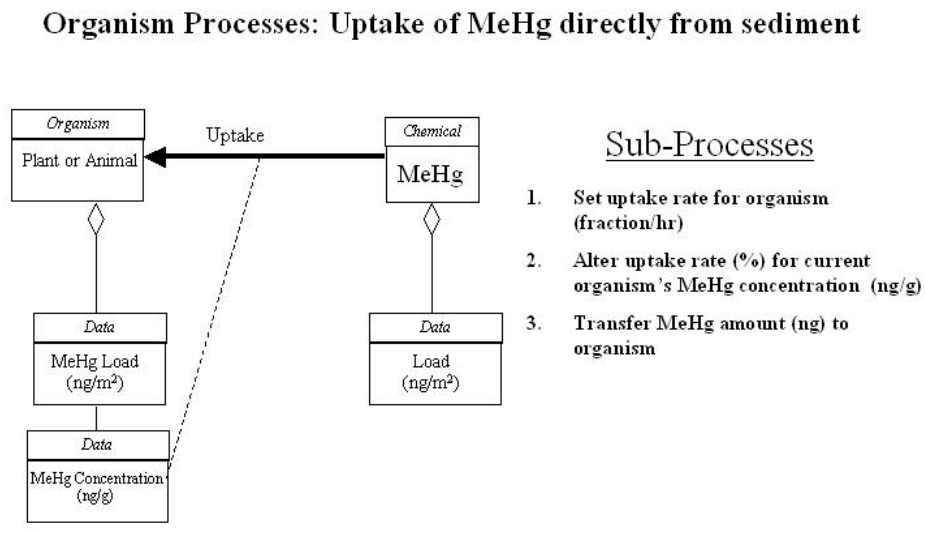

Figure 6. Overview of the QnD:HAAF organism MeHg intake from sediment.

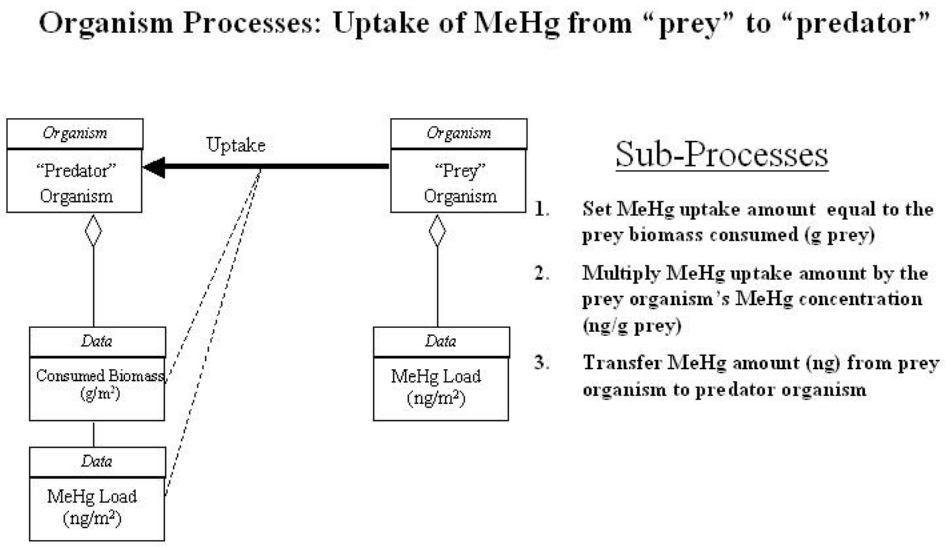

Figure 7.Overview of the QnD:HAAF organism MeHg intake from biomass.

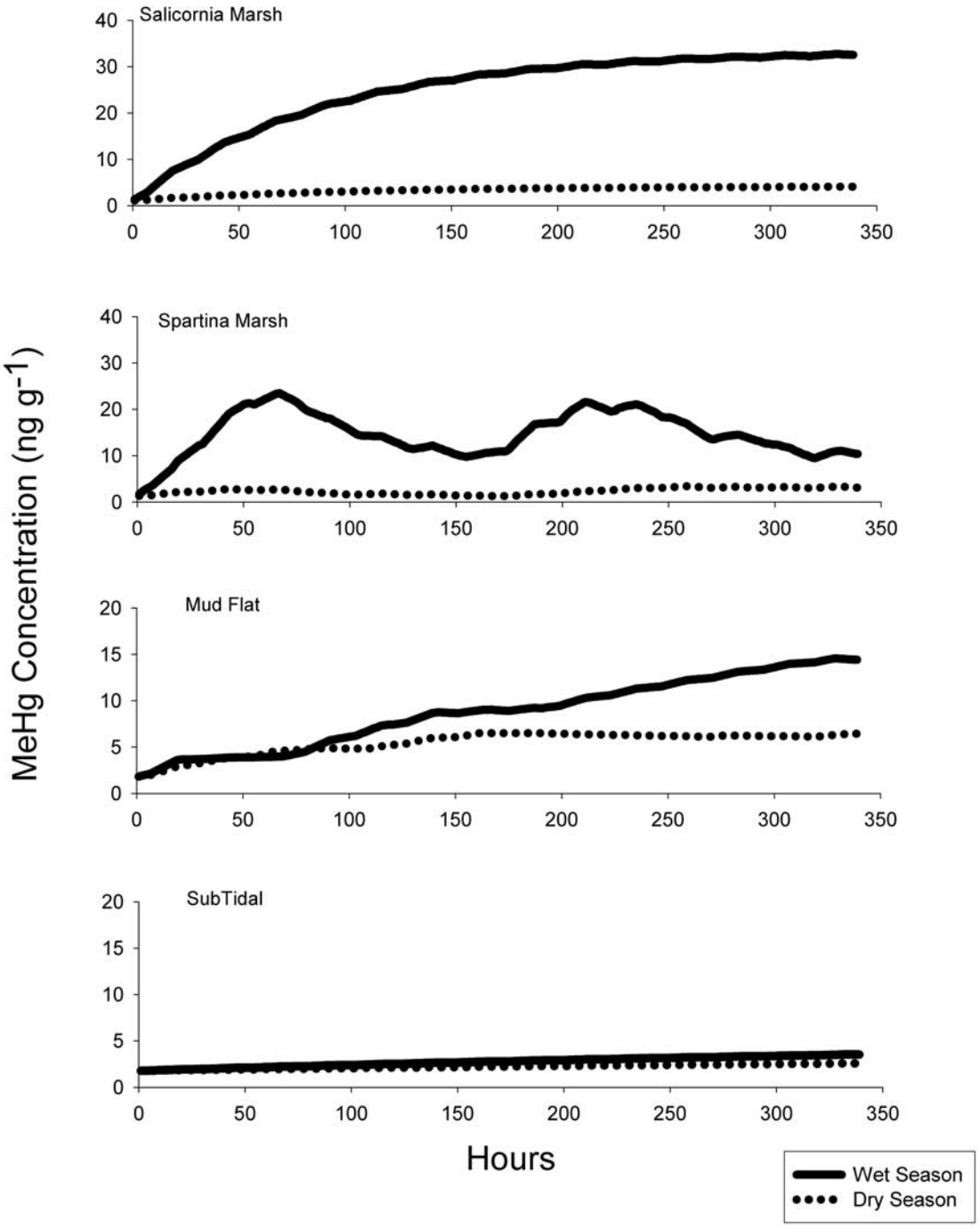

Figure 8. Simulated MeHg concentrations in surface sediments of four spatial areas.

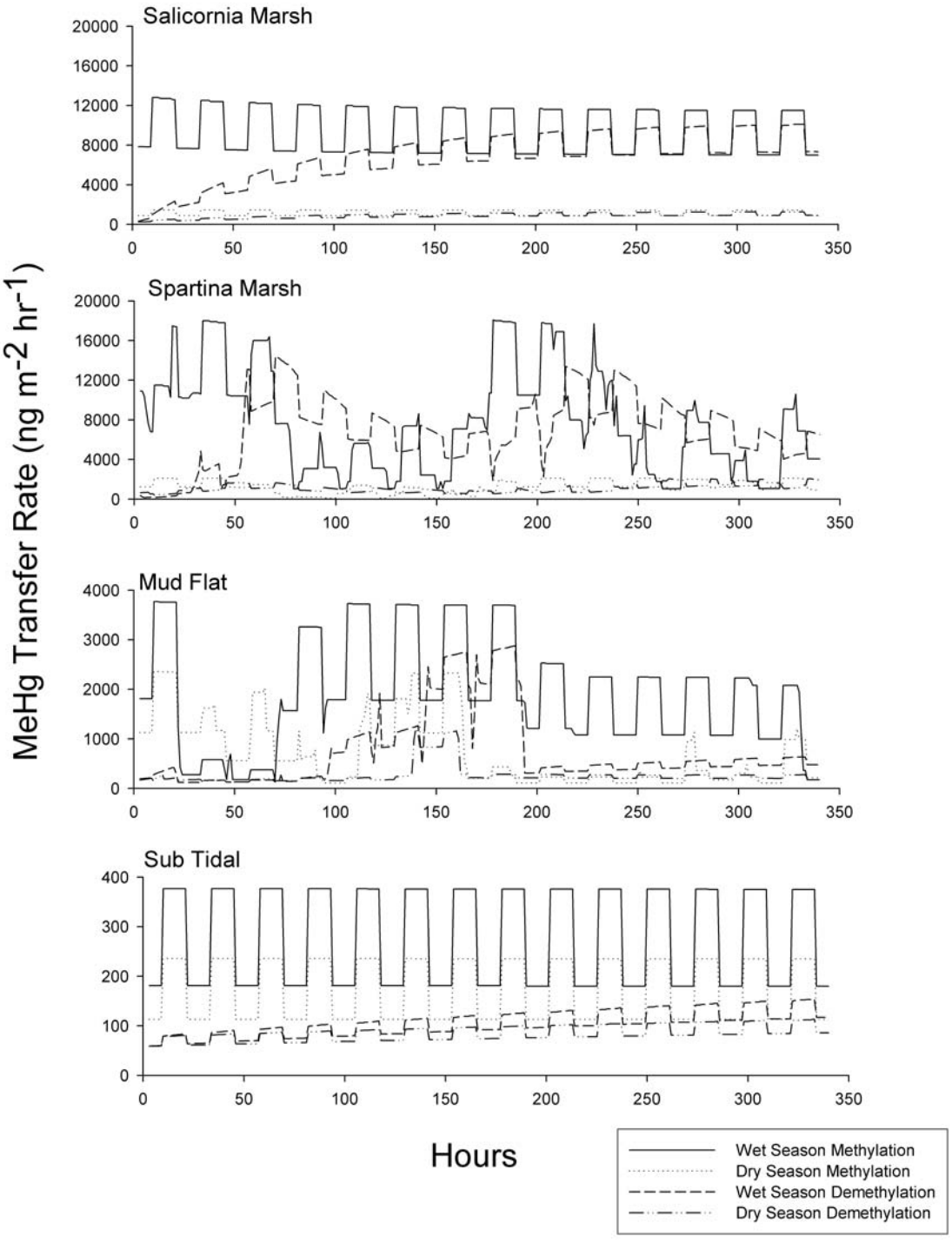

.

Figure 9. Simulated methylation and demethylation rates in surface sediments of four spatial areas.

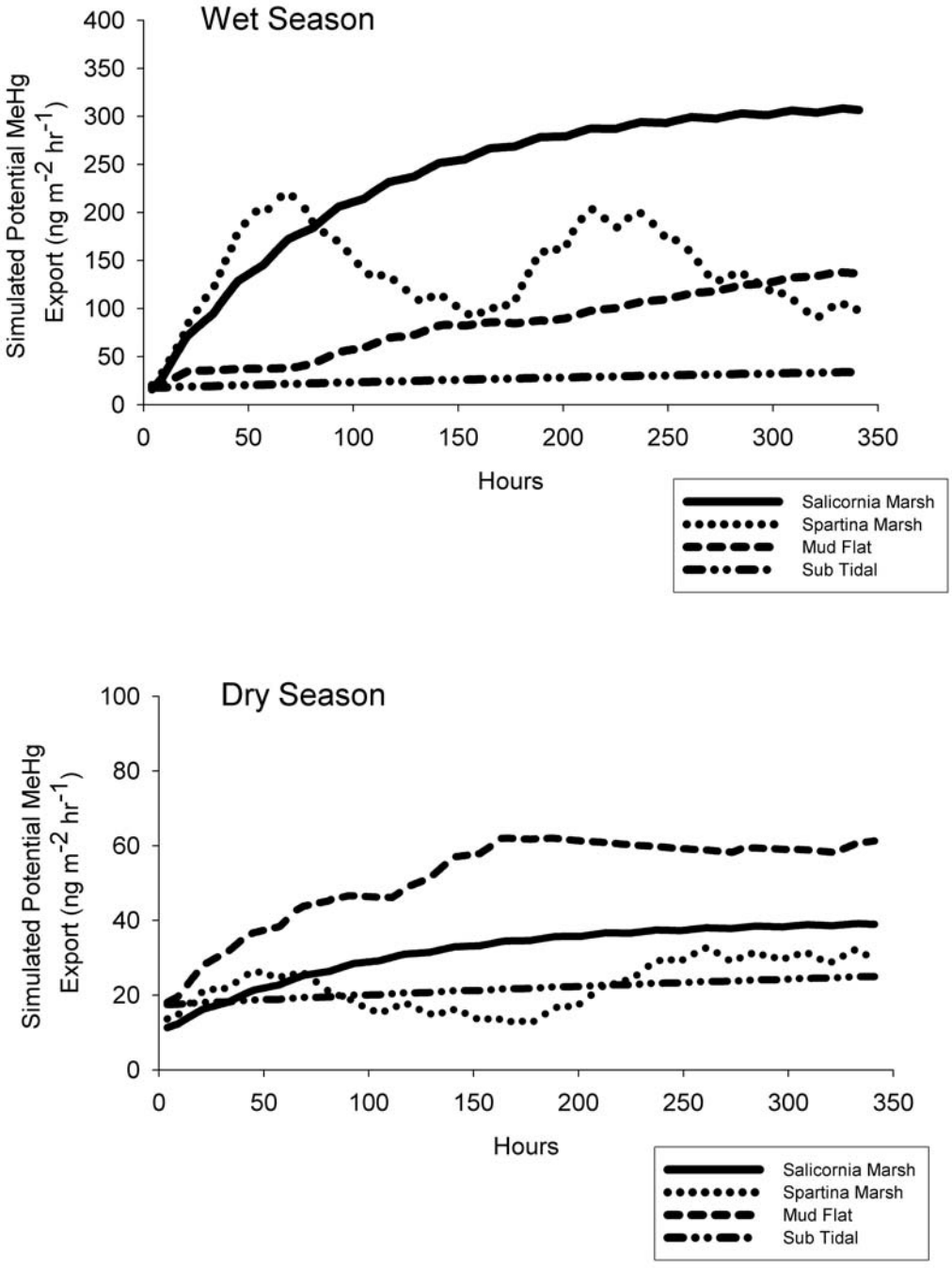

Figure 10. Simulated MeHg export rates from surface areas of four for HAAF spatial areas.

Table 1. Simulated potential export and contribution to the MeHg TMDL .

Spatial Area	Potential Export Simulated by QnD:HAAF		Potential Contribution HAAF To MeHg TMDL [1]	
	Wet Season ($ng\ m^{-2}\ hr^{-1}$)	Dry Season ($ng\ m^{-2}\ hr^{-1}$)	Wet season ($kg\ MeHg\ yr^{-1}$)	Dry season ($kg\ MeHg\ yr^{-1}$)
Salicornia Marsh	300	38	5.3	0.68
Spartina Marsh	200-100	10-30	3.6-1.8	0.18 - 0.53
Mud Flat	130	60	2.3	1.1
Sub Tidal	33	24	0.6	0.4

[1] Assuming a surface area of 203 ha for the HAAF wetland, and 100 percent cover by only one of the four spatial areas distinguished by QnD:HAAF.

[This Page Intentionally Left Blank]

6- References

Chapter 1, This Report. HAAF sediment mercury pool sizes and dynamics in relation to primary producers.

Chapter 2, This Report. Spatial distribution and concentrations of mercury species in the vegetated marsh zones of salt marshes bordering the HAAF wetland restoration site.

Chapter 3, This Report. Geochemical characterization of HAAF sediment profiles and mercury species levels in macrofauna.

Chapter 4, This Report. Bioavailability of mercury to benthic invertebrates: characterization and remediation effects in HAAF wetland sediments.

Chapter 5, This Report. Screening-level model design: Integrating physical, chemical and biological processes that drive mercury and methylmercury cycling in San Pablo Bay salt marshes.

Allen, J.R.L. (1990). "Salt-marsh growth and stratification: a numerical model with special reference to the Severn Estuary, southwest Britain", *Marine Geology* 95, 77-96.

Allen, J.R.L. (1994). "A continuity-based sedimentological model for temperate-zone tidal salt marshes", *Journal of the Geological Society, London* 151, 41-49.

Alpers, C.N., Hunerlach, M.P. (2000). "Mercury contamination from historic mining in California", U.S. Geological Survey Fact Sheet FS-061-00, Sacramento, CA.

Barber, M.C. (2001). "Bioaccumulation and Aquatic System Simulator (BASS) User's Manual Beta Test Version 2.1." USEPA Report No. 600/R-01/035. http://www.epa.gov/AthensR/staff/members/barbermahlonc/bass21_manual.pdf

Bartlett, P.D., and Craig, P.J. (1981a). "Total mercury and methylmercury levels in British estuarine sediments", *Applied Environmental Microbiology* 63: 37-47.

Bartlett, P.D., and Craig, P.J. (1981b). "Total Mercury Levels in British Estuarine Sediments-II," *Water Research* 15, 37-47.

Batten, K.M. and Scow, K.M. (2003). "Sediment microbial community composition and methylmercury pollution at four mercury mine-impacted sites", *Microbial Ecology* 46, 429-441.

Bednar, A.J. (2002). "Arsenic speciation and redox chemistry in natural waters", Ph.D. Dissertation, Department of Chemistry and Geochemistry, Colorado School of Mines, Golden, CO.

Benoit, J.M, Gilmore, C.C., Heyes, A., Mason, R.P., and Miller C.L. (2003). "Geochemical and biological controls over methylmercury production and degradation in aquatic ecosystems", ACS Symposium Series 835, *Biogeochemistry of Environmentally Important Trace Elements*, Y. Cai and O.C. Braids (eds.), American Chemical Society, Washington, D.C.

Bloom, N. (1989). "Determination of picogram levels of methylmercury by aqueous phase ethylation, followed by cryogenic gas chromatography with cold vapor atomic fluorescence detection", *Canadian Journal of Fisheries and Aquatic Sciences* 46, 1131-1140.

Boehn, H.L. (1971). "Redox potentials", *Soil Science* 112, 39-45.
Brannon, J., Plumb, R.H., and Smith, I. (1980). "Long term release of heavy metals from sediments," In: R.A. Baker (Ed.), *Contaminants and sediments*, Vol. 2, Chapter 13, Ann Arbor Science Publ.: 221-266.
Callaway, J.C. (2001). "Hydrology and substrate," In: J.B.Zedler (Ed.). "*Handbook for restoring tidal wetlands*", CRC Press, Boca Raton, London, New York, Washington D.C., Chapter 3, 89-111.
Callaway, J.C., Sullivan, G., and Zedler, J.B. (2003). "Species-rich plantings increase biomass and nitrogen accumulation in a wetland restoration experiment," *Ecological Applications* 13, 1626-1639.
Chan, H.M., Scheuhammer, A.M., Ferran, A., Loupelle, C., Holloway, J., and Weech, S. (2003). "Impacts of mercury on freshwater fish-eating wildlife and humans", Human and Ecological Risk Assessment 9, 867-883.
Day, P.R. (1956). "Report of the Committee on Physical Analyses (1954-1955)", *Soil Science Society of America Proceedings* 20: 167-169.
Delta Tributaries Mercury Council and the Sacramento River Watershed Program (2002). "Final Strategic Plan for the Reduction of Mercury-Related Risk in the Sacramento River Watershed: Appendices 1 and 4." (http://www.sacriver.org/subcommittees/dtmc/documents.html)
Demuth, N. and K. G. Heumann. (2001). "Validation of methylmercury determinations in aquatic systems by alkyl derivatization methods for GC analysis using ICP-IDMS', *Analytical Chemistry* 73, 4020.
Dong, W., Lindberg, S.E., Meyers, T., Chatton, J. (2002). "A proposed mechanism of gaseous mercury emission mediated via aquatic plants in the Florida Everglades", In preparation.
Faulkner, S.P., Patrick, W.H. Jr., Gambrell, R.P. (1989). "Field techniques for measuring soil parameters", *Soil Science Society of America Journal* 53, 883-890.
Fredrickson, H.L., Cappenberg, T. and de Leeuw, J. (1986). "Polar lipid ester-linked fatty acid composition of Lake Vechten seston: an ecological application of lipid analysis". *FEMS Microbial Ecol*ogy 38, 381-396.
Gardner, W. S., Kendall, D. R., Odom, R. R., Windom, H. L., and Stephens, J. A. (1978). "The distribution of methyl mercury in a contaminated salt marsh ecosystem", *Environmental Pollution* 15, 243-251.
Gill, R.G. (1979). "Status and distribution of the California clapper rail (*Rallus longirostris obsoletus*)," *California Fish Game* 65, 36-49.
Goals Project (1999). "Baylands Ecosystem Habitat Goals. A report of habitat recommendations prepared by the San Francisco Bay Area Wetlands Ecosystem Goals Project", First Reprint. U.S. Environmental Protection Agency, San Francisco, CA/S.F. Bay Regional Water Quality Control Board, Oakland, CA.
Gilmour, C.C. and Henry, E.A. (1991). "Mercury methylation in aquatic systems affected by acid decomposition. *Environmental Pollution* 71:131-169.
Grossinger, R. (1995). "*Historical evidence of freshwater effects on the plan form of tidal marshlands in the Golden Gate Estuary*", Masters thesis, Department of Marine Sciences, University of California at Santa Cruz, Santa Cruz, CA. 130 pp.
Hammerschmidt, C.R., and Fitzgerald, W.F. (2001)."Formation of artifact methylmercury during extraction from a sediment reference material", *Analytical Chemistry* 73, 5930-5936.

Heller, A.A. and Weber, J.H. (1998). "Seasonal study of speciation of mercury II and monomethylmercury in *Spartina alterniflora* from the Great Bay Estuary, NH", *The Science of Total Environment* 221, 181-188

Heyes, A. (1996). "Methylmercury in natural and disturbed wetlands", Ph. D. Thesis. McGill University, Montreal, CA.

Heyes, A., Moore, T.R., and Rudd, J.W.M. (1998). "Mercury and methylmercury in decomposing vegetation of a pristine and impounded wetland", *Journal of Environmental Quality* 27, 591-599.

Hintelmann, H. and Ogrinc, N. (2003). "Determination of stable mercury isotopes by ICP/MS and their application in environmental studies", In: *Biogeochemistry of environmentally important trace elements*, Y. Cai and C.O. Braids (eds), ACS Symposium Series Volume 835, Washington, DC, 321-338.

Hintelmann, H., Keppel-Jones, K., and Evans, R. D. (2000). "Constants of mercury methylation and demethylation rates in sediments and comparison of tracer and ambient mercury availability", *Environmental Toxicology and Chemistry* 19, 2204-2211.

Hintelmann, H., and Evans, R.D. (1997). "Application of stable isotopes in environmental tracer studies – Measurements of monomethylmercury (CH_3Hg^+) by isotope dilution ICP-MS and detection of species transformation", *Fresenius Journal of Analytical Chemistry* 358, 378-385.

Horvat, M., Bloom, N.S., and Liang, L. (1993). "Comparison of distillation with other current isolation methods for the determination of methyl mercury compounds in low level environmental samples", *Analytica Chimica Acta* 281,135-152.

Hudson, R. J. M., Gherini, S. A., Watras, C. J., and Porcella, D. B. (1994). "Modeling the Biogeochemical Cycle of Mercury in Lakes: The Mercury Cycling Model (MCM) and its Application to the MTL Study Lakes." In: C. J. Watras and J. W. Huckabee (eds.), Mercury pollution: integration and synthesis, Lewis Publishers, 473-523.

Kamman, R.Z., Phillip Williams and Associates (1998). "Conceptual design for tidal wetland restoration for the Hamilton Airfield focused feasibility study. Vol.1. Prepared for IT Corporation, January 1998. 103 pp.

Kannan, K., Smith, Jr. R. G., Lee, R. F., Windom, H. L., Heitmuller, P. T., Macauley, J. M., and Summers, J. K. (1998). "Distribution of total mercury and methyl mercury in water, sediment, and fish from south Florida estuaries", *Archives of Environmental Contamination and Toxicology* 34, 109-118.

King, J.K., Gladden, J.B., Harmon, S.M., and Fu, T.T. (2001). "Mercury removal, methylmercury formation, and sulfate-reducing bacteria profiles in wetland mesocosms containing gypsum-amended sediments," WSRC-TR-2001-00063

Kwak, T.J., and Zedler, J.B. (1997). "Food web analysis of southern California coastal wetlands using multiple stable isotopes," *Oecologia* 110, 262-277.

Lambers, H., Chapin III, F.S., and Pons, T.L. (1998). "*Plant physiological ecology*", Springer . Chapter 6. Mineral nutrition, 239-263.

Langmuir, D. (1997). *Aqueous Environmental Geochemistry.* Prentice Hall, Upper Saddle River, NJ, 600pp.

Lee, C. R., et al. (2000). "Field Survey of Contaminated Concentrations in Existing Wetlands in the San Francisco Bay Area," ERDC/EL SR-00-15, U. S. Army Engineer Research and Development Center, Vicksburg, MS.

Leonard, E.N., Cotter, A.M., and Ankley, G.T. (1996). "Modified diffusion method for analysis of acid volatile sulfide and simultaneously extractable metals in freshwater sediments", *Environmental Toxicology and Chemistry* 15: 1479-81.

Light, T.S. (1972). "Standard Solution for Redox Potential Measurements", *Analytical Chemistry* 44, 1038-1039.

Lindberg, S.E., Dong, W., Meyers, T. (2002). "Transpiration of gaseous elemental mercury through vegetation in a subtropical wetland in Florida", *Atmospheric Environment* 36, 5207-5219.

Marvin-DiPasquale, M.C., J.L. Agee, R.M. Bouse, and B.E. Jaffe. (2003). "Microbial cycling of mercury in contaminated pelagic and wetland sediments of San Pablo Bay, California", *Environmental Geology* 43, 260-267.

Mason, R. P., Reinfelder, J. R., and Morel, F. M. M. (1996). "Uptake, toxicity, and trophic transfer of mercury in a Coast diatom," *Environmental Science and Technology* 30, 1835-1845.

McFarland, V.A., and Lee, C.R. (2002). "Dredging-Related Mercury Issues in the San Francisco Bay-Delta Region," White Paper prepared for the USACE District, San Francisco. USACE Engineer Research and Development Center, Waterways Experiment Station, Vicksburg, MS.

McFarland, V.A., Clarke, J.C., Lutz, C.H., MacMillan, D.K. (2002). "Mercury concentrations bordering the Hamilton Army Air Field remediation site: September, 2001." Report to: USACE District, San Francisco, by USACE Engineer Research and Development Center, Waterways Experiment Station. October 4, 2002 + Appendices A-F.

McFarland, V.A., Lutz, C., Clarke, J.U., MacMillan, D.K. (2003). "Mercury Concentrations Bordering The Hamilton Army Air Field Remediation Site: February, 2003: Wet Season - Dry Season Contrast," Report to USACE District, San Francisco. USACE Engineer Research and Development Center, Waterways Experiment Station, Vicksburg, MS.

Millward, R.N., Bridges, T.S, Ghosh, U., Luthy, R.G., Zimmerman, J.R. "Addition of granular activated carbon (GAC) and coke to reduce PCB bioavailability in sediments: Bioaccumulation and toxicity tests," Environmental Science and Technology, Submitted.

Mills, A.L. (1997). "Metal requirements and tolerance", In *Manual of Environmental Microbiology*, C. J. Hurst, G. R. Knudsen, M/ J. McInerney, L. D. Stetzenbech, and M. V. Walter (eds.), American Society For Microbiology Press, Washington, D.C.

Morel, F. M. M., Kraepiel, A.M., and Amyoy, M. (1998). "The chemical cycle and bioaccumulation of mercury", *Annual Review of Ecology and Systematics* 29, 543-566.

Onuf, C.P. (1987). "The ecology of Mugu Lagoon, California: an estuarine profile", *U.S. Fish and Wildlife Service Biological Report* 85, 122 pp.

Patrick, W.H., Jr. (1958). "Modification of method of particle size analysis", *Soil Science Society of America Proceedings* 22, 366-367.

Pethik, J.S. (1992). "Saltmarsh geomorphology", In: J.R.L. Allen and K. Pye (eds). "*Saltmarshes: morphodynamics, conservation and engineering significance*", Cambridge University Press, New York, USA.

Phillip Williams and Associates (1998). See: Kamman et al.

Pinkart, H.C., Ringelberg, D.B., Piceno, Y.M., MacNaughton, S.J. and White, D.C. (2002). "Biochemical approaches to biomass measurements and community structure analysis", In: *Manual of Environmental Microbiology*, C.J. Hurst (Ed.), American Society of Microbiology Press, Washington, D.C.

Rogers, D.W. (1994). "You Are What You Eat and a Little Bit More: Bioenergetics-Based Models of MethylMercury Accumulation in Fish Revisited." In: C. J. Watras and J. W. Huckabee (eds.), Mercury pollution: integration and synthesis, Lewis Publishers, 473-523.

Roulet, M., Guimaraes, J.-R.D., and Lucotte, M. (2001). "Methylmercury production and accumulation in sediments and soils of an Amazonian floodplain – Effect of seasonal inundation," *Water Air and Soil Pollution* 128, 41-60, 2001.

SAS Institute Inc. (2001). *The SAS® System for Windows, Release 8.02*. SAS Institute Inc., Cary, NC.

Schlesinger, W.H. (1991). "*Biogeochemistry: an analysis of global change*", Academic Press, San Diego.

St.Louis, V.L., Rudd, J.W.M., Kelly, C.A., Beaty, K.G., Bloom, N.S., and Flett, R.J. (1994). "The importance of wetlands as sources of methyl mercury to boreal forest ecosystems", *Canadian Journal of Fisheries and Aquatic Sciences* 51, 1065-1076.

St.Louis, V.L., Rudd, J.W.M., Kelly, C.A., Beaty, K.G., Flett, R.J., and Roulet, N.T. (1996). "Production and loss of total mercury from boreal forest catchments containing different types of wetlands", *Environmental Science and Technology* 30, 2719-2729.

St. Louis, V.L., Rudd, J.W.M., Kelly, C.A., Hall, B.D., Rolfhus, K.R., Scott, K.J., Lindberg, S.E., and Dong, W. (2001). "Importance of the forest canopy to fluxes of methyl mercury and total mercury to boreal ecosystems," *Environmental Science and Technology* 35, 3089-3098.

Tsui, M.T.K., and Wang, W. (2004). "Uptake and elimination routes of inorganic mercury and methylmercury in *Daphnia magna*", *Environmental Science and Technology* 38, 808-816.

Ullrich, S.M., Tanton, T.W., Abdrashitova S.A. (2001). "Mercury in the Aquatic Environment: A Review of Factors Affecting Methylation," *Critical Reviews in Environmental Science and Technology* 31, 241-293.

U.S. Environmental Protection Agency (1989). "Guidance Manual: Bedded Sediment Bioaccumulation Tests. EPA/600/x-89/302", U.S. Environmental Protection Agency, ERL-N, Pacific Ecosystems Branch, Newport, OR.

USEPA Test Methods for Evaluating Solid Waste, SW-846, Method 7421.

USEPA. (1992a). "Acid Digestion of Sediments, Sludges, and Soils, Method 3050B, Test Methods for the Analysis of Solid Waste, Physical/Chemical Methods", Update II, Third Edition, July 1992, U.S. Environmental Protection Agency (EPA).

USEPA. (1992b). "Inductively Coupled Plasma-Atomic Emission Spectrometry, Method 6010B, Test Methods for the Analysis of Solid Waste, Physical/Chemical Methods", Update II, Third Edition, July 1992, U.S. Environmental Protection Agency (EPA).

USEPA. (1992c). "Mercury in Solid or Semisolid Waste (Manual Cold-Vapor Technique), Method 7471A, Test Methods for Evaluating Solid Waste Methods, SW-846", Third Edition, Update II, July 1992, U.S. Environmental Protection Agency (EPA).

USEPA (1994). "Mercury in solid or semi-solid waste (manual cold-vapor technique)," http://www.epa.gov/epaoswer/hazwaste/test/pdfs/7471a.pdf. Washington, DC.

USEPA (1997). "Mercury Study Report to Congress. Volume VIII. An evaluation of mercury control technologies and costs," EPA 452/R-97-010. Washington, DC

U.S. Fish and Wildlife Service (2003). "Evaluation of the Clean Water Act Section 304(a) human health criterion for methylmercury: protectiveness for threatened and endangered wildlife in California. U.S. Fish and Wildlife Service, Sacramento Fish and Wildlife Office, Environmental Contaminants Division. Sacramento California.

Van Handel, E. (1985). "Rapid determination of total lipids in mosquitoes", *Journal of American Mosquito Control Association* 1, 302-304.

Vitaliano, J.J, and Bejda, A.J. (2001). "Age, Growth, and Allometric Relationships of Ribbed Mussels (Geuken demissa)," NOAA Technical Memo 167. (http://nefsc.noaa.gov/nefsc/publications/tm/tm167/tm167p5.htm)

Windham, L., Weis, J.S., Weis, P. (2001). "Patterns and processes of mercury release from leaves of two dominant salt marsh macrophytes, *Phragmites australis* and *Spartina alterniflora*", *Estuaries* 24, 787-795.

Winfield, T.P. (1980). "Dynamics of carbon and nitrogen in a southern California salt marsh", Ph. D. Dissertation, University of California Riverside, and San Diego State University, San Diego. 76 pp.

Winfrey, M.R., and Rudd, J.W.M. (1990). "Environmental factors affecting the formation of methylmercury in low ph lakes", *Environmental Toxicology and Chemistry* 9, 853-869.

Zedler, J.B., Winfield, T., and Williams, P. (1980). "Salt marsh productivity with natural and altered tidal circulation", *Oecologia* 44, 236-240.

Zimmerman, J.R., Ghosh, U., Luthy, R.G., Millward, R.N., Bridges, T.S. "Addition of carbon sorbents to reduce bioavailability of PAH and PCB in marine sediments," Physicochemical tests. *Environmental Science and Technology* In Press.

APPENDIX - CHAPTER 3

Table 1. Sediment quality characteristics of Bel Marin (BM-50a; n = 1) and HAAF upland (SM-10U; n = 1) soil/sediment cores. Mean (SD)

Depth Section (cm)	Eh (mV)	AVS (µg/g)	TOC (%)	Sand (%)	Silt (%)	Clay (%)	Fines (%)
SM-10U							
0 – 7.6	----	0.53	19	----	----	----	----
7.6 – 10.2	----	<0.22	17	----	----	----	----
10.2 –14.0	----	<0.23	13	13	58	29	0.87
14.0 – 17.8	----	2.7	7.8	5.9	50	45	0.94
17.8 – 24.1	----	9.4	7.5	0.96	61	38	0.99
24.1 – 30.5	----	74	3.9	0.58	51	48	0.99
30.5 – 40.6	----	1600	3.3	0.37	55	45	1
BM-50a							
0 - 2.5	516	<0.06	1.7	13	45	43	0.87
2.5 - 5.1	454	0.09	1.6	6.5	54	39	0.94
5.1 - 7.6	440	0.43	1.7	8.8	50	41	0.91
7.6 - 10.2	265	0.71	1.7	23	38	40	0.78
10.2 - 12.7	136	8.7	1.8	3.5	52	45	0.96
12.7 - 15.2	141	1100	1.9	6.1	52	42	0.94

Table 2. Major and trace elements of Bay Edge (SM-1, SM-10) and Reference (R-44) soil/sediment cores. Mean (SD).

Depth Section (cm)	Al (%)	Fe (%)	Cs (μg g^{-1})	Li (μg g^{-1})	Mn (μg g^{-1})	P (μg g^{-1})	Se (μg g^{-1})
SM-1							
0 - 2.5	2.9 (0.3)	4.3 (0.2)	3.2 (0.3)	33 (3)	430 (66)	720 (120)	1.0 (0.1)
2.5 - 5.1	3.0 (0.4)	4.5 (0.1)	3.2 (0.3)	36 (4)	480 (230)	590 (180)	1.1 (0.1)
5.1 - 7.6	3.2 (0.2)	4.4 (0.3)	3.3 (0.3)	38 (3)	410 (93)	520 (120)	1.1 (0.1)
7.6 - 10.2	3.3 (0.3)	4.5 (0.1)	3.3 (0.2)	40 (3)	400 (84)	630 (320)	1.1 (0.1)
10.2 - 12.7	3.5 (0.2)	4.5 (0.1)	3.4 (0.2)	42 (2)	430 (97)	500 (30)	1.1 (0.1)
12.7 - 15.2	3.8 (0.3)	4.4 (0.3)	3.5 (0.2)	44 (3)	450 (110)	490 (10)	1.0 (0.1)
SM-10							
0 - 2.5	2.6 (0.4)	3.5 (0.4)	2.6 (0.3)	29 (3)	440 (120)	790 (160)	0.84 (0.15)
2.5 - 5.1	2.5 (0.4)	3.5 (0.3)	2.6 (0.2)	29 (4)	320 (91)	510 (61)	0.82 (0.09)
5.1 - 7.6	2.8 (0.3)	3.8 (0.1)	2.6 (0.4)	33 (3)	380 (94)	530 (210)	0.80 (0.08)
7.6 - 10.2	3.0 (0.3)	4.1 (0.2)	2.9 (0.2)	37 (2)	450 (59)	480 (14)	0.84 (0.09)
10.2 - 12.7	3.2 (0.1)	4.2 (0.1)	2.9 (0.2)	39 (1)	510 (66)	470 (25)	0.80 0.07)
12.7 - 15.2	3.4 (0.0)	4.2 (0.1)	3.0 (0.3)	41 (1)	490 (59)	470 (29)	0.76 (0.05)
R-44							
0 - 2.5	3.6 (0.3)	4.8 (0.6)	3.7 (0.2)	41 (2)	370 (100)	740 (190)	0.93 (0.08)
2.5 - 5.1	3.8 (0.3)	4.6 (0.4)	3.7 (0.1)	43 (2)	350 (80)	690 (120)	1.0 (0.1)
5.1 - 7.6	3.7 (0.2)	4.4 (0.3)	3.5 (0.1)	42 (1)	310 (29)	650 (120)	0.97 (0.06)
7.6 - 10.2	3.8 (0.3)	5.0 (0.4)	3.5 (0.1)	43 (2)	410 (160)	660 (200)	0.98 (0.11)
10.2 - 12.7	3.8 (0.4)	5.1 (0.3)	3.6 (0.1)	43 (2)	450 (88)	670 (220)	1.1 (0.1)
12.7 - 15.2	3.8 (0.3)	4.8 (0.4)	3.54(0.2)	43 (2)	490 (62)	650 (210)	0.94 (0.12)

Table 3. Major and trace elements of Bel Marin (BM-50a; n = 1) and HAAF upland (SM-10U; n = 1) soil/sediment cores. Mean (SD).

Depth Section (cm)	Al (%)	Fe (%)	Cs (μg g^{-1})	Li (μg g^{-1})	Mn (μg g^{-1})	P (μg g^{-1})	Se (μg g^{-1})
SM-10U							
0 – 7.6	2.2	3.9	2.1	22	5300	1600	1.5
7.6 – 10.2	2.7	4.5	2.6	29	1900	1300	2.1
10.2 –14.0	2.6	5.6	2.7	29	540	1600	1.6
14.0 – 17.8	3.4	4.6	3.2	36	260	1200	1.5
17.8 – 24.1	3	3.5	2.9	34	220	820	1.4
24.1 – 30.5	3.5	3.8	3.2	39	240	790	1.2
30.5 – 40.6	3.8	4.3	3.3	42	280	970	1.1
BM-50a							
0 - 2.5	4.4	4.9	3.5	42	440	950	1.0
2.5 - 5.1	3.7	4.0	3.4	37	270	770	0.96
5.1 - 7.6	4.1	4.3	3.4	40	270	740	0.96
7.6 - 10.2	3.6	4.1	3.5	38	250	790	1.1
10.2 - 12.7	3.8	4.3	3.6	39	260	980	1.0
12.7 - 15.2	3.7	4.2	3.3	40	300	860	0.91

Table 4. THg statistical analysis by depth profile.

Location	Depth (cm)	N	Median (ug g^{-1})	Mean of Ranks	Tukey Ranking*	Mean (ug g^{-1})	St. Dev. (ug g^{-1})
SM-1	0 –2.5	5	0.33	12	BC	0.33	0.06
	2.5 – 5.1	5	0.34	8.9	C	0.33	0.04
	5.1 – 7.6	5	0.36	11	BC	0.33	0.05
	7.6 – 10.2	5	0.36	14	ABC	0.35	0.03
	10.2 – 12.7	5	0.41	23	AB	0.40	0.03
	12.7 – 15.2	5	0.42	25	A	0.41	0.04
SM-10	0 – 2.5	5	0.32	8.0	A	0.33	0.04
	2.5 – 5.1	5	0.35	12	A	0.34	0.04
	5.1 – 7.6	5	0.35	16	A	0.36	0.04
	7.6 – 10.2	5	0.35	20	A	0.38	0.04
	10.2 – 12.7	5	0.34	14	A	0.35	0.03
	12.7 – 15.2	5	0.38	22	A	0.38	0.02
R-44	0 – 2.5	5	0.29	10	A	0.32	0.04
	2.5 – 5.1	5	0.32	15	A	0.34	0.04
	5.1 – 7.6	5	0.34	17	A	0.35	0.04
	7.6 – 10.2	5	0.34	14	A	0.34	0.05
	10.2 – 12.7	5	0.37	17	A	0.37	0.08
	12.7 –15.2	5	0.43	20	A	0.41	0.10

* Medians with same letter designation do not differ statistically ($P < 0.050$) by One-way ANOVA on Ranks followed by Tukey's post hoc test

Table 5. MeHg statistical analysis by depth profile.

Location	Depth (cm)	N	Median (ug kg^{-1})	Mean of Ranks	Tukey Ranking*	Mean (ug kg^{-1})	St. Dev. (ug kg^{-1})
SM-1	0 –2.5	5	3.4	18	A	3.3	3.2
	2.5 – 5.1	5	2.2	16	A	2.2	2.0
	5.1 – 7.6	5	4.2	20	A	0.99	1.2
	7.6 – 10.2	5	1.5	13	A	1.1	1.1
	10.2 – 12.7	5	1.0	14	A	0.84	1.2
	12.7 – 15.2	5	0.54	11	A	0.34	0.27
SM-10	0 –2.5	5	5.2	25	A	4.4	3.6
	2.5 – 5.1	5	3.9	20	AB	2.9	2.3
	5.1 – 7.6	5	1.4	18	AB	1.2	1.1
	7.6 – 10.2	5	0.31	11	B	0.28	0.26
	10.2 – 12.7	5	0.23	11	B	0.22	0.13
	12.7 – 15.2	5	0.15	9	B	0.16	0.16
R-44	0 –2.5	5	4.2	20	A	3.6	3.7
	2.5 – 5.1	5	3.4	18	A	2.0	1.5
	5.1 – 7.6	5	2.2	16	A	3.9	3.1
	7.6 – 10.2	5	1.0	14	A	2.6	3.8
	10.2 – 12.7	5	1.5	13	A	1.8	1.9
	12.7 – 15.2	5	0.54	11	A	0.91	0.76

* Medians with same letter designation do not differ statistically ($P < 0.050$) by One-way ANOVA on Ranks followed by Tukey's post hoc test.

Table 6. Statistical analysis of phosphorus (P) by depth profile.

Location	Depth (cm)	N	Median (ug g^{-1})	Mean of Ranks	Tukey Ranking*	Mean (ug g^{-1})	St. Dev. (ug g^{-1})
SM-1	0 –2.5	5	710	25	A	720	120
	2.5 – 5.1	5	530	16	A	590	180
	5.1 – 7.6	5	500	12	A	520	110
	7.6 – 10.2	5	490	15	A	630	320
	10.2 – 12.7	5	500	14	A	500	29
	12.7 – 15.2	5	480	10	A	490	10
SM-10	0 –2.5	5	850	27	A	790	160
	2.5 – 5.1	5	510	19	AB	510	61
	5.1 – 7.6	5	460	10	B	530	210
	7.6 – 10.2	5	470	13	B	480	14
	10.2 – 12.7	5	470	11	B	470	25
	12.7 – 15.2	5	480	13	B	470	29
R-44	0 –2.5	5	850	19	A	740	190
	2.5 – 5.1	5	740	17	A	690	120
	5.1 – 7.6	5	610	17	A	650	120
	7.6 – 10.2	5	530	15	A	660	200
	10.2 – 12.7	5	540	14	A	670	220
	12.7 – 15.2	5	510	12	A	650	210

* Medians with same letter designation do not differ statistically ($P < 0.050$) by One-way ANOVA on Ranks followed by Tukey's post hoc test.

Table 7. Statistical analysis of manganese (Mn) by depth profile.

Location	Depth (cm)	N	Median (ug g^{-1})	Mean of Ranks	Tukey Ranking*	Mean (ug g^{-1})	St. Dev. (ug g^{-1})
SM-1	0 –2.5	5	420	15	A	430	66
	2.5 – 5.1	5	380	14	A	480	230
	5.1 – 7.6	5	420	14	A	410	93
	7.6 – 10.2	5	410	14	A	400	84
	10.2 – 12.7	5	470	18	A	430	97
	12.7 – 15.2	5	480	19	A	450	110
SM-10	0 –2.5	5	423	16	AB	440	120
	2.5 – 5.1	5	285	6.6	B	320	91
	5.1 – 7.6	5	346	10	AB	380	94
	7.6 – 10.2	5	468	17	AB	450	59
	10.2 – 12.7	5	544	22	A	510	66
	12.7 – 15.2	5	458	22	A	490	59
R-44	0 –2.5	5	340	15	AB	370	100
	2.5 – 5.1	5	320	11	AB	350	80
	5.1 – 7.6	5	290	7.0	B	310	29
	7.6 – 10.2	5	360	14	AB	410	160
	10.2 – 12.7	5	430	22	A	450	88
	12.7 – 15.2	5	500	24	A	490	62

* Medians with same letter designation do not differ statistically ($P < 0.050$) by One-way ANOVA on Ranks followed by Tukey's post hoc test.

Table 8. Statistical analysis of total organic carbon (% TOC) by depth profile.

Location	Depth (cm)	N	Median (ug g^{-1})	Mean of Ranks	Tukey Ranking*	Mean (ug g^{-1})	St. Dev. (ug g^{-1})
SM-1	0 –2.5	5	4.6	22	AB	4.4	0.9
	2.5 – 5.1	5	4.4	24	A	4.5	0.8
	5.1 – 7.6	5	4.3	21	AB	4.2	0.5
	7.6 – 10.2	5	3.4	14	BC	3.6	0.5
	10.2 – 12.7	5	3.3	8.6	C	3.2	0.7
	12.7 – 15.2	5	2.9	4.2	C	3.0	1.2
SM-10	0 –2.5	5	4.6	22	AB	4.7	1.1
	2.5 – 5.1	5	4.4	24	A	4.7	0.5
	5.1 – 7.6	5	4.3	21	AB	4.2	0.7
	7.6 – 10.2	5	3.4	14	BC	3.6	0.5
	10.2 – 12.7	5	3.3	8.6	C	3.2	0.3
	12.7 – 15.2	5	2.9	4.2	C	2.9	0.1
R-44	0 –2.5	5	2.9	9.6	A	3.1	0.4
	2.5 – 5.1	5	3.5	16	A	3.6	0.7
	5.1 – 7.6	5	3.5	17	A	3.7	0.8
	7.6 – 10.2	5	3.9	18	A	3.7	0.6
	10.2 – 12.7	5	3.8	20	A	3.8	0.6
	12.7 – 15.2	5	3.0	12	A	3.3	0.5

* Medians with same letter designation do not differ statistically ($P < 0.050$) by One-way ANOVA on Ranks followed by Tukey's post hoc test.

Table 9. Statistical analysis of redox potential (Eh) by depth profile.

Location	Depth (cm)	N	Median (mV)	Mean of Ranks	Tukey Ranking*	Mean (mV)	St. Dev. (mV)
SM-1	0 –2.5	4	70	18	A	52	81
	2.5 – 5.1	4	-98	14	AB	-87	42
	5.1 – 7.6	4	-124	7.9	B	-131	34
	7.6 – 10.2	2	-118	11	AB	-118	1.3
	10.2 – 12.7	4	-151	5.0	B	-152	19
	12.7 – 15.2	2	-140	5.3	B	-140	0.4
SM-10	0 –2.5	4	296	24	A	311	183
	2.5 – 5.1	5	352	23	AB	268	223
	5.1 – 7.6	5	70	18	ABC	93	176
	7.6 – 10.2	5	-63	12	BC	-26	146
	10.2 – 12.7	5	-83	8.2	C	-100	50
	12.7 – 15.2	5	-135	6.6	C	-117	31
R-44	0 –2.5	5	368	25	A	348	42
	2.5 – 5.1	5	266	21	AB	284	86
	5.1 – 7.6	5	255	19	AB	187	201
	7.6 – 10.2	5	40	14	ABC	84	199
	10.2 – 12.7	5	-80	10	BC	-12	143
	12.7 – 15.2	5	-135	5.2	C	-110	56

* Medians with same letter designation do not differ statistically ($P < 0.050$) by One-way ANOVA on Ranks followed by Tukey's post hoc test.

Table 10. Statistical analysis of acid-base characteristics (pH) by depth profile.

Location	Depth (cm)	N	Median (mV)	Mean of Ranks	Tukey Ranking*	Mean (mV)	St. Dev. (mV)
SM-1	0 –2.5	5	6.4	4.3	C	6.3	0.2
	2.5 – 5.1	5	6.4	5.0	BC	6.4	0.1
	5.1 – 7.6	5	6.6	11	AB	6.6	0.1
	7.6 – 10.2	3	6.7	14	A	6.6	0.1
	10.2 – 12.7	4	6.7	16	A	6.7	0.1
	12.7 – 15.2	1	6.8	18	A	6.8	0.2
SM-10	0 –2.5	4	5.4	9.4	BC	5.4	0.3
	2.5 – 5.1	5	5.1	7.0	C	5.0	0.7
	5.1 – 7.6	5	5.1	9.1	BC	5.3	0.4
	7.6 – 10.2	5	5.9	18	AB	5.9	0.1
	10.2 – 12.7	4	6.0	24	A	6.0	0.2
	12.7 – 15.2	5	6.0	26	A	6.2	0.3
R-44	0 –2.5	5	6.1	11	A	6.0	0.2
	2.5 – 5.1	5	6.0	9.4	A	6.0	0.1
	5.1 – 7.6	5	6.0	13	A	6.1	0.2
	7.6 – 10.2	5	6.0	16	A	6.2	0.2
	10.2 – 12.7	5	6.2	20	A	6.3	0.1
	12.7 – 15.2	5	6.4	24	A	6.3	0.1

* Medians with same letter designation do not differ statistically ($P < 0.050$) by One-way ANOVA on Ranks followed by Tukey's post hoc test.

Table 11. Mineralogy of six depth sections from composite cores from HAAF (SM-1)[1].

Mineralogy parameter	Depth (cm)					
(Weight Percent)	0 – 2.5	2.5 – 5.1	5.1 – 7.6	7.6 – 10.2	10.2 – 12.7	12.7 – 15.2
Whole Rock Mineralogy						
Quartz	28.9 %	30.1 %	22.4 %	25.7 %	22.5 %	19.1 %
K-Feldspar	1.8 %	0.4 %	1.6 %	2.1 %	2.0 %	1.0 %
Plagioclase	29.2 %	29.5 %	35.4 %	26.5 %	23.1 %	21.5 %
Amphibole	2.8 %	2.7 %	2.3 %	3.8 %	2.9 %	3.0 %
Pyrite	5.3 %	6.9 %	5.0 %	6.2 %	6.3 %	5.9 %
Natrojarosite	2.2 %	0.0 %	1.0 %	1.2 %	2.0 %	1.3 %
Gypsum	0.9 %	0.6 %	0.7 %	0.6 %	2.4 %	1.7 %
Halite	0.0 %	0.0 %	0.8 %	0.9 %	1.1 %	1.2 %
Phyllosilicate Mineralogy						
R=0 M-L I/S (90%S)[2]	9.0 %	7.7 %	9.0 %	11.2 %	11.0 %	13.3 %
Illite & Mica	9.6 %	11.5 %	10.2 %	10.0 %	12.4 %	15.1 %
Kaolinite	3.6 %	3.1 %	3.8 %	3.8 %	4.8 %	6.4 %
Chlorite	6.6 %	7.5 %	7.9 %	8.1 %	9.6 %	10.5 %

[1]N = 1 composite sample at each depth.

[2]R=0 M-L I/S (90%S) - Randomly Ordered Mixed-Layer Illite/Smectite with 90% Smectite Layers

Table 12. Mineralogy of six depth sections from composite cores from HAAF (SM-10)[1].

Mineralogy parameter (Weight Percent)	Depth (cm) 0 – 2.5	2.5 – 5.1	5.1 – 7.6	7.6 – 10.2	10.2 – 12.7	12.7 – 15.2
Whole Rock Mineralogy						
Quartz	35.7 %	33.5 %	34.0 %	33.1 %	26.9 %	29.3 %
K-Feldspar	1.0 %	1.1 %	0.9 %	0.4 %	2.1 %	3.5 %
Plagioclase	31.9 %	32.7 %	31.0 %	30.9 %	30.3 %	26.2 %
Amphibole	3.0 %	3.5 %	3.7 %	2.6 %	3.0 %	3.9 %
Pyrite	1.8 %	2.9 %	4.8 %	5.6 %	7.4 %	4.1 %
Natrojarosite	0.5 %	3.5 %	2.2 %	1.3 %	1.4 %	1.5 %
Gypsum	0.4 %	1.1 %	1.2 %	1.0 %	1.0 %	1.5 %
Halite	1.0 %	0.3 %	0.3 %	0.2 %	0.8 %	0.4 %
Phyllosilicate Mineralogy						
R=0 M-L I/S (90%S)[2]	7.7 %	6.7 %	8.1 %	8.8 %	9.5 %	9.0 %
Illite & Mica	8.1 %	7.2 %	6.7 %	7.5 %	8.6 %	9.4 %
Kaolinite	2.6 %	2.1 %	2.8 %	3.0 %	2.5 %	4.1 %
Chlorite	6.4 %	5.4 %	4.4 %	5.7 %	6.4 %	7.1 %

[1]N = 1 composite sample at each depth.

[2]R=0 M-L I/S (90%S) - Randomly Ordered Mixed-Layer Illite/Smectite with 90% Smectite Layers

Table 13. Mineralogy of six depth sections from composite core samples from China Camp (R-44)[1].

Mineralogy parameter (Weight Percent)	Depth (cm) 0 – 2.5	2.5 – 5.1	5.1 – 7.6	7.6 – 10.2	10.2 – 12.7	12.7 – 15.2
Whole Rock Mineralogy						
Quartz	23.5 %	25.7 %	24.8 %	24.6 %	24.6 %	22.5 %
K-Feldspar	2.3 %	2.0 %	2.4 %	2.2 %	2.0 %	1.6 %
Plagioclase	25.7 %	28.2 %	27.4 %	27.3 %	25.5 %	23.4 %
Amphibole	4.0 %	1.5 %	5.0 %	3.0 %	1.8 %	2.6 %
Pyrite	0.9 %	0.0 %	4.0 %	5.2 %	8.3 %	8.1 %
Natrojarosite	0.0 %	0.0 %	0.0 %	1.6 %	2.0 %	1.5 %
Gypsum	2.9 %	1.5 %	1.9 %	1.6 %	1.6 %	1.3 %
Halite	2.0 %	0.9 %	1.2 %	1.0 %	0.8 %	1.2 %
Phyllosilicate Mineralogy						
R=0 M-L I/S (90%S)[2]	11.9 %	14.0 %	10.7 %	10.8 %	10.2 %	11.2 %
Illite & Mica	13.0 %	12.1 %	10.5 %	10.7 %	10.8 %	13.9 %
Kaolinite	4.1 %	4.4 %	3.3 %	4.5 %	4.4 %	4.8 %
Chlorite	9.8 %	9.7 %	8.8 %	7.4 %	7.8 %	7.9 %

[1]N = 1 composite sample at each depth.

[2]R=0 M-L I/S (90%S) - Randomly Ordered Mixed-Layer Illite/Smectite with 90% Smectite Layers

Table 14. Mineralogy of six depth sections from core samples from Bel Marin (BM-50a)[1].

Mineralogy parameter	Depth (cm)					
(Weight Percent)	0 – 2.5	2.5 – 5.1	5.1 – 7.6	7.6 – 10.2	10.2 – 12.7	12.7 – 15.2
Whole Rock Mineralogy						
Quartz	30.6 %	29.7 %	29.8 %	26.2 %	26.9 %	29.0 %
K-Feldspar	1.9 %	2.2 %	2.9 %	2.9 %	2.6 %	2.1 %
Plagioclase	29.1 %	30.1 %	27.0 %	30.7 %	31.6 %	29.4 %
Amphibole	2.3 %	2.8 %	3.3 %	3.9 %	3.9 %	2.6 %
Pyrite	0.0 %	0.0 %	0.0 %	0.0 %	1.3 %	1.1 %
Natrojarosite	0.0 %	0.0 %	0.0 %	0.0 %	0.8 %	1.9 %
Gypsum	1.3 %	2.1 %	1.4 %	1.1 %	0.4 %	1.7 %
Halite	0.0 %	0.0 %	0.0 %	0.0 %	0.0 %	0.0 %
Phyllosilicate Mineralogy						
R=0 M-L I/S (90%S)[2]	14.0 %	12.5 %	12.2 %	13.7 %	12.4 %	12.2 %
Illite & Mica	9.1 %	8.8 %	9.9 %	9.3 %	10.0 %	9.4 %
Kaolinite	6.6 %	6.2 %	8.8 %	8.8 %	4.0 %	4.8 %
Chlorite	5.1 %	5.6 %	4.8 %	3.5 %	6.1 %	5.8 %

[1]N = 1 sample at each depth.

[2]R=0 M-L I/S (90%S) - Randomly Ordered Mixed-Layer Illite/Smectite with 90% Smectite Layers

Table 15. Mineralogy of seven depth sections from cores from Hamilton upland site (SM-10U)[1].

Mineralogy parameter	Depth (cm)						
(Weight Percent)	0–7.6	7.6–10.2	10.2–14.0	14.0–17.8	17.8–24.1	24.1–30.5	30.5–40.6
Whole Rock Mineralogy							
Quartz	30.3 %	29.9 %	26.8 %	25.2 %	25.5 %	24.7 %	26.6 %
K-Feldspar	3.6 %	1.7 %	2.1 %	1.8 %	1.3 %	1.7 %	2.0 %
Plagioclase	22.3 %	19.3 %	20.7 %	23.6 %	25.4 %	20.5 %	19.3 %
Amphibole	0.0 %	2.3 %	0.0 %	0.0 %	2.4 %	2.6 %	2.6 %
Pyrite	1.3 %	1.0 %	0.7 %	0.6 %	0.9 %	1.3 %	1.3 %
Natrojarosite	0.0 %	0.0 %	0.0 %	0.0 %	0.0 %	0.0 %	0.0 %
Gypsum	0.0 %	0.0 %	0.0 %	0.0 %	0.0 %	0.0 %	0.0 %
Halite	6.7 %	2.6 %	2.1 %	2.6 %	2.9 %	2.2 %	3.1 %
Phyllosilicate Mineralogy							
R=0 M-L I/S (90%S)[2]	12.6 %	12.8 %	16.6 %	15.2 %	11.0 %	15.1 %	12.9 %
Illite & Mica	10.2 %	15.3 %	14.1 %	14.8 %	14.4 %	14.7 %	13.8 %
Kaolinite	4.4 %	6.3 %	6.5 %	7.7 %	6.9 %	8.0 %	8.4 %
Chlorite	8.6 %	8.8 %	10.4 %	8.5 %	9.3 %	9.3 %	10.0 %

[1]N = 1 sample at each depth.

[2]R=0 M-L I/S (90%S) - Randomly Ordered Mixed-Layer Illite/Smectite with 90% Smectite Layers

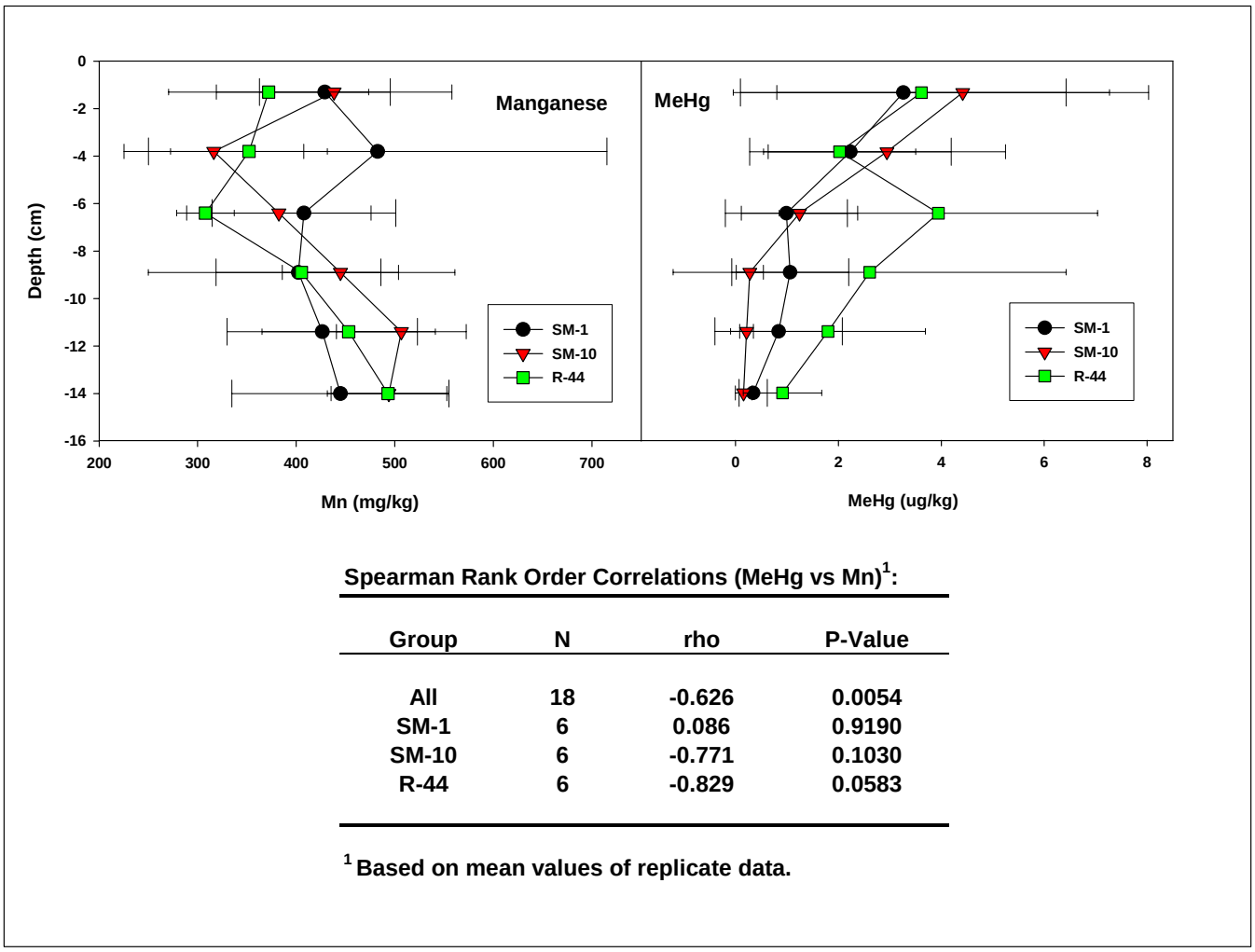

Spearman Rank Order Correlations (MeHg vs Mn)[1]:

Group	N	rho	P-Value
All	18	-0.626	0.0054
SM-1	6	0.086	0.9190
SM-10	6	-0.771	0.1030
R-44	6	-0.829	0.0583

[1] Based on mean values of replicate data.

Figure 1. Depth profile comparisons and correlations for Manganese (Mn) and Methylmercury (MeHg) from replicate core samples collected at HAAF (SM-1 & SM-10) and China Camp (R-44). Symbols represent mean of replicate data (n=5); error bars indicate standard deviation.

[This Page Intentionally Left Blank]

APPENDIX CHAPTER 5

QnD:HAAF Model Design – Technical Description, Equations and Calibration

Overview of the QnD Model System

The *Questions and Decisions* ™ (QnD) screening model system was created to provide an effective tool to incorporate ecosystem, management, economics and socio-political issues into a user-friendly model framework. The model is written in object-oriented Java and can be deployed as a stand-alone program or as a web-based (browser-accessed) 'applet'. The QnD model links the spatial components within geographic information system (GIS) files to the abiotic, climatic, and biotic interactions that exist in an ecosystem.

The model can be constructed using any combination of measured data or estimated interactions of the ecological, management, social,and/or economic forces influencing an ecosystem. The model development is iterative and can be initiated quickly through conversations with users or stakeholders. Model alterations and/or more detailed processes can be added throughout the model development process.

The configuration of QnD is meant to be iterative to enable the exploration of concepts of interest, and the subsequent expansion or disposal as further learning occurs. The major inputs of QnD:HAAF include the following (Fig.1):

- Four spatial areas (land areas, river reaches, wetlands), interconnected or individual ('stand-alone' mode)
- Habitats, i.e., forest, grassland, and bare patches within the Spatial Areas
- Environmental drivers (rainfall, temperature, tidal activity) and time scales (hours, days, months, quarters, years)
- Chemicals (total mercury, methylmercury)
- Biota (microbes, plants, invertebrate and vertebrate animals)
- Estimated relationships between chemicals, biota and drivers

The next section describes these QnD model components in more detail for the HAAF wetland ecosystem.

QnD:HAAF Model Description

The various objects used in the initial version of QnD:HAAF are presented in Fig. 1. These objects (Chemicals, Organisms and Drivers) exist within a "virtual" landscape of spatial areas and habitats. The Chemical and Organism objects participate in specific processes that cause changes in the ecosystem. For example: within a High Marsh (spatial area object), a crab (organism object) may take MeHg up from the sediment (chemical object). A more complete description of the spatial areas, habitats, chemicals and organism objects and their associated processes is given in further detail in the sections below.

Spatial Areas

While QnD can simulate ecosystem components and processes for an entire map of linked spatial areas, the initial version of QnD:HAAF utilizes four stylized wetland areas (Fig. 2). This spatial simplification allows the use of the data of initial feasibility studies with simplified modeling concepts, instead of attempting to fit a complex model to an ecosystem in which no data have been collected. In QnD:HAAF, the selected scale of each spatial area is 10 x 10 m (100 m^2), all mass data are on a dry weight basis, and all simulated data are on a m^2 basis.

The 'High Marsh' area represents *Salicornia virginica* (pickle weed)-dominated areas that are rarely flooded. The 'Mid Marsh' area represents *Spartina foliosa* (cord grass)-dominated areas that are partially flooded as a part of the daily tidal cycle. The third spatial area represents the 'Mud Flat' zone that is partially submerged. The fourth spatial area represents the 'Sub Tidal' zone that is completely submerged. The elevation of each spatial area is kept constant. High Marsh was kept at 3.0 feet (1 m) above Mean High Water (MHW), Mid Marsh at 1.0 foot (0.333 m), Mud Flat at 0.5 foot (0.167 m) and Sub Tidal at –1.0 feet (-0.333 m). Each spatial area has resident biota listed in Fig. 2. Upgrades of QnD:HAAF will expand these elementary spatial areas into linked maps of wetlands that can be managed separately or in groups for ecosystem/management objectives.

Habitats

Habitats exist within, and occupy a fraction of each spatial area. The habitats are assumed to be homogeneous and harbor different combinations of biota and chemicals. In the initial version of QnD:HAAF, no specialized habitats within the spatial areas are distinguished, *i.e.* one "default" habitat occupies 100% of the spatial area . In later model versions, a plant- and a non-plant influenced habitat within each spatial area may be introduced. This modification would allow QnD to simulate the effects of depositing dredged material on a vegetated area. This management action may convert a portion of a vegetated wetland temporarily into a mud flat with altered mercury dynamics.

Environmental Drivers and Time Scales

Three environmental drivers were selected to link processes at time scales varying from current (on site measured methylation and demethylation rates in light versus in darkness, Chapter 1, This Report) to seasonal (wet versus dry season data on THg and MeHg concentrations in the sediment, cf. McFarland et al., 2003). An on-line tide simulator for the bay area was used to provide initial estimates of tidal water levels for selected time periods on an hourly basis (http://tbone.biol.sc.edu/tide/sitesel.html). Values pertaining to the mouth of the Petaluma River were selected, since these were considered as representative for the nearby HAAF. In general, SI units are used. The only exception is water depth, where feet are used for easy import of water level data from the on-line tide simulator.

For initial QnD:HAAF v1.0 testing, two hourly time series were constructed, representing a dry season, i.e. 1 – 14 June 2003, and a wet season, i.e., 1 – 14 February 2004), respectively. QnD:HAAF v1.0 utilizes a default time step of one hour, and can model results can, thus, easily be converted into daily values by multiplication with a factor of 24.

Tidal and Redox Processes

Water depth on each spatial area is calculated by subtracting its' local elevation hourly from tidal water level, using the following equation (1):

$$WaterDepth = TidalDepth - Elev_{base} \quad (1)$$

where *WaterDepth* = local water depth on the spatial area (ft),
TidalDepth = hourly tidal depth (ft),
$Elev_{base}$ = base elevation of the surficial sediment layer (ft)

If the calculated local water depth (*WaterDepth*) has a positive sign, then the spatial area is considered as being submerged and susceptible to decreasing oxygen diffusion. Vice versa, if the calculated local water depth has a negative sign, then the spatial area is considered as extending above the water level and thus susceptible to oxygen diffusion from the ambient air.

WaterDepth is used subsequently to calculate the number of hours in which the spatial area is submerged or extended above the water level, which, in turn, governs changes in redox potential. The simplified relationship between water depth and change in number of hours under water is presented in Fig. 3. Subsequently, the cumulative numbers of hours under and above the water level, respectively, are used to calculate the hourly change in redox potential (mV; Fig. 4). The maximum and minimum values of the hourly change in redox potential do not change as they represent the stable redox potential values of areas that are, respectively, above and below the water level for longer periods (for example, the High Marsh or SubTidal spatial zones). The hourly change in redox potential is then added to the cumulative redox potential for each spatial zone. The fluctuations in redox potential in all spatial areas were delimited by an assigned upper boundary of 300 mV and a lower boundary of –300 mV. These initial redox relationships were estimated from redox dynamics reported in Bartlett and Craig (1981) and should be further validated through site measurements.

Mercury Dynamics

Two chemical mercury pools are assumed to exist and available for transformation: total mercury (THg) and methylmercury (MeHg) (Fig. 1). Both pools are assumed to reside in the surficial 5-cm sediment layer and its associated pore water. The pools change in mass per unit area (ng m^{-2}), but have an associated, calculated, concentration (ng g^{-1}). The pools are considered as fully active, i.e., the whole THg pool is available for conversion into the MeHg pool, and vice versa. THg is transformed into MeHg as a function of time of year (dry or wet season), redox potential (dependent on tidal movements) and time of day (light or dark conditions). The values assigned to the pools of mercury are defined by the analytical procedures used to measure THg and MeHg. I assume that all THg and MeHg is reactive, but am aware that this is an overestimate since only a fraction may be reactive and/or is bioavailable. However, it is currently not known what and how large the reactive and bioavailable fractions are.

The inputs of the THg and MeHg pools originate from the TotalLoad pools (objects) that contain the chemical mass values (ng m^{-2}) and are calculated using equation (2):

$$Load = Conc * Depth * BD * 10000 \quad (2)$$

where Load = the total mass (ng m^{-2}) of Hg^{2+} or MeHg,
Conc = Hg^{2+} or meHg concentration (ng g^{-1} DW),
Depth =depth (cm) sediment, assumed to be 5 cm,

BD = bulk density sediment on a dry weight basis,
10,000 = conversion from cm^2 to m^2.

Bulk density was derived as follows. A bulk density on wet weight basis of 1.29 g wet wt cm^{-3} was measured by M. Marvin-DiPasquale, USGS Menlo park, CA, Unpublished Results 2004). The latter value was converted to BD on a dry weight basis, assuming that 1 g wet sediment represents 0.438 g DW (Chapter 1-Table 5, This Report). The calculated BD was 0.565 g DW cm^{-3}.

The initial concentrations and calculated loads of THg and MeHg are presented in Table 1. Initial concentrations have been derived from data collected at HAAF in 2003 (Chapter 1, This Report). All mercury-related calculations are carried out in nanograms on a dry weight basis, and subsequently the nanograms are converted into concentrations.

Mercury Methylation

The methylation process is presented in Fig. 5. In the model, methylation is affected by redox potential, tidal water movements, season, and light/dark conditions. The calculations of water depth and redox potential, prerequisites for the calculation of methylation, have been described in the previous section.

The base THg methylation rates have been derived from the rates measured in the field in 2003, under dry season, daylight, and oxic conditions (Table 2).

In the model, the amount of Hg methylated hourly in each spatial area is calculated as a percentage of the total available, inorganic Hg^{2+} pool (TotalHg), and follows equation (3):

$$meHg_n = BaseRate_{meth} \times Season(month) \times \mathrm{Re}dox_m(hours) \times Light_m(daylight) \times TotalHg \quad (3)$$

where $BaseRate_{meth}$ = THg methylation (ng MeHg methylated ng^{-1} Hg^{2+} hr^{-1}),
Season(month) = seasonal, month-specific, effect on methylation rate (-),
$Redox_m$(hours) = redox potential effect on methylation rate, depending on the cumulative number of hours under water or extending above the water level (-),
$Light_m$(daylight) = daylight effect on methylation rate depending on time of day (-),
TotalHg = size Hg^{2+} pool (ng DW)

MeHg concentrations in the sediments were found to be higher in the wet season than in the dry season by McFarland et al. (2003). It is not clear if these differences were caused by higher methylation or lower demethylation rates, or both. Nevertheless, to enable the calculation of methylation rates accounting for effects of dry and wet season on methylation rates, multiplication factors relating wet season activity to dry season activity were derived from mean dry season and mean wet season MeHg concentrations in the sediment as ratios (McFarland et al., 2003, Table 2). The seasonal factors for the spatial areas are listed in Table 3. Since base methylation rates were measured in the dry season of 2003, the multiplication factors for the dry season are 1.0. The multiplication factors accounting for the effects of a wet season range from 1.6 in the Mud Flat and Sub Tidal spatial areas to 8.8 in the High and Mid Marsh spatial areas vegetated by *Salicornia* and *Spartina*, respectively. The dry season in the model lasts from April through October, and the wet season from November through March.

Methylation rates were found to be generally 40 to 50 percent lower in darkness than in light (Chapter 1, This Report). In QnD:HAAF, factors accounting for the decreasing effect of darkness have been derived from the field data. These factors are listed in Table 4. Night time in the model lasts from 6 PM to 6 AM.

The relative effect of redox potential on the methylation of Hg follows a stylized Gauss curve with a maximum of 1 at a redox potential between -100 and +100 mV, and minima of 0.1 at redox potential values more negative than -300 mV and more positive than 300 mV (Fig. 5). This curve has been fitted to data of Bartlett and Craig, 1981; and modified by McFarland and Lee, 2002). Methylation proceeds at the highest rate between –100 and 100 mV potential.

Methylmercury Demethylation

The demethylation process is represented in Fig. 6. MeHg is demethylated and returns as Hg to the active Hg^{2+} pool following a simplified, first-order, rate equation (DTMC /SRWP, 2002), which is affected by redox potential, tidal water movements, season, and light/dark conditions.

The base MeHg demethylation rates have been derived from the rates measured in the field in 2003, under dry season, daylight, and aerobic conditions (Table 5).

In the model, the amount of MeHg demethylated hourly in each spatial area is calculated as a percentage of the MeHg pool, and follows equation (4):

$$demethHg_t = BaseRate_{Demeth} \times \mathrm{Re}dox_d(hours) \times Light_d(daylight) \times meHg_t \qquad (4)$$

where $BaseRate_{demeth}$ = MeHg demethylation rate (ng MeHg demethylated ng^{-1} MeHg hr^{-1}),

$Redox_d$ (hours) = redox potential effect on demethylation rate depending on the cumulative number of hours under water or extending above the water level (-),

$Light_d$ (daylight)= daylight effect on demethylation rate depending on time of day (-),

MeHg = size MeHg pool (ng DW)

Demethylation rates were found to be generally 25 percent lower in darkness than in light, except in the *Spartina*-vegetated Mid Marsh where it was elevated by almost 50 percent (Chapter 1, This Report). In QnD:HAAF, factors accounting for the effect of darkness have been derived from the field data. These factors are listed in Table 6.

The relative effect of redox potential on demethylation of MeHg follows a linearized saturation curve with a maximum of 1 at a redox potential more positive than 100 mV, and a minimum of 0.1 at a redox potential more negative than -100 mV (Fig. 8). This curve has been fitted to data of Bartlett and Craig (1981), modified by McFarland and Lee (2002), and data Chapter 1, This Report.

Simple MeHg Export From Sediments

In QnD:HAAF, MeHg is exported from the sediments at a constant rate as described in Chapter 1-Table 12, This Report. It is assumed that 0.8 percent of the MeHg in the sediment is exported per day (i.e., 0.0333 percent per hour). This amount of MeHg enters into a non-returnable pool that estimates the potential MeHg export to the bay.

Biota

Selected organisms are included in the QnD:HAAF model, i.e., plants, invertebrates and one vertebrate animal (a bird). Two emergent macrophytic plant species and one microalgal group are represented in the current version of QnD:HAAF. *Salicornia virginica* (Pickle weed) and *Spartina foliosa* (Cord grass) are simulated at the simplest level as an established standing crop with constant biomass over the two-week simulation. Plant MeHg load (ng) and potential contribution to export were assumed to be the primary data of interest in these simulations. The epipelon (algae living on the sediments) are also potential contributors to the export of MeHg. The values on plant biomass and THg and meHg concentrations used to calibrate the model are reported in Chapter 1, This Report. The following wetland invertebrates are modeled as potentially resident in all four spatial areas, but with population size and –biomass being spatial area-specific: Ribbed Mussel (*Geukensia Demissa*), Yellow Shore Crab (*Hemigrapsus Oregonensis*) and the Eastern Mud Snail (*Iyanassa obsoleta*). These animals have been identified in HAAF field samples (Chapter 1, This Report). For exploring the trophic transfer and bioaugmentation of MeHg to higher levels in the food chain, the California Clapper Rail (*Rallus longirostris obsoletus*) is included as potentially resident in all four spatial areas. For the time being, it is assumed that biota do not migrate between spatial areas.

The initial MeHg pool ($MeHg_{Load}$) for each organism is calculated using equation (5) :

$$MeHg_{Load} = Org_{biom} \times Conc_{MeHg} \quad (5)$$

where Org_{biom} = organism biomass (g DW),
$Conc_{MeHg}$ = MeHg concentration (ng g^{-1} DW)

Population and biomass data of the biota were estimated from literature values, since they had not been collected at HAAF (Table 7). Population densities may vary with spatial area, e.g., ribbed mussels, and in those cases different starting values were used. The initial concentrations and calculated loads of MeHg in the biota are presented in Table 8. Initial concentrations have been derived from data collected at HAAF and China Camp (Chapter 1 and Chapter 4, This Report).

Uptake of Biomass

In this QnD:HAAF version the relationships between consumers and their food sources are formulated as a predator-prey relationship (Fig. 8). According to this approach, when a mud snail grazes epipelon, the mud snail would be a predator and the epipelon would be a prey. The uptake of prey biomass by the predator is calculated using equation (6):

$$Intake_{pred} = Biom_{pred} \times DemandRate_{prey} \quad (6)$$

where $Intake_{pred}$ = amount of prey biomass ingested by a specific predator (g DW),
$Biom_{pred}$ = predator biomass (g DW),
$DemandRate_{prey}$ = amount of prey required per unit weight of the predator (g DW prey per g DW predator)

The biomass of the prey is transferred from the prey pool to the predator pool ($Intake_{pred}$). If the prey pool is smaller than the demand of the predator, all available prey biomass is transferred to the predator. The predators and prey demand rates are listed in Table 9.

Biomass Loss

Long-term changes in biomass due to growth and respiration are not included. The biomass of plants (*Salicornia*, *Spartina* and epipelon) and ribbed mussels is assumed to be constant within the two-week simulation period. However, for animals that consume prey organisms (mud snails, shore crabs and clapper rails) and thus would increase in biomass, a mass-loss rate is introduced that is set equal to the biomass uptake rate to enable the simulation of trophic transfer of MeHg. The mass loss rates are listed in Table 10.

Uptake of MeHg Directly from Sediment

In QnD:HAAF, all biota have uptake and loss processes that allow them to potentially bioaccumulate and release MeHg. This methodology is in accordance with DTMC/ SRWP (2002), recommending an initial simplified approach, followed by a detailed bioenergetic approach once MeHg data become available on higher trophic levels. Data on uptake and bioaccumulation of MeHg from soil, sediment, and pore water are still extremely scarce in the literature, and they are, therefore, largely estimated from most recent research reported in the Chapters 1, 2, 3, and 4 of This Report, and from (Mason et al., 1996; Rogers, 1994; Barber, 2001).

Uptake of MeHg from sediment is represented in Fig. 9, and calculated using equation (7):

$$MeHgIntake_{sed} = Biomass \times Transfer_{sed} \times Sat(MeHg_{conc}) \qquad (7)$$

where $MeHgIntake_{sed}$ = uptake of MeHg from sediment (ng),
Biomass = biomass organism (g DW),
$Transfer_{sed}$ = potential MeHg transfer rate from sediment into organism ($ng\ g^{-1}$ organism-DW),
$Sat(MeHg_{conc})$ = relative function that reduces MeHg uptake to 0.0 when the species-characteristic initial (equilibrium) MeHg concentrations (Table 8) are reached

MeHg will only be taken up from the sediment when the MeHg concentration in the organism is below the concentration measured in the field, since the latter is assumed to be in equilibrium with the environment. One potential MeHg transfer rate from sediment into organism is used for all organisms, i.e. (0.14042 ng MeHg g^{-1} DW hr^{-1}).
This $Transfer_{sed}$ value was measured in preliminary uptake experiments with Hg^{2+} on a *Macoma* species that filters sediment (Chapter 3, This Report). It is planned to include more species-characteristic uptake/transfer rates when these become available.

Uptake of MeHg from Grazing or Predation by Predator

Uptake of MeHg by ingestion of biotic food sources is represented in Fig. 10, and is calculated using equation (8). This equation has been formulated after Rogers (1994).

$$MeHgIntake_{prey} = Biomass_{pred} \times \Pr eyConsumed \times MeHg_{prey} \quad (8)$$

where $MeHgIntake_{prey}$ = uptake of MeHg from ingesting a prey (ng),
$Biomass_{pred}$ = biomass predator (g DW),
Prey Consumed = biomass prey consumed (g prey-DW),
$MeHg_{prey}$ = MeHg concentration prey (ng g^{-1} prey-DW)

MeHg Loss From Biota

All macrophytes lose 50 percent of their biomass per year (estimate Chapter 1, This Report), and, based on this estimate they would also lose that fraction of the MeHg contained in the plant biomass. In QnD:HAAF all plants, i.e. macrophytes and epipelon, are modeled as losing 50 percent of the MeHg contained in their maximum standing crop per year, i.e., 5.7078x 10^{-3} percent hr^{-1}. All animals, including the ribbed mussels with constant biomass, are assumed to release 10 percent of their resident MeHg load per day, i.e., 0.4167 percent hr^{-1}. The latter value is based on a study on elimination of THg and MeHg by the zooplankter *Daphnia magna* feeding on phytoplankton (Tsui and Wang, 2004). This amount of MeHg released enters into a general pool that quantifies the potential MeHg export to the bay.

QnD:HAAF MODEL RESULTS

Comparison of Simulated and Measured Methylation Rates

An important means to build confidence in the capabilities of QnD:HAAF to generate results that reflect what is happening in the ecosystems of interest, is to compare simulated results with measured values. Here, I illustrate one such case.

The QnD model was used to simulate methylation and demethylation rates in the *Salicornia*-vegetated High Marsh spatial area over a two-week period. The simulated values were compared with values measured in a *Salicornia*-vegetated High marsh along San Francisco Bay by Marvin-DiPasquale et al. (2003). The simulated methylation and demethylation rates of 7.85 and 7.37 ng g^{-1} DW day^{-1}, respectively, were in the same range as the rates described by Marvin-DiPasquale et al. (2003). A more detailed analysis and comparison of methylation and demethylation rates used for model calibration and those measured by Marvin-DiPasquale et al. (2003) is given in Chapter 1, This Report.

As with any modeling effort, more comparisons of simulated values with measured ones will increase the confidence of a model's performance.

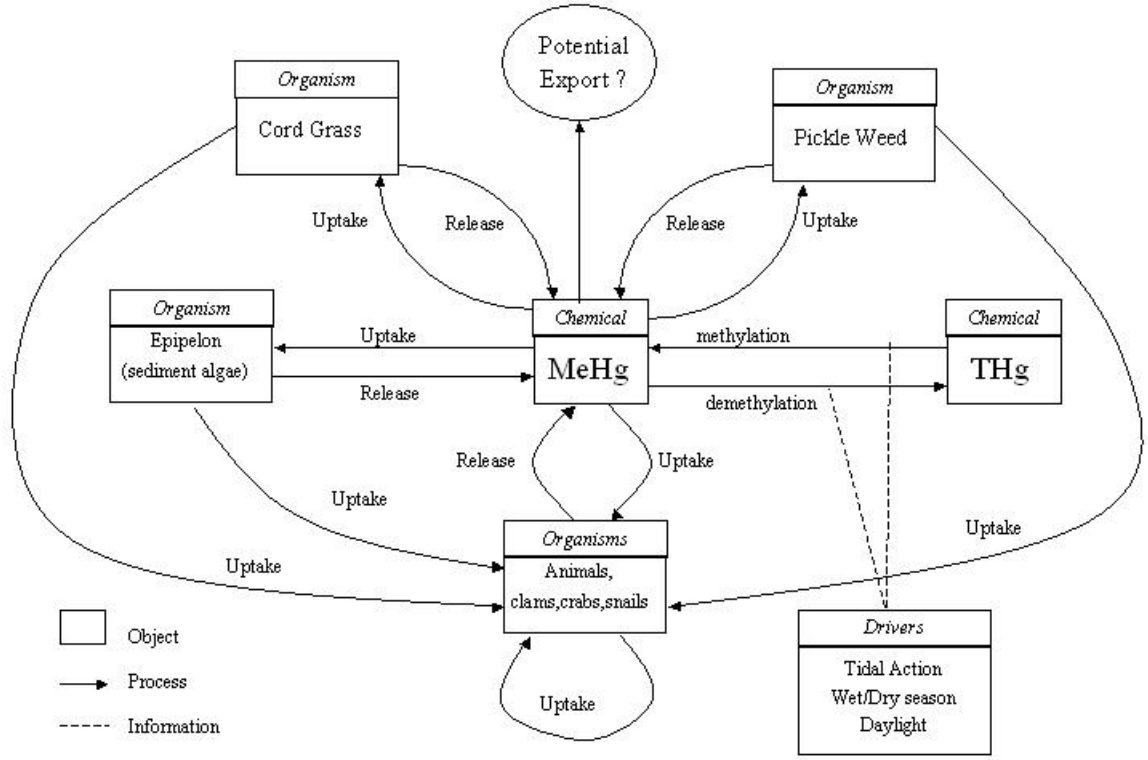

Figure 1. Overview of QnD:HAAF objects, drivers and processes.

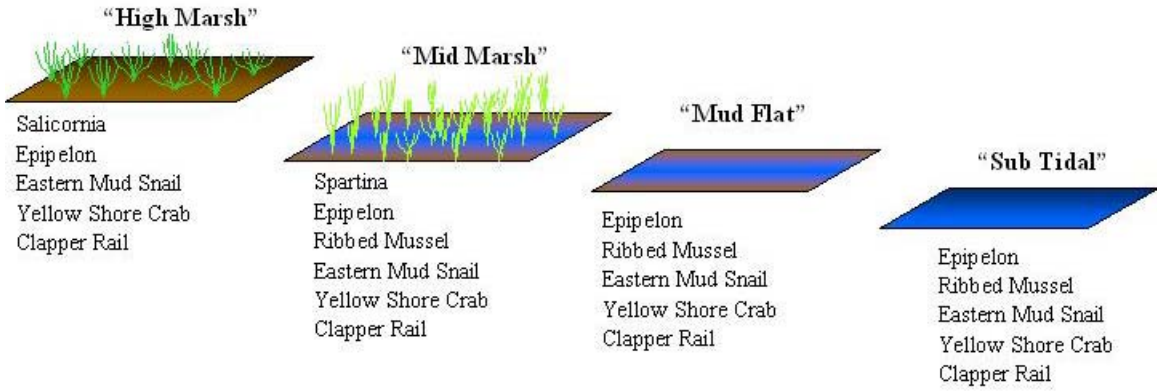

Figure 2. Spatial areas with associated biota within QnD:HAAF version 1.0.

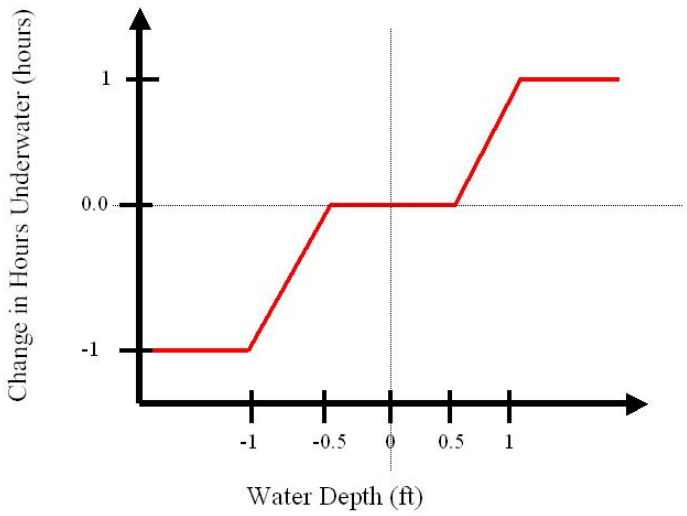

Figure 3. Simplified relationship between local water depth and change in number of hours under water.

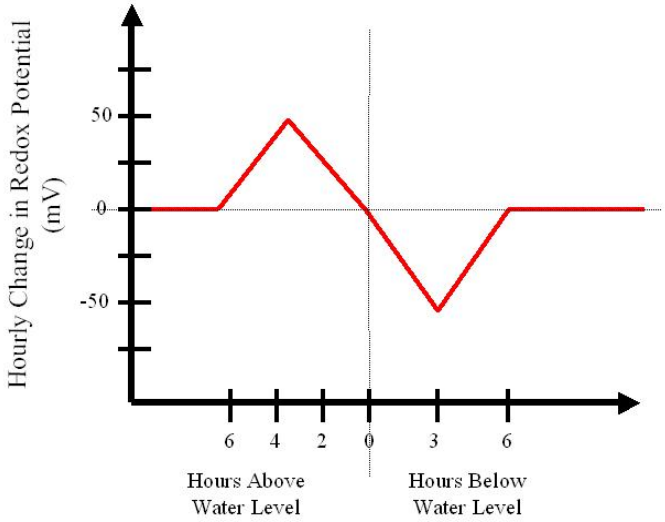

Figure 4. Relationship between hours above and under water, and the hourly change in redox potential.

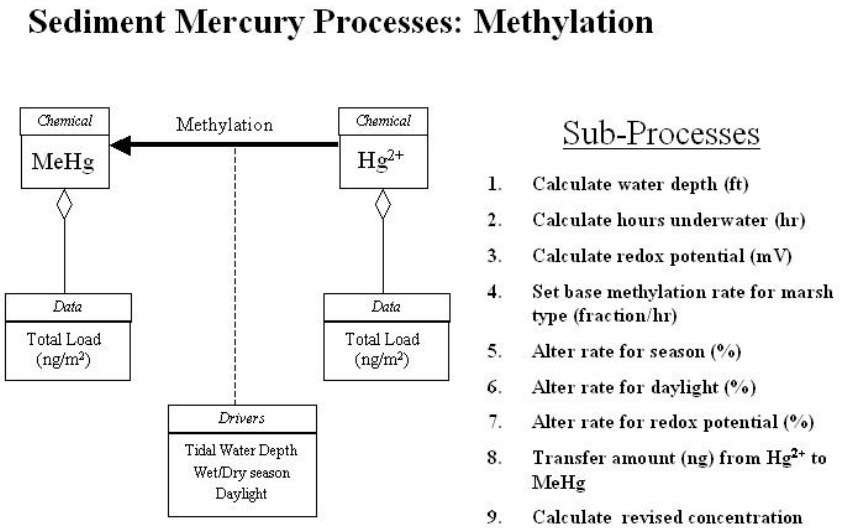

Figure 5. Overview of the QnD:HAAF mercury methylation process.

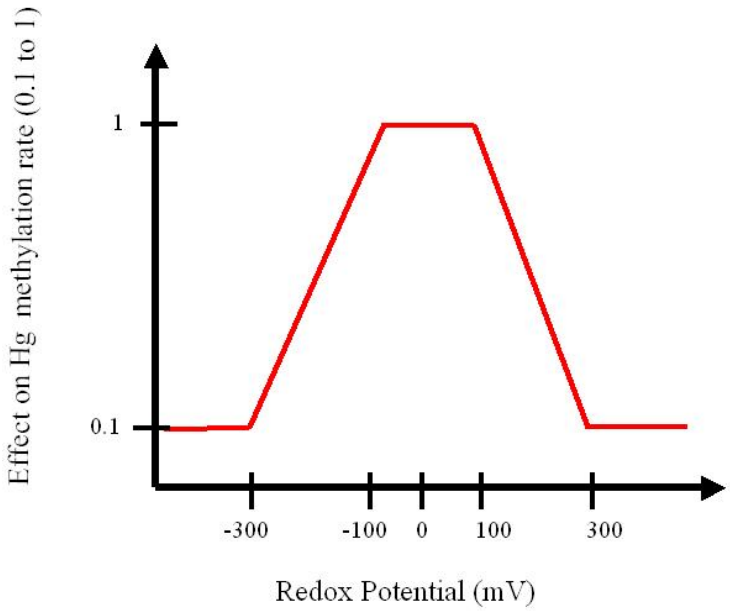

Figure 6. Effect of redox potential on mercury methylation rate (relative).

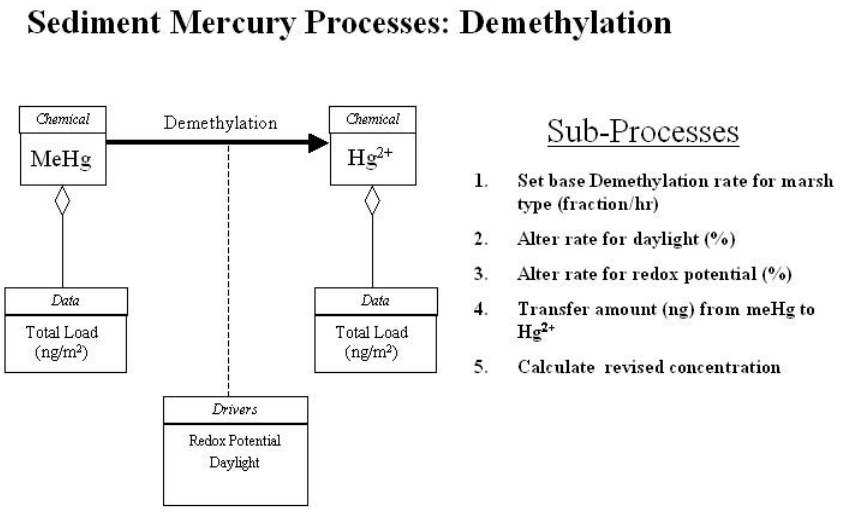

Figure 7. Overview of the QnD:HAAF methylmercury demethylation process.

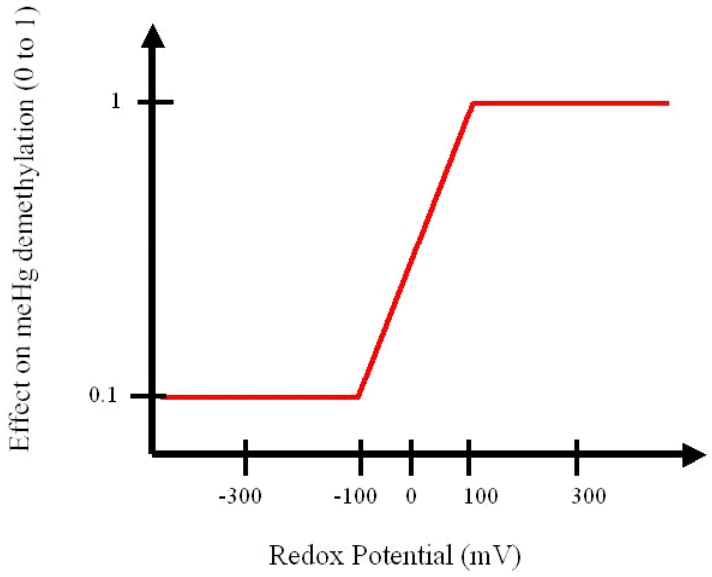

Figure 8. Effect of redox potential on methylmercury demethylation rate (relative).

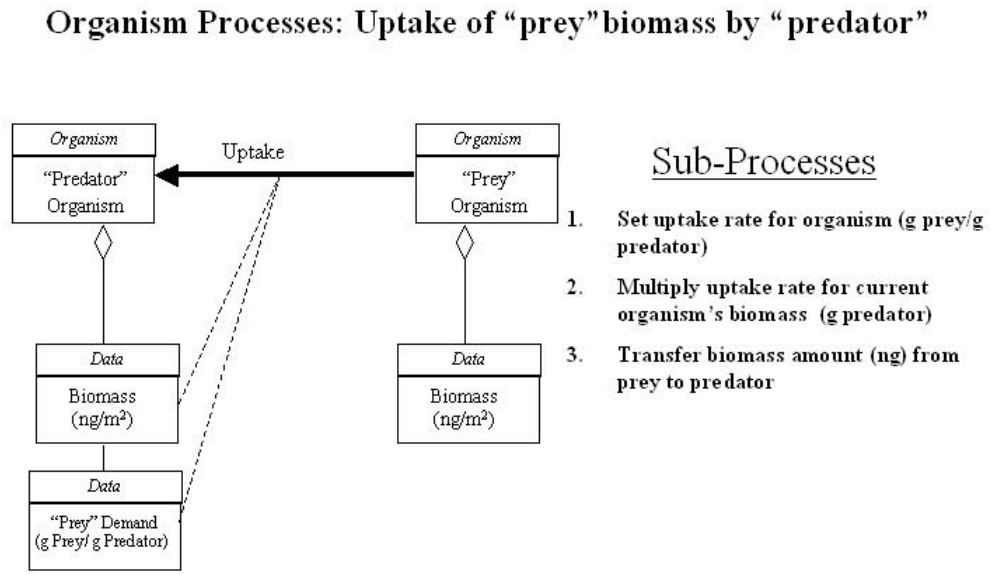

Figure 9. QnD:HAAF uptake of biomass.

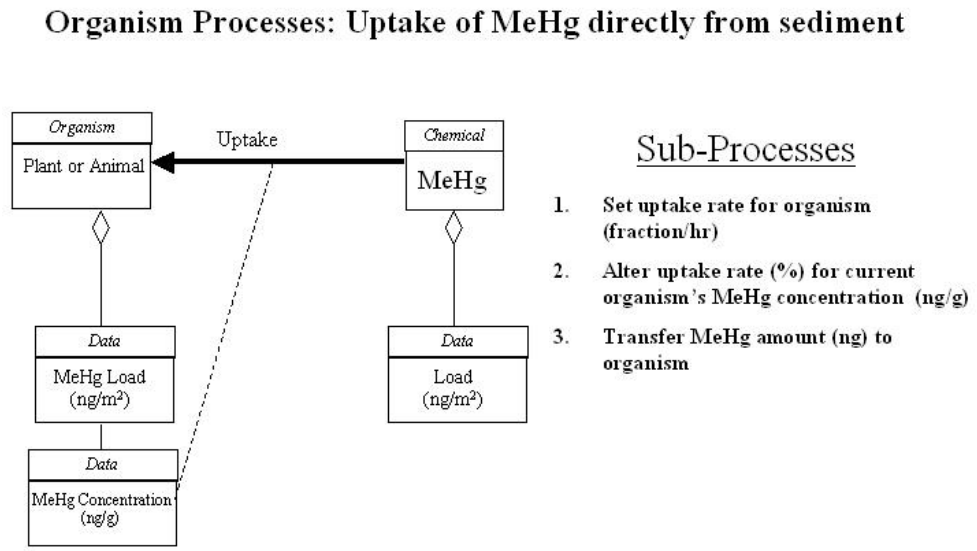

Figure 10. QnD:HAAF uptake of MeHg by organisms directly from sediment.

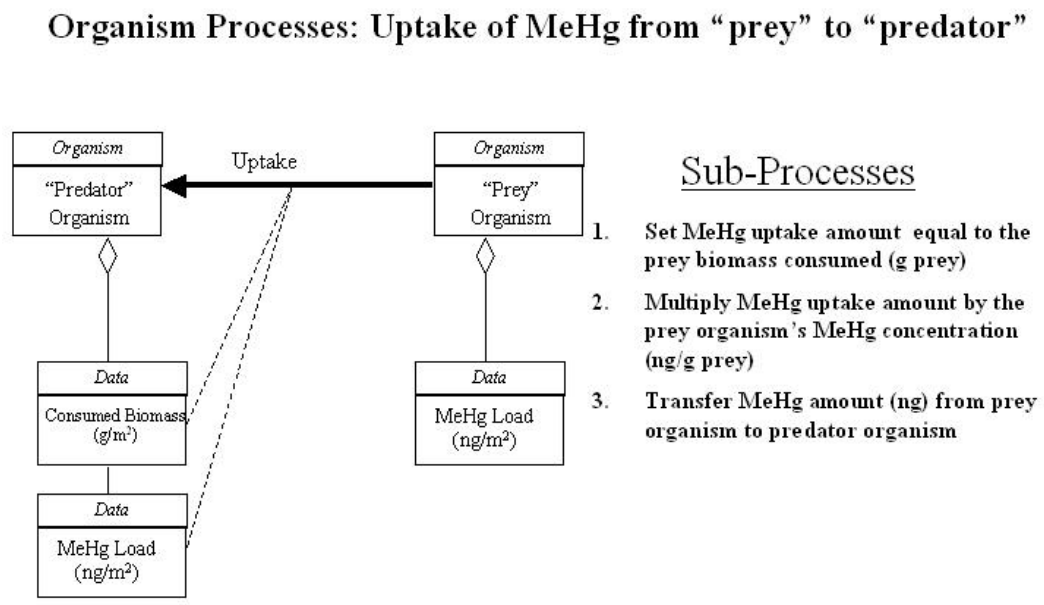

Figure 11.QnD:HAAF uptake of MeHg through biomass ingestion.

Table 1. Initial concentrations and calculated loads of Hg and MeHg for spatial areas.

Spatial Area	Hg^{2+}		MeHg	
	Conc[1] (ng g^{-1})	Load (ng m^{-2})	Conc[1] (ng g^{-1})	Load (ng m^{-2})
Salicornia Marsh	314	8,870,500	1.11	31,358
Spartina Marsh	407	11,497,750	1.35	38,138
Mud Flat	378	10,678,500	1.78	50,285
Sub Tidal	378	10,678,500	1.78	50,285

[1] Field data Chapter 1, Table 5

Table 2. Base mercury methylation rates for QnD:HAAF spatial areas, under dry season, day-time, aerobic conditions[1].

Spatial Area	Methylation Rate (Fraction Hg^{2+} hr^{-1})	Fraction Hg^{2+} Pool Converted (Percent hr^{-1})
Salicornia Marsh	3.00×10^{-4}	0.0300
Spartina Marsh	1.833×10^{-4}	0.01833
Mud Flat	2.083×10^{-4}	0.02208
Sub Tidal [2]	2.083×10^{-4}	0.02208

[1] Field data Chapter 1, Table 7
[2] SubTidal assumed to equal Mud Flat

Table 3. Multiplication factors accounting for seasonal effects on methylation rate[1] .

Spatial Area	Wet Season Factor	Dry Season Factor
Salicornia Marsh	8.8	1.0
Spartina Marsh	8.8	1.0
Mud Flat	1.6	1.0
Sub Tidal	1.6	1.0

[1] Ratios estimated from field data McFarland et al. (2003)

Table 4. Multiplication factors for daylight effects on methylation rate [1].

Spatial Area	Night-time Dark Factor	Day-time Light Factor
Salicornia Marsh	0.61	1.0
Spartina Marsh	0.59	1.0
Mud Flat	0.48	1.0
Sub Tidal	0.48	1.0

[1] Ratios estimated from data Chapter 1, Table 7

Table 5. Base demethylation rates[1], under dry season, day-time, aerobic conditions.

Spatial Area	Demethylation Rate (Percent MeHg hr^{-1})	Fraction MeHg Pool Converted (Percent hr^{-1})
Salicornia Marsh	1.083×10^{-2}	1.083
Spartina Marsh	1.458×10^{-2}	1.458
Mud Flat	1.542×10^{-2}	1.542
Sub Tidal	1.542×10^{-2}	1.542

[1] Field data Chapter 1, Table 8

Table 6. Multiplication factors for day-time light effects on demethylation rate[1].

Spatial Area	Dark Factor (6 pm – 6 am)	Light Factor (6 am – 6 pm)
Salicornia Marsh	0.73	1.0
Spartina Marsh	1.48	1.0
Mud Flat	0.76	1.0
Sub Tidal	0.76	1.0

[1] Ratios calculated using field data Chapter 1, Table 8

Table 7. Initial numbers of individuals and biomass of biota in QnD:HAAF.

Biota	Population (N m^{-2})	Individual Weight (g DW $individual^{-1}$)	Biomass (g DW m^{-2})
Salicornia virginica			2000.0 [1]
Spartina foliosa			2000.0 [1]
Epipelon (all areas)			286.0 [2]
Ribbed Mussel (High Marsh area)	12.0 [3]	0.2 [5]	2.4
Ribbed Mussel (Mid Marsh area)	156.0	0.2	31.2
Ribbed Mussel (Mud Flat area)	412.0	0.2	82.4
Ribbed Mussel (Sub Tidal area)	412.0	0.2	82.4
Eastern Mud Snail (High Marsh area)	1.0 [5]	0.1 [5]	0.1
Eastern Mud Snail (Mid Marsh area)	1.0	0.1	0.1
Eastern Mud Snail (Mud Flat area)	10.0	0.1	1.0
Eastern Mud Snail (Sub Tidal area)	10.0	0.1	1.0
Yellow Shore Crab	1.0 [5]	2.0 [5]	2.0
Clapper Rail	0.000125 [6]	69.2 [7]	0.00865

[1] Biomass levels estimated in Chapter 1, Table 11)
[2] 130 g C m^{-2} y^{-1}, with 1 g C = 2.22 g DW (listed in Chapter 1, This Report, Table 1; after Onuf, 1987) [3]
[4] Vitaliano and Bejda (2001)
[5] Estimated from current field research effort.
[6] One rail per 0.8 ha assumed, based on density ranges Gill (1979)
[7] Weight per rail: 346.1 g wet or 69.22 g dry (US Fish and Wildlife Service, 2003)

Table 8. Initial MeHg concentrations and MeHg loads of biota in QnD:HAAF

Biota	Biomass ($g\ DW\ m^{-2}$)	MeHg Concentration ($ng\ g^{-1}\ DW$)	Load ($ng\ m^{-2}$)
Salicornia virginica [1]	2000.0	1.64	3280.0
Spartina foliosa[1]	2000.0	2.52	5040.0
Epipelon (all areas) [1]	286.0	1.5	429.0
Ribbed Mussel (High Marsh area)	2.4	1.86	4.46
Ribbed Mussel (Mid Marsh area)	31.2	1.86	58.0
Ribbed Mussel (Mud Flat area)	82.4	1.86	153.3
Ribbed Mussel (Sub Tidal area)	82.4	1.86	153.3
Eastern Mud Snail (High Marsh area)	0.1	7.9	0.79
Eastern Mud Snail (Mid Marsh area)	0.1	7.9	0.79
Eastern Mud Snail (Mud Flat area)	1.0	7.9	7.9
Eastern Mud Snail (Sub Tidal area)	1.0	7.9	7.9
Yellow Shore Crab	2.0	1.72	3.44
Clapper Rail	0.00865	0.1 [2]	0.00865

[1] Field data Chapter 1, Tables 5 and 11
[3] Assumed initial load

Table 9. Predators and prey demands

Predator	Prey Demand ($g\ prey\text{-}DW\ g^{-1} predator\text{-}DW\ hr^{-1}$)	
Eastern Mud Snail [1]	Epipelon Demand	= 0.0042
Yellow Shore Crab[2]	Epipelon	= 0.0003
	Eastern Mud Snail	= 0.0003
	Ribbed Mussel	= 0.0003
Clapper Rail[3]	Ribbed Mussel	= 0104
	Eastern Mud Snail	= 0.0052
	Yellow Shore Crab	= 0.0052

[1] Assumed demand is 10 percent predator-biomass per day
[2] Assumed demand is 20 percent predator-biomass per day
[3] Assumed demand is 50 percent predator-biomass per day. Food source composed by: ribbed mussels (0.5), mud snails (0.25) and shore crabs (0.25). After US Fish and Wildlife Service (2003).

Table 10. Predators and mass loss rates to keep biomass pools constant over short periods.

Predator	Mass loss rate (g lost-DW g^{-1} predator-DW hr^{-1})
Eastern Mud Snail [1]	0.006
Yellow Shore Crab[2]	0.006
Clapper Rail[3]	0.021

[1] Assumed mass loss rate is 10 percent predator-biomass per day
[2] Assumed mass loss rate is 20 percent predator-biomass per day
[3] Assumed mass loss rate is 50 percent predator-biomass per day.

Table 11. Comparison of daily methylation and demethylation rates for *Salicornia*-vegetated High Marsh, measured by Marvin-DiPasquale et al. (2003; mean values and standard deviations) versus simulated by QnD:HAAF.

Process	Marvin-DiPasquale et al.(2003)[1]		QnD:HAAF	
	Potential Rate (ng g^{-1} DW day^{-1})	In-situ Rate (ng g^{-1} DW day^{-1})	Wet season (ng g^{-1} DW day^{-1})	Dry season (ng g^{-1} DW day^{-1})
Methylation	6.2 (2.84)	3.6 (1.8)	7.85	0.99
Demethylation	6.3 (2.0)	1.1 (0.8)	7.37	0.93

[1] Rates measured in March were converted from a wet-weight basis to a dry-weight basis, assuming 50 percent water, 50 percent solids.